USE OF CALIX[4]ARENES TO RECOVER THE SELF-ASSEMBLY ABILITY OF MUTATED p53 TETRAMERIZATION DOMAINS

Susana Gordo Villoslada

2008

Memòria presentada per

Susana Gordo Villoslada

per optar al grau de doctor per la Universitat de Barcelona
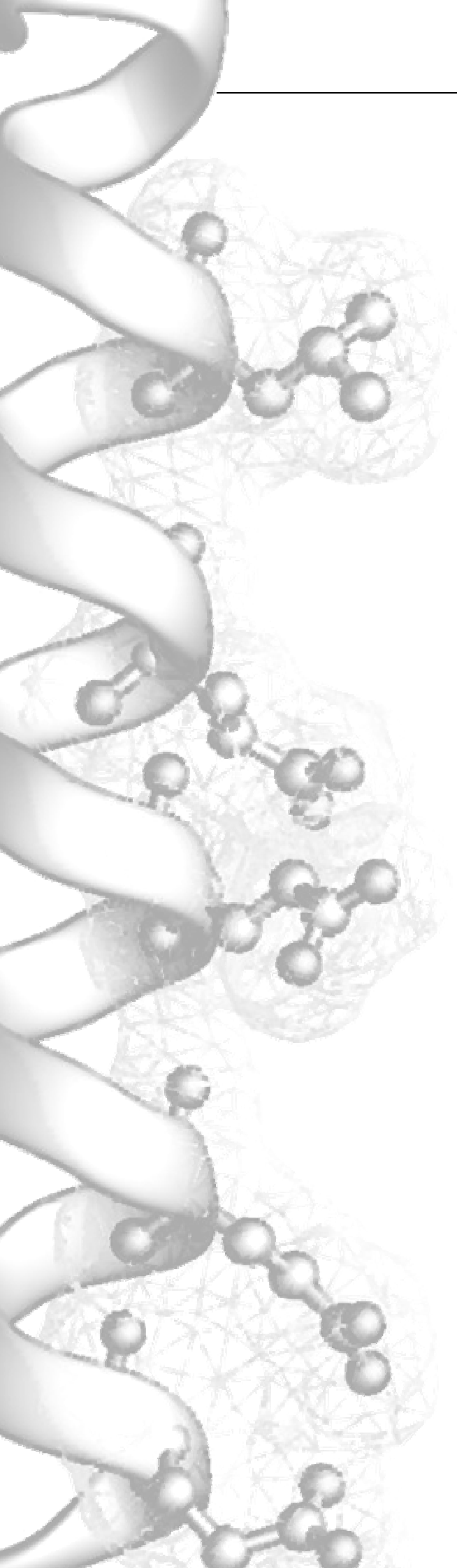
Revisada per:

Prof. Ernest Giralt i Lledó

Universitat de Barcelona

Director

Programa de Química Orgànica

Bienni 2003-2005

Barcelona, abril de 2008

RESULTS

Calix4bridge:

# a designed ligand for the

p53 tetramerization

domain

Calix4bridge is a ligand designed to bind and stabilize the tetrameric structure of p53TD. Its abilities on stabilizing the tetrameric assembly of mutated proteins, as well as the study of the structure of the complex and the binding mechanisms are presented in this chapter.

2.1. Calix4bridge: the design

The previous chapter illustrated how mutations in the tetramerization domain of p53 can seriously compromise the stability of the protein. Said destabilization is directly related to the inability of the mutant species to assemble into a compact tetrameric structure. Hence, the tetramerization domain of protein p53 and its mutants with compromised oligomerization properties represent an excellent case for designing ligands able to recognize and stabilize the native state of oligomeric proteins.

Taking as a model the structure of the wild-type p53TD, Prof. Javier de Mendoza envisioned a multivalent calix[4]arene ligand able to interact simultaneously with the four units of the tetramer, thereby holding together the whole structure of the protein. The rational binding model is shown in **Figure 2.1**. The multivalent ligand in question is the 5,11,17,23-tetraguanidinomethyl-25,26-27,28-biscrown-3-calix[4]arene, named **calix4bridge** for shorter.
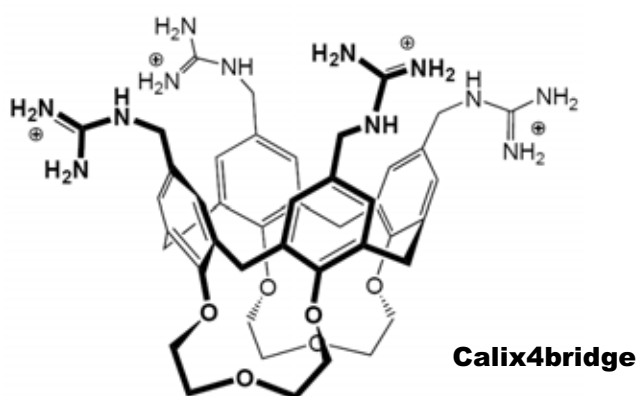
Calix4bridge

Calix4bridge presents two biscrown loops in the lower rim of the calix[4]arene platform; they outline an hydrophobic surface that can fit into a hydrophobic pocket on the protein surface, formed by the α-helices of the four monomers. Moreover, the loops bridging vicinal phenol rings keep the calixarene into an almost perfect conical shape and prevent winged conformations.[1,2]

On the upper rim of the calixarene ligand, four guanidinomethyl residues might additionally establish interactions via hydrogen bonding and ion pairing with the side-chain carboxylates of glutamates E336 and E339, which come from two monomers belonging to two different primary dimers. The methylene link positions the guanidinium groups on top of the platform, thus easily orienting their H-donors to the protein surface.

The simultaneous contribution of multiple hydrophobic and electrostatic interactions from calix4bridge elegantly illustrates the concept of *multivalency*, which should result in a stronger binding.[3]

Due to the high symmetry of p53TD, the protein presents two of those hydrophobic pockets; it was thus envisaged that two molecules of the calixarene could interact with and support the tetrameric

assembly. However, the ligand was designed according to the wild-type protein structure; hence, whilst calix4bridge might also bind to mutant proteins that adopt a tetrameric, native-like conformation –and in doing so, shift the tetramerization equilibrium and/or stabilize the protein as a pharmacological chaperone would– it would not be able to bind to mutants that do not adopt even the secondary structure elements (*e.g.* L344P).

The calix4bridge molecule was synthesized and purified by Vera Martos from the de Mendoza's laboratory at the Institut Català d'Investigacions Químiques (Tarragona). The synthetic scheme and the characterization of the synthetic product are provided in Appendix I. The final product used for the biophysical characterization was the corresponding tetrachloride salt.
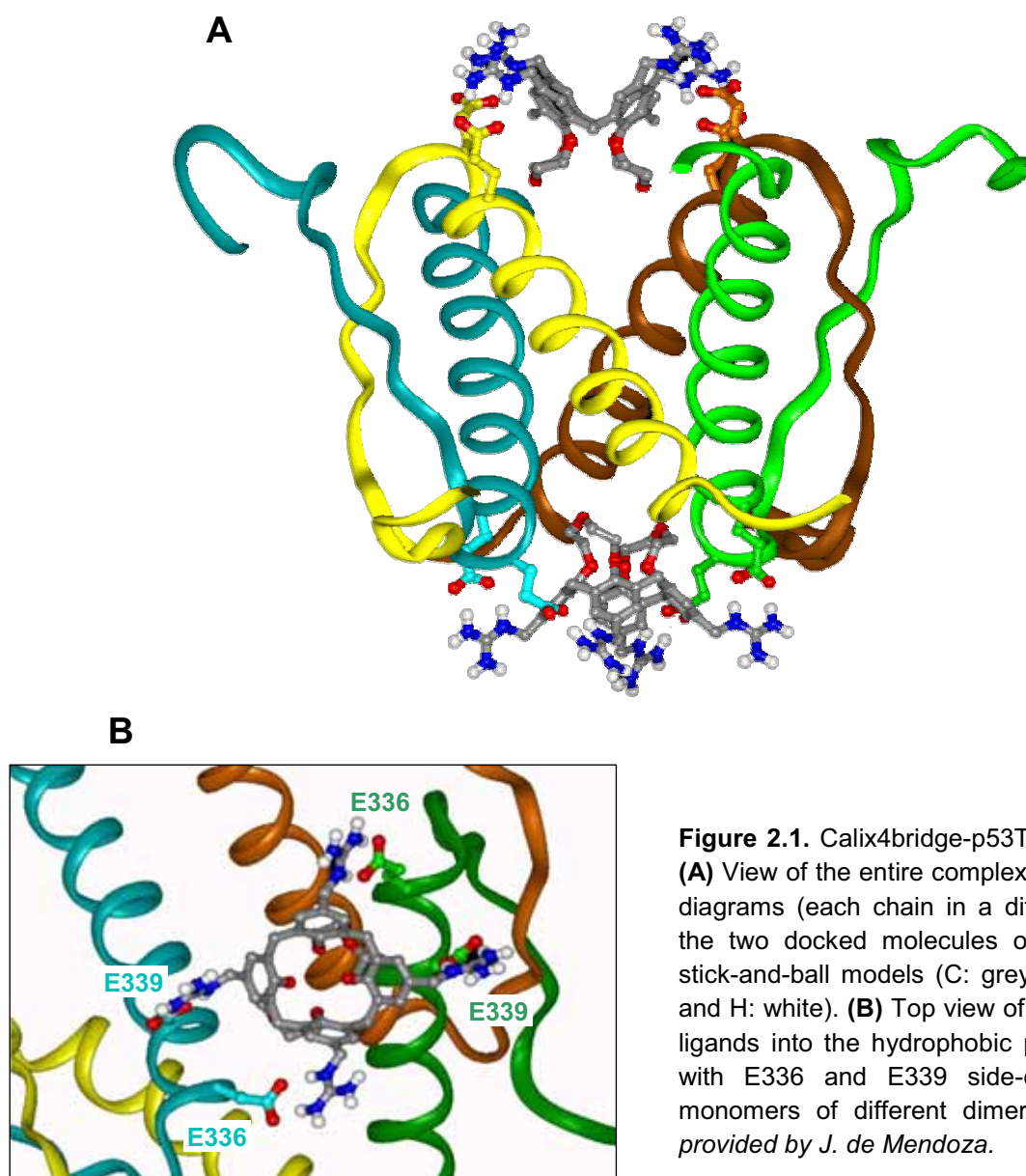
Figure 2.1. Calix4bridge-p53TD binding model. **(A)** View of the entire complex; protein in ribbon diagrams (each chain in a different color) and the two docked molecules of calix4bridge as stick-and-ball models (C: grey; O: red, N: blue and H: white). **(B)** Top view of one of the bound ligands into the hydrophobic pocket interacting with E336 and E339 side-chains from two monomers of different dimers. *Images kindly provided by J. de Mendoza.*

The proximity of the four guanidinium groups in the calixarene upper rim certainly influences their acidity. Although the pK_as would be expected to be fairly lower than standard values for a guanidinium group (pK_a ~12.5), all the basic moieties should be considered as protonated at the neutral pH range employed in the biophysical assays.[4]

Prior to discuss the experimental results, certain facts which affected the experimental working conditions must be explained.

The tetraguanidinium biscrown calix[4]arene is water soluble, a requirement for its evaluation in biological systems. However, its solubility is rather limited (at least at neutral pHs), and markedly reduced in high ionic strength buffers. In fact, the calixarene precipitated in phosphate buffer (or in the presence of any other bidentate anion), most likely due to the neutralization of the positives charges by the strong chelation of the phosphate anions to the guanidinium groups.[4] This effect was worse at the high ligand concentrations employed for some biophysical techniques. For this reason, the experiments were performed in water. However, water is not an ideal or appropriate medium: firstly, the lack of buffering properties of water complicates pH control and accurate reproduction of conditions; and secondly, the absence of ionic strength enhances the chance of non-specific electrostatic interactions.

In the next sections the protein concentration and the ligand molar ratios are always provided considering the tetramer (unless otherwise stated) since, according to the model, calix4bridge interacts with the tetrameric assembly.

2.2. Thermal effects of calix4bridge on protein stability

The most direct way to determine if the designed calixarene ligand could bind and stabilize the tetrameric state of p53 was to assess its effects on the thermal stability of the protein.

2.2.1. Differential Scanning Calorimetry

When a ligand interacts with a protein in its native state, the thermal stability of the biomolecule increases; hence, the DSC endotherm of the protein in the presence of the interacting ligand is shifted towards higher temperatures.[5-8]

Regrettably, mutant G334V could not be studied by DSC, because it aggregated under the experimental conditions. Therefore, DSC studies were done only for p53wt and R337H.

(a) Protein p53wt

The presence of calix4bridge hardly affected the thermal unfolding profile of the wild-type p53TD (**Figure 2.2**). In the presence of a high molar ratio of ligand, the maximum of the transition peak (T_m) for p53wt was barely shifted: from 85.5ºC for the free protein (25μM tetramer), to 86.8ºC in the presence of 16 equivalents of ligand (ligand-to-tetramer molar ratio) (**Figure 2.3B**).

In spite of being minute, the change in T_m was real and reproducible, not mere experimental error. However, the smallness of the change brought its origin into question. Since the experiments were done in water, the protein "stabilization" might simply be the result of the increase in ionic strength introduced by the calixarene, rather than from its specific interaction. This hypothesis was ruled out considering the destabilizing effects of ionic strength on p53wt (RESULTS - section 1.3.1). Therefore, it should be the interaction with the ligand which eventually caused an increase in the thermal stability of the protein.

The shape of the transition peak was perfectly preserved in the presence of calix4bridge; in fact, all the thermograms could fit the mathematical model developed for p53wt (fittings provided in the Supplementary Material);[9] hence, the interaction with calix4bridge did not affect the unfolding pathway for p53wt.[9]

Moreover, the melting enthalpy did not significantly change either –or changed within the range of uncertainty (**Figure 2.3A**); hence, at the melting temperature, the binding enthalpy of the complex could be assumed to be much lower than that of the protein unfolding ($|\Delta H_m| >> |\Delta H_B|$),.
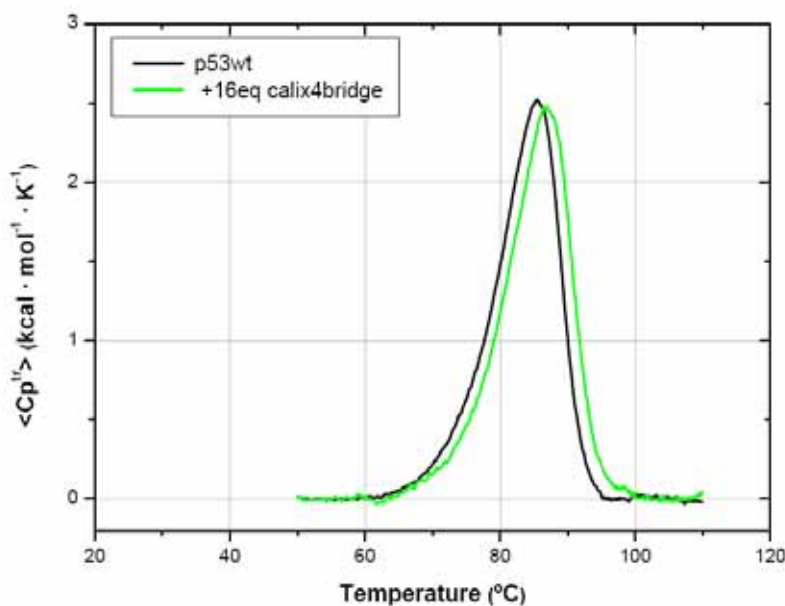
Figure 2.2. DSC thermograms of 25µM tetramer p53wt, alone (black) and in the presence of 400µM of calix4bridge (green), in water at pH 7, heating at 30ºC/h. Intermediate ratios evolved accordingly.
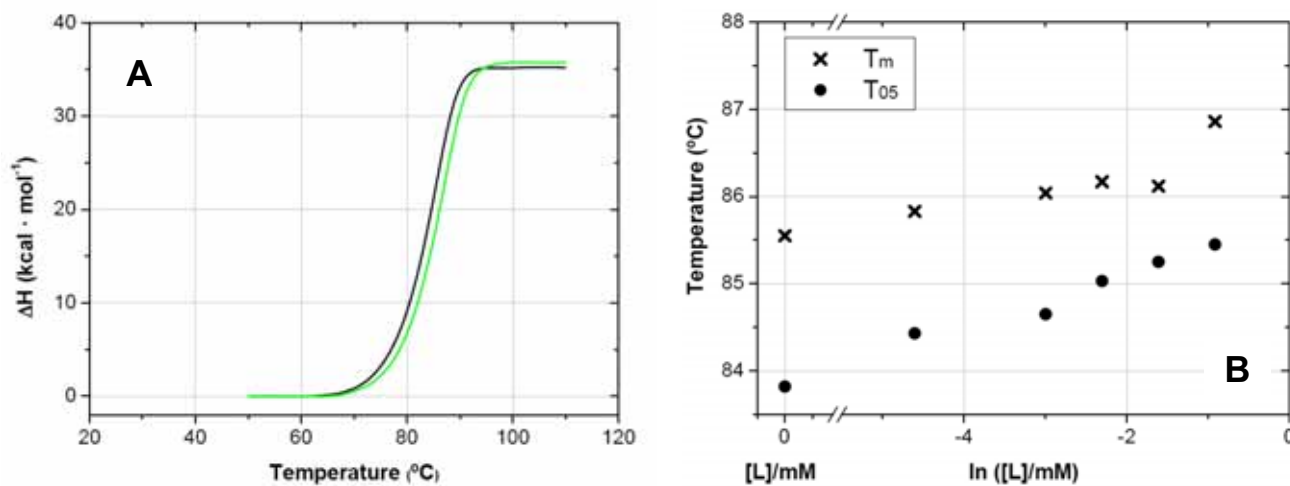
Figure 2.3. (A) Enthalpy change of the unfolding of p53wt at 25µM (tetramer), alone (black) and with 16eq of calix4bridge (green). For the sake of simplicity, lower ligand ratios are not displayed, although there were not significant differences. **(B)** Melting temperatures for the DSC thermograms of p53wt in the presence of increasing amounts of calix4bridge (represented versus the logarithm of calix4bridge concentration).[8] T_m (**x**) represents the temperature at which C_P reaches its maximum. T_{05} (●) corresponds to the temperature at which the transition is half completed (namely, ½ ΔH_m). As expected, the melting temperature increased with the ligand concentration: the shift in the binding equilibrium towards the bound form, also shifted the unfolding equilibrium towards the native form.[8]

Based on the minor thermal stabilization detected, the affinity of calix4bridge for p53wt at the melting temperature could be estimated to be rather low. However, shifts in the melting profile can not always be directly correlated with affinity.[10] Firstly, binding is evaluated indirectly, on the basis of how the ligand affects the unfolding equilibrium of the protein at the melting temperature, which is far from the "standard" temperatures of interest; and secondly, the ligand can also interact with the unfolded protein, thus shifting the melting temperature backwards.

Although calix4bridge was designed to interact specifically with a pocket of the native protein structure, nonspecific interactions with the unfolded species would likely occur, since the experiments were done in water at large concentrations of ligand. Nevertheless, the nonspecific nature of these interactions was unlikely to decrease the thermal stability of the protein; hence, the small change in the melting temperature might ultimately be the result of a very low affinity (at the melting temperature), specific interaction between the protein and the ligand. Because the change was so small, and because the ligand ratios were moderate, no reliable dissociation constant for the protein-ligand binding equilibrium could be calculated.[5,7,8]

The use of water as media also conferred low accuracy to the experimental data and precluded a rigorous analysis of the thermodynamics of the system.[11] It is well known how critical it is in DSC the perfect matching of the buffer solutions in the sample and reference cells,[12] however, working in plain water made this impossible. Although the transition peaks were reproducible, the energetic parameters which could be extracted from the thermograms were not completely reliable, especially those regarding the baseline evolution in the presence of ligand. The DSC traces were corrected by a sigmoidal baseline between the extrapolated C_P before and after the transition peak (resulting in C_P^{tr}), and consequently, the effects of calix4bridge on the change in heat capacity (ΔC_P) were lost.[13]

(b) Mutant R337H

Changes in the thermal stability of mutant R337H in the presence of calix4bridge were more evident, as shown in **Figure 2.4**. The melting temperature was shifted nearly 20ºC: from 63ºC for the free protein (25µM tetramer) to 82ºC in the presence of 16 equivalents of ligand (ligand-to-tetramer molar ratio). Moreover, the unfolding enthalpy was also increased markedly (**Figure 2.5A** and **C**). Both of these observations strongly supported the notion that the ligand interaction did stabilize the tetrameric structure of the mutant protein.

Rather than a continuous shift of the former transition peak towards higher temperatures, the presence of ligand induced bimodal denaturation of R337H. This phenomenon should not to be confused with either slow kinetics of the interaction with the ligand[6] or cooperative binding.[14] Bimodal endotherms are expected at sub-saturating ligand conditions, depending on the binding constant, the binding enthalpy change, the number of binding sites and the protein concentration.[6,14]
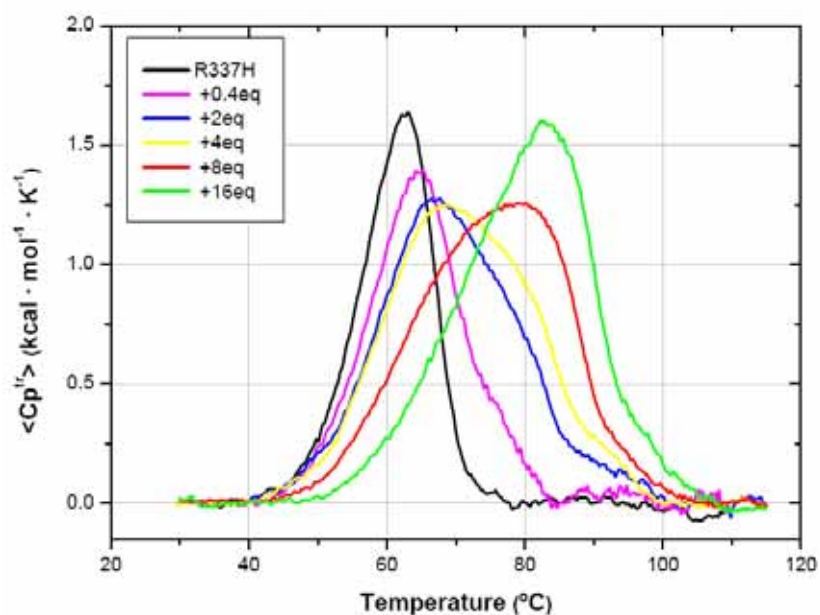
Figure 2.4. DSC transition endotherms of R337H (25μM tetramer) in the presence of calix4bridge (ligand-to-tetramer molar ratios), in water at pH 7, heating at 30ºC/h.

Each of the two transitions in the endotherm of R337H in the presence of calix4bridge was due to the unfolding of different protein populations: the ligand-free one and the ligand-bound one. Under sub-saturating ligand concentrations, the free protein is the first to unfold in the low-temperature range of the transition curve. The unfolding of some bound protein then releases bound ligand, thereby arising the free ligand concentration, and consequently, shifting the binding equilibrium and increasing the melting temperature of the ligand-bound protein. The higher the affinity, the greater the release of ligand; hence the larger the shift in the equilibrium, and the higher the tendency for bimodal denaturation.[14]

Moreover, although both the singly and the doubly-bound complexes are present at low temperatures, as the melting temperature of the native protein is approached and exceeded, the bound ligands rearrange. This increases the population of the doubly-bound protein at the expense of the single form. Therefore, no transition is seen for the singly-bound protein (at least if both sites present similar affinities), and the new transition peak only corresponds to the doubly-bond complex, regardless of whether the two sites are identical or different, independent or sequential.[6]

Since the proteins unfolded at the high-temperature range are mainly ligand-bound, the area under the curve is not linearly proportional to the number of unfolded molecules throughout the entire transition peak (**Figure 2.5A** and **B**). Biphasic distortion of the melting curve is over at saturating ligand concentrations, when all protein is ligand-bound. Interestingly, at this point, the endotherm of R337H is not as symmetric as that of the free protein (green trace in **Figure 2.4**). Indeed, the shape of the thermogram –skewed to the lower temperatures– resembles that of a tetrameric assembly in which unfolding is coupled to dissociation.

Figure 2.5B shows the normalized enthalpy curves for R337H in the presence of calix4bridge (normalized assuming a two-state unfolding). The asymmetry of the unfolding transitions, and the non-uniform shift towards higher temperatures, are clearly appreciated. Since the unfolding enthalpy for the bound protein was larger than that for the free species, the normalized curves did not linearly correlate with the unfolded fraction, at least for the lower concentrations of ligand. Therefore, the value for T_{05} –at which half of the unfolding enthalpy has been completed– was an overestimation of the real temperature at which half of the protein was unfolded (**Figure 2.5D**).
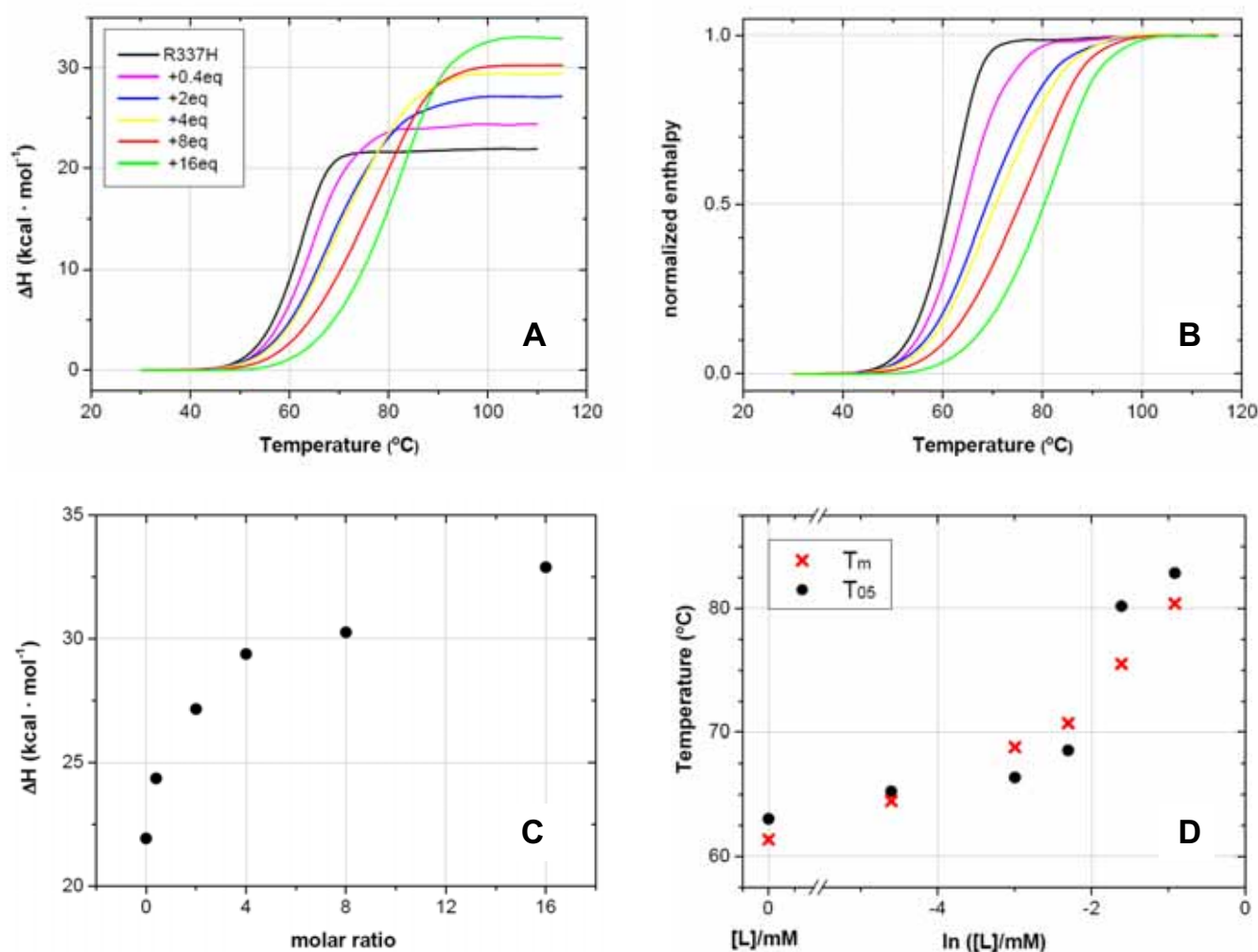
Figure 2.5. Enthalpy change of the unfolding of R337H in the presence of calix4bridge represented over **(A)** the temperature and **(B)** the normalized enthalpy curves. **(C)** Experimental ΔH_m represented against the ligand-to-tetramer ratio. **(D)** Thermal stability considering T_m (●) and T_{05} (**x**). As expected, the melting stability always increased with ligand concentration: the ligand binding equilibrium is coupled to the unfolding equilibrium; hence, the higher the ligand concentration, the higher the temperature required to unfold half of the protein.[8]

Regarding the affinity, the complexity of the system made impossible to deal with the thermodynamic data to estimate the dissociation constant for R337H and calix4bridge. All the

models proposed in the literature are simplified for systems with large excesses of free ligand (*i.e.* the system is by far saturated and [P]<<[L]), and most of these consider that the binding enthalpy for the protein-ligand complex is negligible if compared with that of the protein unfolding (*i.e.* ΔH_B<<ΔH_m). For the case at hand, neither of those two conditions was satisfied. Firstly, the ligand concentrations used were still far from the total saturation of the system (only the larger ligand concentration seemed to be closer, but due to the limited amount of calixarene available, no higher concentrations of ligand were considered). Secondly, the unfolding of the ligand-bound protein seemed to be more energetic, although it was unclear whether the increase was due only to the binding enthalpy itself, or to a change in the unfolding mechanism of the protein.

The aforementioned change of DSC curve shape of the protein-ligand complex strongly suggested that the ligand-bound protein underwent a different unfolding pathway, although this change could not be unequivocally attributed. One possibility is that the complex protein-ligand had been so tight and so stable that the dissociation of the ligand and the unfolding of the protein (as a tetramer) occurred simultaneously. However, the binding of calix4bridge might also promote a different tetrameric structure which is more stable, regardless of whether the release of ligand occurs before or during the unfolding. Moreover, the binding of the ligand to the tetrameric structure might also result in the protonation of the H337 side-chain, thus further stabilizing the mutant protein to thermal unfolding (as seen in the previous chapter, the thermal stability of R337H critically depends on the protonation state of H337).

The DSC data were not sufficient for understanding the events taking place. Moreover, even if the structure of the complex at room temperature were known, it might not provide any concluding evidence about the unfolding mechanisms at higher temperatures.

The lack of a mathematical model was not the only inconvenience in analyzing the thermodynamics of the system. As discussed for p53wt, working in water introduced some uncertainty in the experimental values and therefore, the baseline of the endotherms had to be corrected. For R337H, tracing said baselines was not trivial and was further complicated by the broadness of the transitions peaks and the precipitation of the unfolded species at high temperatures for some samples. Consequently, the resulting transition curves were probably not completely accurate.

Regardless of these limitations, the thermograms of R337H, at least, could be compared with those of p53wt. Bimodality, for the same concentration of binding sites, depends on the binding constant;[14] hence, the affinity of calix4bridge for R337H should be larger than that for p53wt (at the melting temperature). Nonetheless, the shift in the melting temperature for R337H might not only be due to the affinity, but also to changes in the structure of the protein (*e.g.* protonation of the H337).

2.2.2 Circular Dichroism

Circular dichroism was an excellent spectroscopic tool for examining the effects of calix4bridge on protein structure and stability. The former was readily determined by changes in the CD spectrum; the latter, by changes in the thermal unfolding curve of the protein in the presence of ligand.

In contrast to DSC, the thermal stability information provided by CD results from tracking the loss of secondary structure that the protein experiences upon heating. Therefore, thermodynamic parameters determined by CD are not measured directly but calculated with approximate equations. For our system, this was actually a great advantage, rather than a drawback. As discussed in the previous section, working in water compromised the DSC experimental data because of an inappropriate reference sample. However, CD does not require any reference, and the measured spectroscopic properties depend only on the system itself.

Furthermore, the concentration of protein in CD experiments is considerably less than that needed for DCS. The greatest benefit of this was that the thermal effects of calix4bridge on mutant G334V also could be studied.

The CD melting curves of proteins p53wt, R337H and G334V alone and in the presence of calix4bridge are compared in **Figure 2.6**. In spite of working with samples ten times more diluted than in DSC (2.5µM *vs.* 25µM of tetramer), the ligand also thermally stabilized the protein This means that the effect of calix4bridge –actually, the binding– was specific. And not only that, reproducibility would further support the correctness of the DSC curves (despite the aforementioned inconveniences associated with water).

The asymmetry of the CD unfolding curve of R337H in the presence of calix4bridge correlated well with the distortions in the DSC transition peak under sub-saturating conditions (**Figure 2.5C**). The degree of stabilization reached by CD was proportionally less (**Table 2.1**), as should correspond to the lower concentration used.

Mutant G334V was also thermally stabilized by calix4bridge, but not as much as R337H was, and its shift in the melting curve towards higher temperature appeared to be more uniform, which could suggest lower affinity. Perhaps the presence of the calixarene would have prevented the precipitation of G334V at higher concentrations (*i.e.* in the DSC); unfortunately, those experiments were not done.

Although equations to calculate the affinity constants from the ligand-induced shift in the protein CD melting curves have been developed, none of them was suitable here, given that *(i)* the unfolding enthalpy changed in the presence of calix4bridge[15] (as seen in the DSC curves for R337H), and *(ii)* not all the changes in the free energy could be related only to the binding of the ligand.[16] Hence, just as with DSC, thermodynamic information for the binding of the biscrown calixarene could not be obtained from the protein unfolding CD data.
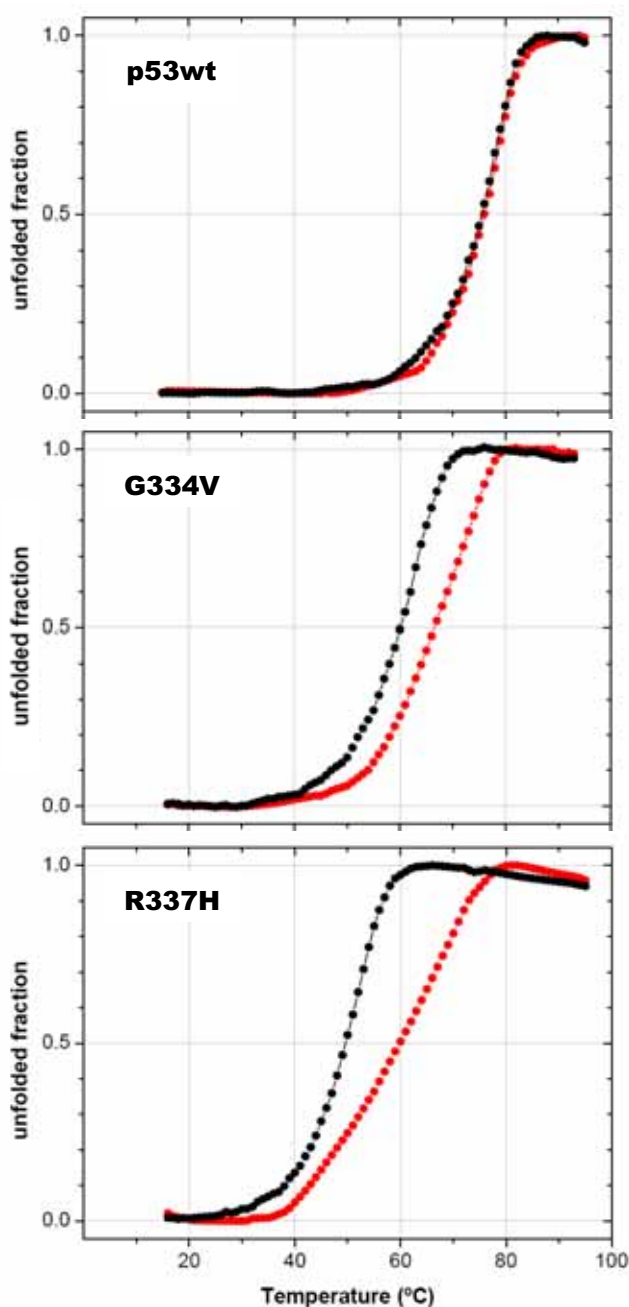
Table 2.1. Thermal stability as T_{05}

	T_{05} DSC [a]		T_{05} CD [b]	
	P	+8eq L	P	+8eq L
p53wt	84	85.5	75.5	76
R337H	61.5	75.5	49.5	60
G334V	-	-	60	66

[a] 100µM monomer; T_{05} at which ½ ΔH_m.

[b] 10µM monomer; T_{05} at which the f_u is ½

Figure 2.6. CD melting curves of 10µM (monomer) p53wt, R337H and G334V, free (black) and in the presence of 20µM calix4bridge (red) (water at pH 7.0, heating at 90ºC/h). Due to the detection limits of the dichrograph, no further ligand excess could be accurately recorded.

In addition, circular dichroism also reported about the effects of the ligand on the secondary structure of the protein (**Figure 2.7**).

For p53wt, the presence of calix4bridge did not affect the CD profile at all. For mutant R337H, at 20ºC, if there had been any ligand-induced structural effect, it would have been within the noise level. More evident were the modifications promoted by calix4bridge on G334V; at room temperature, the presence of ligand clearly increased the structural content for G334V, which could correlate with a shift towards a more structured species, namely, the tetramer.
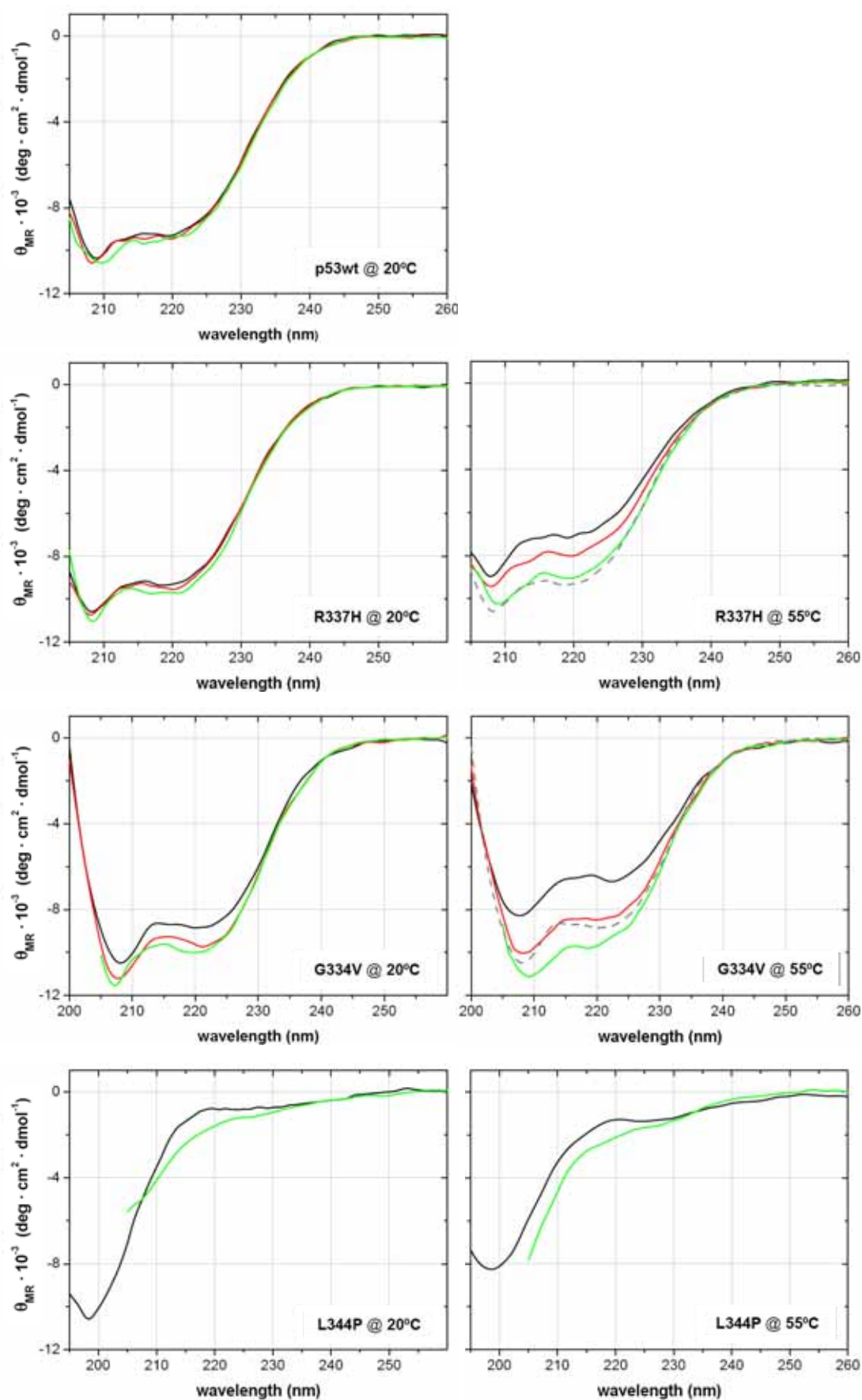
Figure 2.7. CD spectra of p53wt, R337H, G334V and L344P, free (black) and in the presence of 8eq (red) and 16eq (green) of calix4bridge, at 20ºC (left) and 55ºC (right). The grey dashed lines in the right panels, correspond to the CD spectra of the free protein at 20ºC. In water at pH 7.0, at 7.5µM tetramer.

The structural stabilization effects of calix4bridge on mutants R337H and G334V were more evident at higher temperatures (55ºC, **Figure 2.7**). Once gain, the changes for G334V were more pronounced than for R337H, although the thermal stabilization for the latter was proportionally larger (**Figure 2.6**).

Owing to the higher degree of structure of the mutant proteins when bound to the calixarene ligand, the decrease in ellipticity during the temperature scan was not linearly proportional to the number of molecules being unfolded (at least, under sub-saturating conditions); this situation was analogous to that described for the enthalpy in the distorted DSC transition peaks. Thus, the "unfolded fraction" label in **Figure 2.6** is not totally correct, and the normalization of the melting profiles in the presence of ligand (assuming a two-state transition) underestimates the real number of unfolded molecules. Consequently, the experimental temperature at which the melting curve reached its half, T_{05}, is always an overestimation of the real temperature at which half of the protein is unfolded. Nevertheless, this value was taken as a simple parameter to evaluate and compare the effects of the ligand on the thermal stability of the proteins.

Calix4bridge not only stabilized the mutant p53TD to thermal unfolding. Likewise, the calixarene stabilized the protein over time. This long term effect is clearly illustrated in **Figure 2.8**: the presence of the ligand nearly avoided the spontaneous denaturation of G334V. Therefore, the ligand did slow the denaturation process. This is a very interesting property, since the stabilization provided by the interaction with the ligand would also (potentially) prevent undesired side effects of the time-induced unfolding, such as for instance protein aggregation.
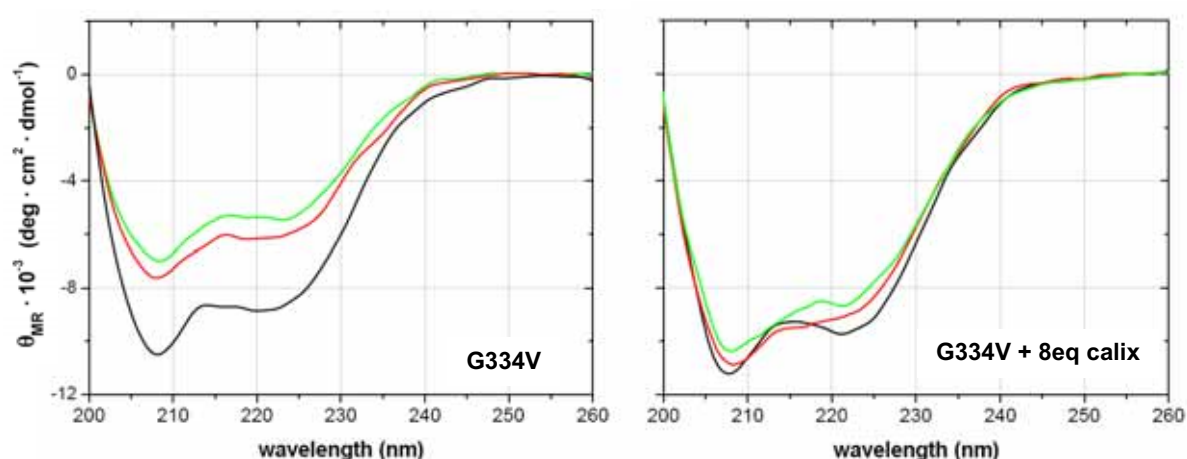
Figure 2.8. Time stabilizing effects of calix4bridge. Spectra show the evolution of G334 structure, for a sample of protein alone (left panel) and in the presence of calix4bridge (right panel), at time zero (black trace) and after 2 days (red) and 4 days (green) incubated at 37ºC. In water at pH 7.0, 7.5µM tetramer; 8eq of ligand (relative to tetramer).

The effects of calix4bridge on the unstructured monomeric L344P were also evaluated (**Figure 2.7**). As expected, the calixarene ligand did not recover any structural feature for the protein.

In conclusion, calix4bridge was only able to *stabilize* the tetrameric structure of those mutants of p53 tetramerization domain that can assemble the tetramer (R337H or G334V); hence, it could *not recover* the structural elements of the mutation L344P. This means that calix4bridge may simply function as a ligand, whose binding to the "native" protein (considering as "native" the tetrameric state), shifts the tetramerization equilibrium and thermodynamically (and kinetically) stabilizes the structure.

2.3. Structural characterization of the complex by NMR. Understanding the binding event

The thermal stabilization induced by calix4bridge on mutant p53TDs provides striking evidence of the interaction between the protein and the ligand. Unfortunately, the complexity of the system and the scarcity of experimental data render mathematical analysis impossible; only a simple qualitative description could be made. Moreover, the unfolding profiles inform on the properties of the binding at the melting temperature, which is far from the temperatures of interest (*i.e.* 20-37ºC), at which the interaction may not behave the same.

NMR was initially chosen for the structural characterization of the complex. However, the NMR spectra proved more than the plain mapping of the binding site; they also enabled estimation of the binding affinity, the kinetics and the mechanism of interaction.

2.3.1. NMR on the protein

2.3.1.1. ^{15}N-^{1}H-HSQC perturbation by calix4bridge

Chemical shift perturbation (CSP) in the ^{15}N-^{1}H-HSQC spectrum was the strategy followed to map the protein binding interface. Interaction with a ligand causes environmental changes on the protein contact surface and, hence, affects the chemical shifts of local nuclei. However, if the interaction with the ligand also promotes structural rearrangements in the protein, other nuclei out of the binding interface will also change their chemical shifts; then CSP would fail as a mapping device but is an indicator of an allosteric process.[17]

The changes induced by calix4bridge on the protein structure were determined by titrating ^{15}N-labelled protein with increasing amounts of ligand, and recording the ^{15}N-^{1}H-HSQC spectrum after each addition. The titration was carried out at 25ºC, in water, carefully adjusting the pH to 7.0 to reproduce the same conditions used for DSC and CD, although the concentration of protein was higher (125µM tetramer). Ligand was added until most of the resonances had nearly stopped moving (*i.e.* until saturation).

(a) Protein p53wt

Structural evaluation

The overlapped ^{15}N-^{1}H-HSQC spectra of several points of the titration are shown in **Figure 2.19** (page 126). For a better appreciation of the changes, only the central region of the spectrum is presented. The progressive and unidirectional perturbation experienced by some of the HSQC peaks is evident, whereas others peaks remained mainly unaltered. With the exception of a few resonances, chemical shift changes were not especially large, likely because the calix4bridge interacted with the protein side-chains and not directly with the backbone amides.

The chemical shift perturbations were quantified by considering the linear vector that connects the peak of the resonance at the beginning and the end of the titration. Applying equation [1] for each residues of the protein, and then plotting the shift versus the sequence, provided the mapping profile shown in the upper histogram of **Figure 2.9A**.

$$\Delta\delta_{NH} = \sqrt{\left(\Delta\delta_H\right)^2 + \left(\frac{\Delta\delta_N}{5}\right)^2}$$

[1]
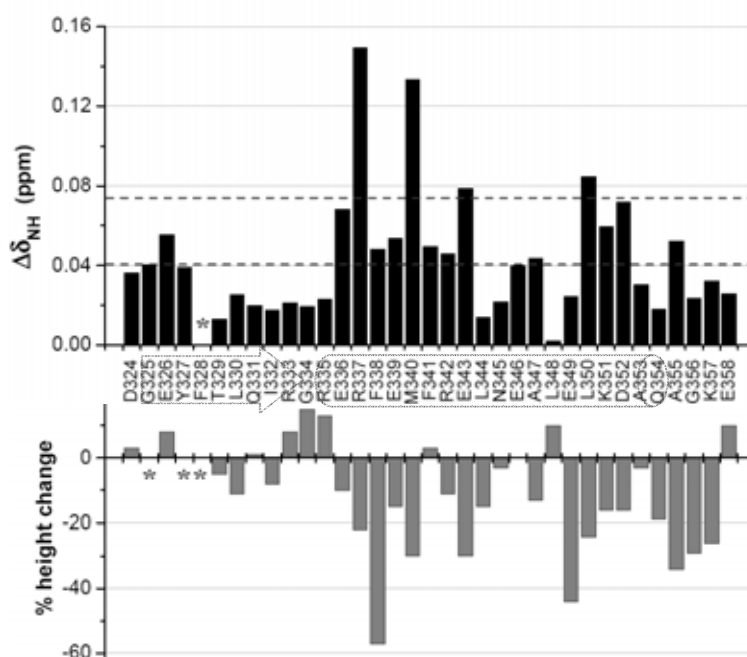
Figure 2.9. p53wt mapping at the end of the titration with calix4bridge (20eq). The upper histogram plots the ligand-induced CSP of the backbone amides, $\Delta\delta_{NH}$, for every residue of p53TD. The dashed lines drawn across represent the cutoff limits (average shift: 0.04ppm, and average shift plus one standard deviation: 0.075ppm) used to categorize the degrees of CSP for mapping the p53TD structure in **Figure 2.10**. The lower histogram represents the change in the peak height, calculated as $(h_o-h_f)/h_o \times 100$, whereby h_o and h_f are the initial and final peak heights, respectively. Asterisks mark that reliable data was not available.

For a clearer interpretation, only changes larger than the mean shift were considered significant.[18] As expected, the α-helix was much more sensitive than the β-strand –according to the model, the binding sites is defined by the four α-helixes–, and residues buried in the deep hydrophobic core of the protein (*e.g.* L344, L348, L330 or I332) were hardly effected. Interestingly, R337, M340 and E343 (*i, i+3, i+6*), all three of which directly constitute the surface of the binding site, were the most affected residues. Likewise, L350, K351 and D352, which participate in the other side of the binding pocket, were also strongly shifted.

Plotting the most affected residues on the 3D-structure of the protein (**Figure 2.10**) revealed how they perfectly outlined the pocket to which calix4bridge was designed to bind (**Figure 2.1**).
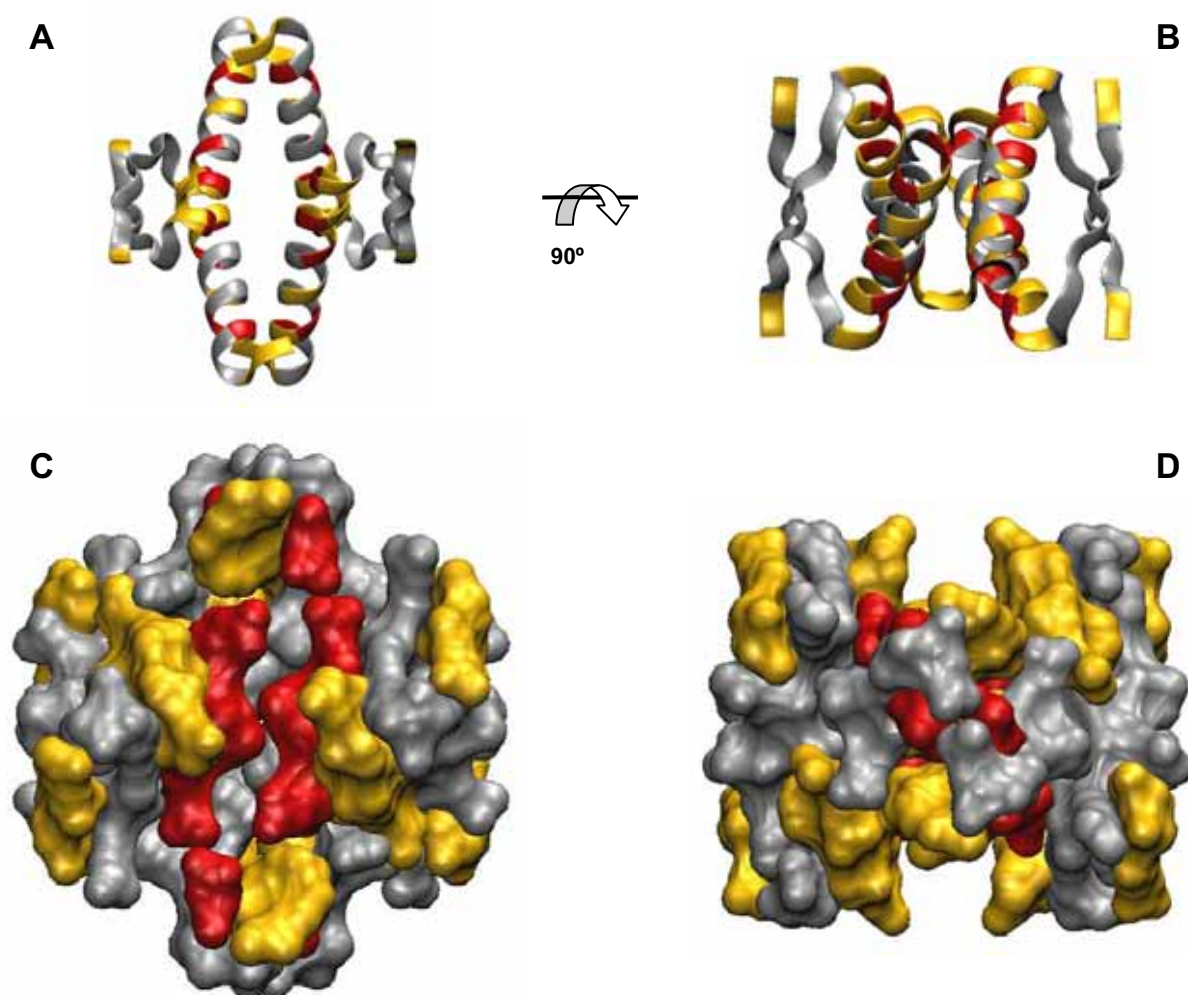
Figure 2.10. Mapping of the ligand binding site on the p53TD structure in **(A)** & **(B)** the ribbon and **(C)** & **(D)** the surface diagrams. The residues colored in red correspond to those shifted >0.075ppm, and those in orange >0.04ppm (see **Figure 2.9**). The representations at the left, **(A)** & **(C)**, show an upper view of the hydrophobic pocket; **(B)** & **(D)** illustrate the side-view.

Besides chemical shift perturbation, some resonances became slightly less intense during the titration; in fact, they became broader. This decrease did not correlate with the CSP of the peak (**Figure 2.9**), although residues within the α-helix appeared to be more sensitive.

Broadening of backbone amide signals can result from several phenomena. Changes in the relaxation time (T2) would be rather unlikely, and more residues would be similarly affected by this factor. Thus, broadening was more likely the result of changes in the kinetics of equilibrium processes. One possibility is that calix4bridge affected the amide proton exchange with water (faster exchange, broader signal). However, since the most affected residues were around the binding interface, it is more probable that the broadening directly resulted from the fast dynamic process of binding-release of the ligand.

Insights into the mechanism of interaction

The evolution of the HSQC resonances during the titration provided information beyond the protein mapping. On the one hand, the interaction was specific, since the most affected residues were within the binding pocket. And on the other hand, only one single set of resonances was detected during the titration, indicating that the complex dissociation was very fast (fast chemical exchange in the NMR time scale); hence, the interaction was likely weak ($K_D > 100 \mu M$).

Furthermore, the two-dimensional trajectories for the perturbation of the amide resonances, were linear and occurred (approximately) at the same rate for all residues (**Figure 2.12**), indicating a single binding event. Hence, should the design model for calix4bridge be correct, that would point out that the two potential binding pockets within the protein were equivalent and completely independent. Considering the symmetry, the tight packing of p53wt and the moderate changes in the HSQC spectra (and also in the CD spectra), major structural rearrangements upon interaction of the ligand could be discarded, and calix4brige binding would resemble a lock-and-key model (**Figure 2.11**).

Overall, these observations led to a conclusion of utmost importance: from the point of view of the protein, the calix4bridge did interact as it had been designed to.
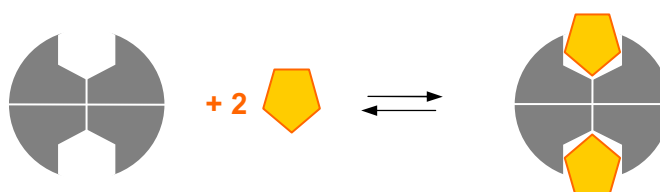
Figure 2.11. Simplified lock-and-key model for the interaction of wild-type p53TD with two molecules of calix4bridge.

Affinity

The simple description of the experimental data provided valuable information about the structure of the complex and the mechanism of interaction. Subsequent quantitative analysis allowed estimation of the binding affinity.

According to the lock-and-key model, the system p53wt - calix4bridge can be described as:

$$P_4 + 2\,L \;\leftrightarrows\; P_4L_2 \qquad\qquad [2]$$

$$K_A = \frac{[P_4]\,[L]^2}{[P_4L_2]} = K_D^{-1} \qquad\qquad [3]$$

whereby P_4 is the tetrameric protein and L the ligand.

According to the fast chemical exchange, changes in the chemical shifts, δ_{NH}, can be expressed as the weighted average between the free, δ_F, and bound, δ_B, states:

$$\delta_{NH} = f_F \cdot \delta_F + f_B \cdot \delta_B \qquad\qquad [4]$$

whereby the fractions of free, f_F , and bound, f_B, protein correspond to:

$$f_F = \frac{[P_4]}{[P_4]_T} \quad\text{and}\quad f_B = \frac{[P_4L_2]}{[P_4]_T} \qquad\qquad [5]\ \&\ [6]$$

whereby $[P_4]_T$ represent the total concentration of protein (as a tetramer).

The expression of these fractions as a function of the equilibrium constant, [3], ultimately enables determination of the affinity.

Unfortunately, from the little data available, it was not possible to work out an exact analytical solution for the resulting third order equation. The mathematical treatment could be simplified by removing the exponential factor from [L], which required the simplification of the system as follows:

$$2\,P_2 + 2\,L \;\leftrightarrows\; 2\,P_2L \quad (=\text{"}P_4L_2\text{"}) \qquad\qquad [7]$$
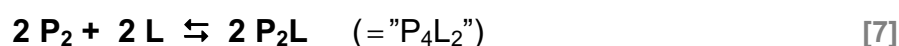
$$K_A = \frac{[P_2]\,[L]}{[P_2L]} = \frac{1}{K_D} \qquad\qquad [8]$$

$$[P_2L] = \frac{1}{2}\left(K_D + [P_2]_T + [L]_T\right) - \sqrt{\frac{1}{4}\left(K_D + [P_2]_T + [L]_T\right)^2 - [L]_T[P_2]_T} \qquad [9]$$

This simplification assumed that the protein virtually existed as dimers, and then, one dimer interacted with one ligand. Since the two binding sites were equivalent and independent, the simplification was not wrong. However, the virtual concentration of dimer was twice that of

tetramer; thus the resulting binding constant would underestimate the actual one. Nevertheless, analyzing the data under this assumption would provide a sufficiently accurate idea of the affinity between p53wt and calix4bridge, using a much simpler procedure.

The two resonances most sensitive to the presence of the calixarene, M340 and R337, were used as probes to determine the binding constant (**Figure 2.12**). The progressive perturbation for these residues, $\Delta\delta_{NH}$, was adjusted to equation [10]:

$$\Delta\delta_{NH} = f_B \cdot \Delta\delta_{NH}^f$$ [10]

thus solving equation [6] and [9]. $\Delta\delta_{NH}^f$ corresponds to the final shift, *i.e.* the vectorial distance separating the resonances of the free and bound species.
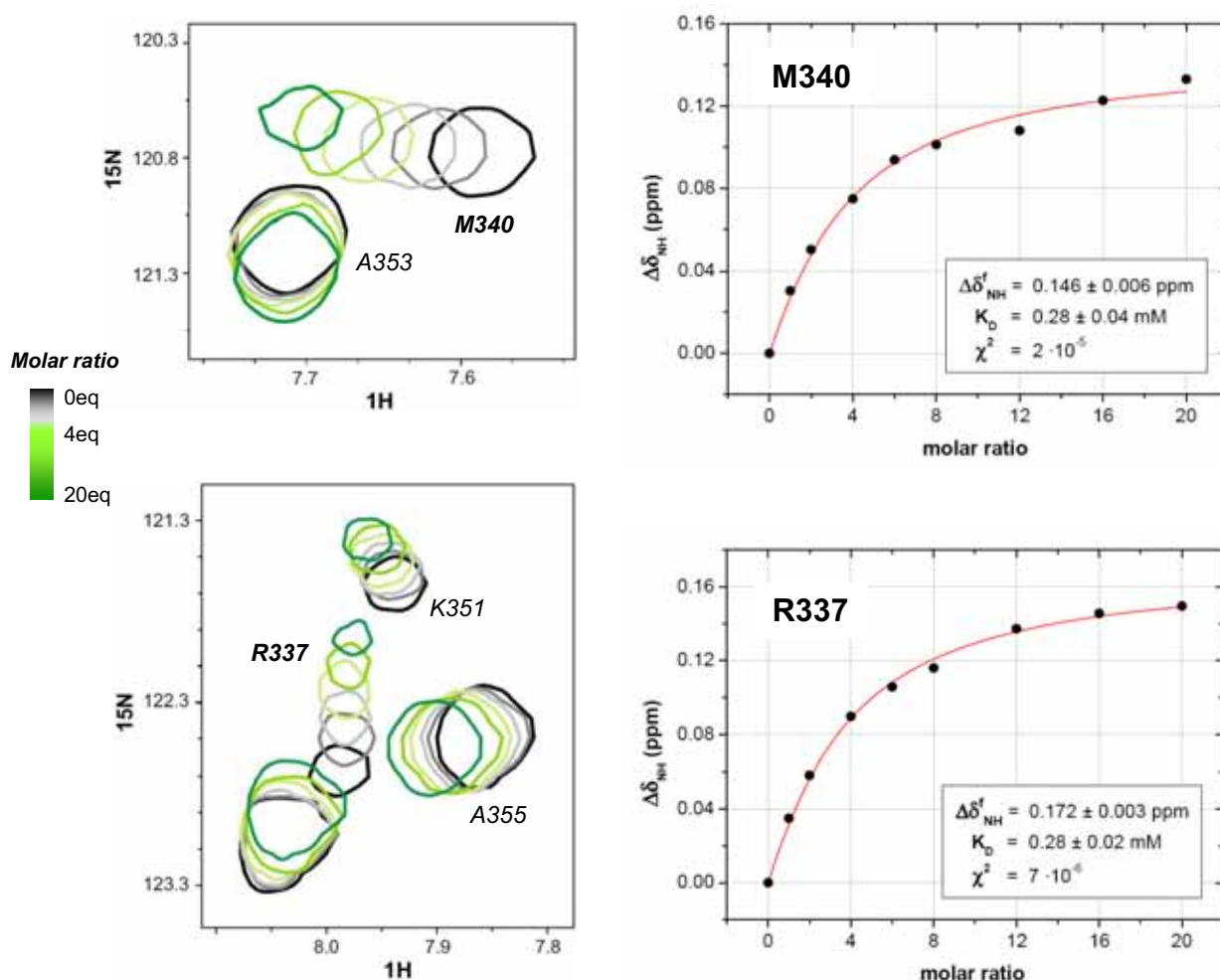
Figure 2.12. Detail of the chemical shift changes for M340 and R337 during the titration with calix4bridge (molar ratio as ligand-to-tetramer). The shifts in the resonances are plotted against the ligand added in the graphs at the right. Experimental data were adjusted to an approximate "one-to-one" binding model (see main text).

The dissociation constant obtained for both residues was 0.28±0.04mM; this is a rather low affinity and agrees with the fast chemical exchange. Moreover, this value would also be in agreement with the minor changes observed in DSC.

The titration was also run in phosphate buffer, but absolutely no changes were detected as the added calix4bridge precipitated (likely due to its interaction with the phosphate anions).[4]

(b) Mutant R337H

The evaluation of calix4bridge by HSQC on R337H revealed a completely different behavior than that described for p53wt. The overlapped spectra for the titration are presented in **Figure 2.20** (page 127), in which the non-conventional changes can be detected at first glance. The titration was performed twice, with protein from different batches, and the alterations in the spectra were perfectly reproduced, thus strengthening the reliability of the experimental data. Furthermore, any possible changes caused by dilution, contaminants, change of salt concentration or pH were ruled out because firstly, the ligand, without detectable impurities, was added lyophilized; secondly, the salts did not significantly affect the position of the HSQC resonances for R337H; and lastly, despite working in water, the pH was scrupulously controlled.

The evolution of the resonances during the titration was clearly divided in two stages; over 4 equivalents of ligand (relative to tetramer), the changes corresponding to the second step became predominant. Interestingly, not all the resonances evolved in the same way during the two stages, although neighboring residues in the protein sequence displayed similar behavior. Moreover, residues located within the β-strand, they all behaved the same. As an example, the details for T329 and R333 in **Figure 2.13**; these residues were at first slightly (or non-) shifted in one direction and changed the course sense in the second stage. The global shift was always small. This behavior was not unique to the β-strand; it was also detected in some residues within the α-helix, although their initial shifts were slightly larger (*e.g.* E336 in **Figure 2.13**). Other resonances from the α-helix, whether shifted or still, all vanished at the end of the first stage, and most of them could not be later re-identified with any of the new resonances emerging during the second stage (*e.g.* G356, M340 and E343 in **Figure 2.13**).

Since resonances did not present a continuous shift towards the final position, no clear mapping of the protein was possible at the end of the titration, although it could be done for the first stage, before the peaks completely disappeared (**Figure 2.14**). Residues within the α-helix were more sensitive to shift than those in the β-strand during the first stage. Interestingly, the most affected residues at this point were all close to the binding pocket (considering that defined for p53wt). It is worth mentioning that residues L344 and L348, located in the deep core of the helix bundle (at least they are there in the wild-type protein structure) were not shifted at all.

A general feature of the whole spectrum was that the intensity decreased during the first stage (the α-helix again being more sensitive, **Figure 2.14**), and was then recovered in the second stage. However, the recovery was not complete and the spectrum at the end of the titration was about a quarter less intense than it was initially (**Figure 2.13**).
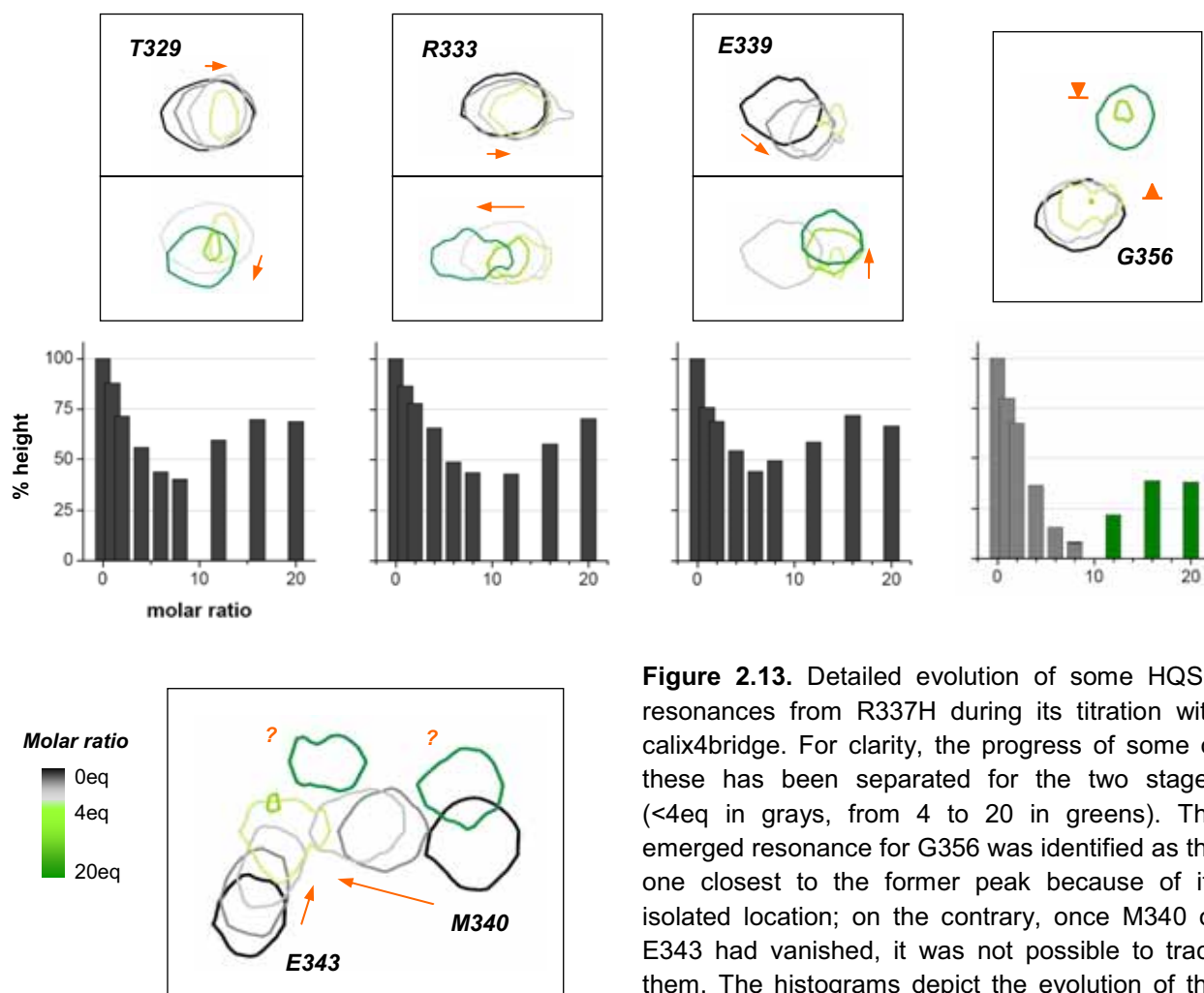
Figure 2.13. Detailed evolution of some HQSC resonances from R337H during its titration with calix4bridge. For clarity, the progress of some of these has been separated for the two stages (<4eq in grays, from 4 to 20 in greens). The emerged resonance for G356 was identified as the one closest to the former peak because of its isolated location; on the contrary, once M340 or E343 had vanished, it was not possible to track them. The histograms depict the evolution of the peak height.

The unlike evolution exhibited by the R337H resonances in the presence of calix4bridge clearly reflected that the mutant and the ligand interacted via a different –and probably more complicated– mechanism than the simple lock-and-key model described for p53wt. The two stages detected in the titration progress required, at least, two processes, each of which probably corresponding to the sequential binding of a molecule of ligand. That no clear singly-bound intermediate (P_4L) could be detected, and that several resonances were relocated in unidentified positions, further suggested a more intricate recognition mechanism, which implied conformational rearrangement that did not affect the whole structure at the same rate.

The decrease in intensity and the relocation of residues within the binding site (*i.e.* the α-helix) could be justified considering the binding of a first ligand, in a fast chemical exchange, followed by a second binding event, in a chemical slow exchange. Hence, the binding of the two molecules of ligand would be sequential and likely cooperative, since the binding of the first one (fast off-rate)

enhanced the affinity for the second one (slower off-rate)[a]. Thus, the structural rearrangements promoted by the first ligand should be important; this would be supported by the relatively large shifts experienced by some of the resonances within the binding site during the first stage (*i.e.* M340, **Figure 2.13**). A few resonances were slightly shifted after re-emerging, which could be explained by minor structural rearrangements taking place after binding of the second ligand.
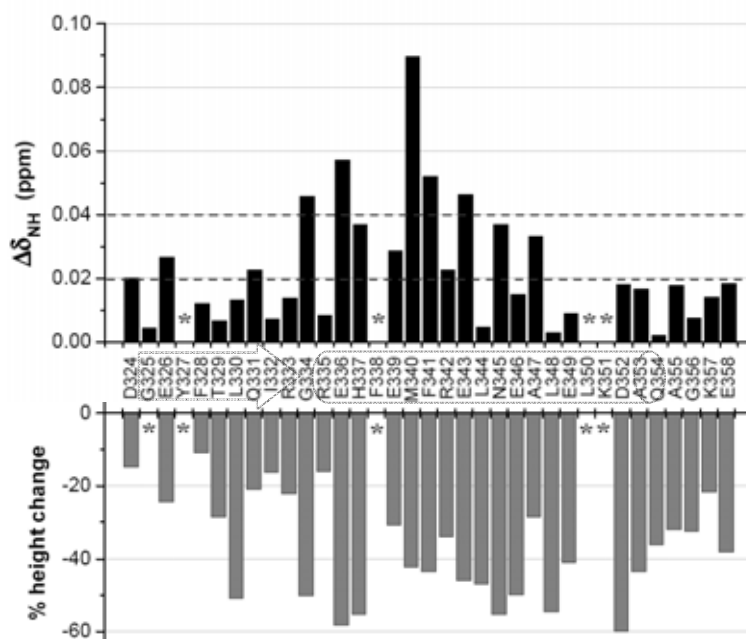
Figure 2.14. Mapping of R337H in the presence of 2 equivalents of calix4bridge (relative to 125µM tetramer).The upper panel plots the ligand induced CSP of the backbone amides, $\Delta\delta_{NH}$ (mean: 0.02ppm, mean + one standard deviation: 0.04ppm). The lower panel represents the change in the peak height. Asterisks mark residues for which confident data was not available due to overlapping.

In addition, residues far from the binding site –namely, those from the β-strand– also experienced changes, although these were minor. The two stages in which they evolved would correlate well with the two sequential binding events, each promoting different structural rearrangements.[17] For these residues, however, both events occurred continuously in the fast exchange regime. This would not contradict the mechanism suggested above, but would indicate that changes in the protein structure occurred at different rates. In other words, changes experienced by the β-strand residues were not consequence of the direct ligand contact, but from the structural rearrangements occurring when the ligand interacted with the binding site. Thus, the fitting of the second ligand molecule into the binding pocket (in a slow exchange) would not "immediately" affect the outer parts of the protein; instead the "latter" structural rearrangement would be detected. Owing to the

---

[a] The kinetics of a chemical exchange in the NMR time scale not only depend on the k_{off} but also on the magnitude of the shift experienced by the resonance. For the present case, in the first stage, even those resonances with large CSP (*e.g.* M340) displayed a fast exchange, and therefore, a fast off-rate; whereas for the second stage, the change of location was not always associated to large shifts (*e.g.* G356), and therefore, it indicated a slow off-rate.

moderate shifts in these resonances, the structural changes induced by the ligand appeared to be minor at the outer surface (far from the binding site).

The decrease in intensity and the broadening of most of the peaks in the HSQC spectrum would agree with the structural rearrangements promoted by the ligand binding (*i.e.* the existence of multiple equilibria, some of which also affected the conformation).[19]

The hypothetical mechanism for the interaction of calix4bridge with R337H is plainly represented in **Figure 2.15**: the binding of the first ligand molecule, in the fast exchange regime, induces structural rearrangements in the second binding site, thus facilitating the binding of the second ligand. In turn, the second ligand would also promote rearrangements, although these would not be sensed equally throughout the structure.

Regarding the affinity, the complexity of the system did not enable ready calculation of the thermodynamic constants for each of the processes (since these were different for each residue[b]). The affinity of calix4bridge for R337H was certainly higher than that estimated for p53wt (K_D ~280µM). For the first binding, the dissociation constant, K_{1D}, was within the fast-medium exchange rate, thus it should be probably in the range of ~50-100µM (or higher, since the second binding is shifting the first). For the second binding, the affinity increased such that it resulted in a slow exchange regime; hence, the dissociation constant K_{2D} might be <50µM.[c] These values would be logical with the DSC biphasic transition, although this behavior might change at higher temperatures.

The question then arising was why the interaction of calix4bridge with R337H differed so much from that with p53wt. First, it must be noted that the side-chain of R337 in the wild-type protein is directly involved in the binding pocket; hence, the mutation R337H affects –for better or worse– the biding site. Second, the mutant protein does not form a tightly packed tetramer as the wild-type does (at least, the mutant is not as stable to thermal unfolding), and this might also condition the binding. Conformational plasticity might help R337H in forming a better pocket and thus, establishing tighter interactions with the bound ligand. That would explain why R337H experiences structural rearrangements (likely minor) upon interaction with the ligand, whereas the inflexible p53wt does not.

It also should be pointed out that the protonation of the H337 side-chain in R337H might also contribute to the changes in the structure. The binding of calix4bridge to the tetramer might enhance the tendency of this residue to be protonated; this would further stabilize the tetramer but also would promote certain changes in the conformation.

---

[b] NMRKIN is a program which simulates line shapes from 2D spectra of proteins upon ligand binding; through iterations the program can determine the kinetic constants for the several processes that occur;[20] unfortunately the software is not open to the public domain, and even so, it requires computational calculations outside of the scope of this work.

[c] It must be mentioned that when structural changes occur, the affinity may not be properly reflected in the exchange regime observed in the spectra. Nevertheless, the estimated values should be a close approximation.
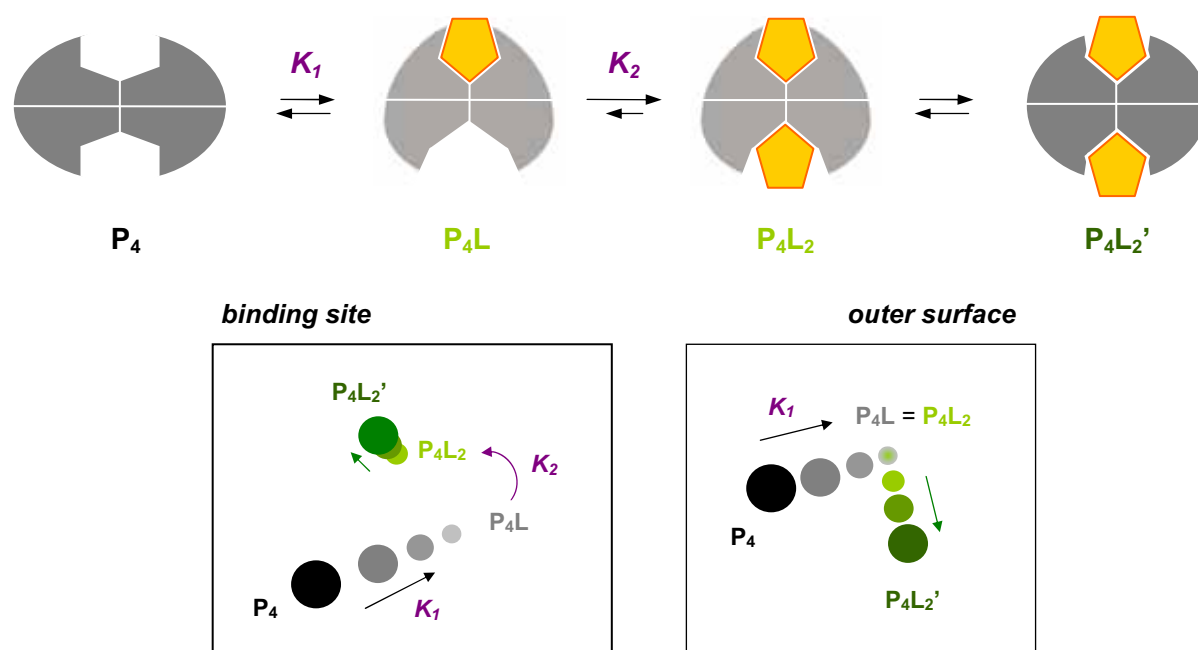
Figure 2.15. Hypothetical mechanism for the intricate binding of calix4bridge with R337H, whereby K_1 and K_2 correspond to the sequential and cooperative binding of two molecules of ligand, followed by structural rearrangements. The lower panels show the evolution of the HSQC resonances of a residue within the binding site (left), which is interacting directly with the ligand, and that of a residue on the outer protein surface (right), only affected by minor structural rearrangements.

(c) Mutant G334V

The changes in the spectra of G334V during its titration with calix4bridge had little to do with those previously described for p53wt and R337H (**Figure 2.21**, page 128).
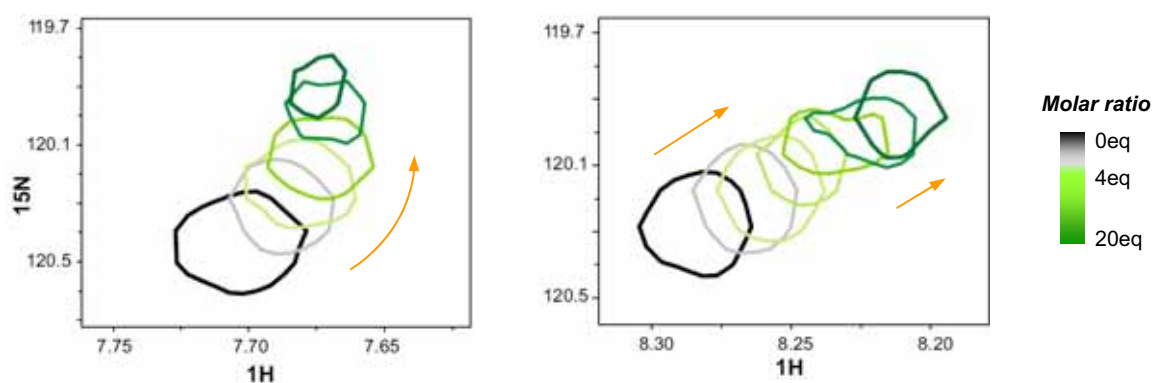
Figure 2.16. Detail of the evolution of two resonances of G334V during the titration with calix4bridge

Close inspection of the HSQC spectra reveals that the shift for many resonances was not unidirectional but rather curved (**Figure 2.16**). For some resonances, it was even possible to detect a new peak emerging next to the former one. The "inflexion" point, at which differences in the initial behavior were detected, was *ca.* 8-12 equivalents of ligand (relative to tetramer). For some of the most shifted resonances, a decrease in the intensity (*i.e.* a broadening of the peak) was also appreciated, although this was not uniform throughout the titration.

Unfortunately, the HSQC spectrum of G334V could not be assigned, and therefore, no mapping was possible. Even so, the changes in the resonances provided valuable information for understanding the interaction mechanism.
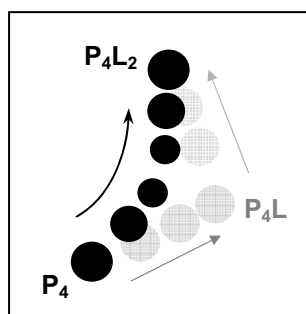

Evidence of a second binding event was found from the curvature of some traces, together with the anomalous broadening observed for several resonances. Curvature arises when a resonance experiences shift changes due to both "primary" and "secondary" binding events, in the fast chemical exchange range (see illustration at the left). This can lead to either a distinct kink in the HSQC traces or a smoother curvature, depending on the difference in affinity for the two bindings. By chance, of course, the second interaction may shift the HSQC peak in the same direction as the first one. For those cases, an indication of a second interaction is given by an exchange broadening for the resonance.[21]

Owing to the symmetry of the protein, the "secondary" binding event should depend on the "primary" one: these would be sequential. One hypothesis is that the interaction with the first molecule of calix4bridge would induce a slight structural rearrangement that would in turn affect the second binding site, and thus its affinity (**Figure 2.17**). Hence, in contrast to p53wt, the G334V binding sites would not be either completely equivalent or independent. This situation would resemble that of R337H; however, the affinity of calix4bridge for G334V was notably lower.

Figure 2.18 shows in detail a resonance (named "M", see **Figure 2.21**) that evolved rather unidirectionally. Its chemical shift perturbation was traced and, at first sight, it seemed to depict a "conventional" saturation curve. Actually, it fit considerably well the model proposed for p53wt of two equivalent and independent binding sites (equation **[7]**), resulting in a large K_D, ~0.5mM, as expected for a fast exchange. However, other resonances, even if they showed linear-like shifts, did not depict a single saturation curve at all, which correlated well with having two binding events. In any case, and despite the fact that numbers could not be properly calculated[d], it did seem that the affinity of calix4bridge for G334V was lower than for the other proteins studied.

---

[d] Changes in resonances were not uniform. Despite the fact that several of them were analyzed with a 2-binding-site model, the fittings usually did not converge and, if they did, the values were too uncertain. Computational analysis of the broadening of HSQC resonances could help in determining the kinetic constants; however the equations to be solved require computational algorithms which are outside of the scope of this thesis.[21,22]
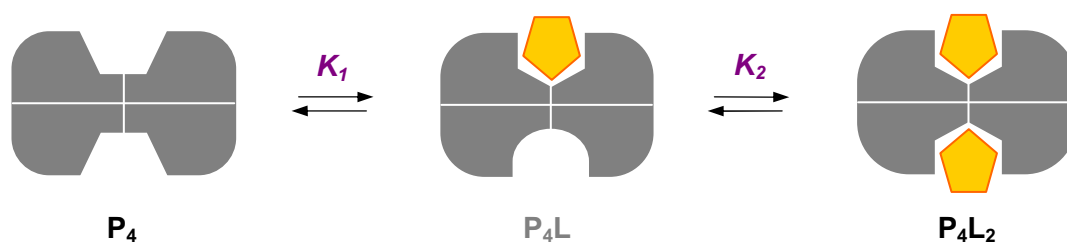
Figure 2.17. Hypothetical mechanism for the interaction of calix4bridge with mutant G334V

Contrariwise to R337H –whose less packed structure was suggested to contribute positively to its interaction with the ligand–, for G334V the same less packed structure could actually be the reason for its less efficient interaction with the ligand. The valine mutation at the hinge of the monomer presumably leads to a "wider" conformation of the protein. Therefore, the binding site for the calixarene ligand (*i.e.* the dimensions of the protein cavity) might not be as "adequate" as it should: the pocket might be too large, causing the ligand to fit loosely and thereby preventing tight interactions (whether by hydrophobic contacts or by chelation of the guanidinium groups to the carboxylates on the protein surface).
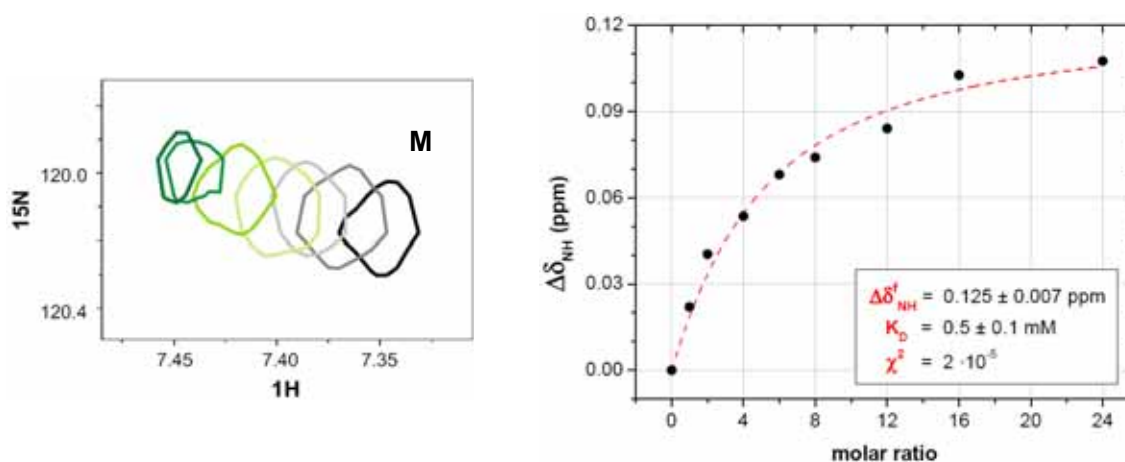

Figure 2.18. Progress of resonance "M" of G334V upon addition of calix4bridge. Its "unidirectional" shift was mathematically adjusted to the 2 equivalent and independent binding sites model proposed for p53wt. Despite the good fitting, the real trend of the shifts was that of two non-equivalent binding sites.
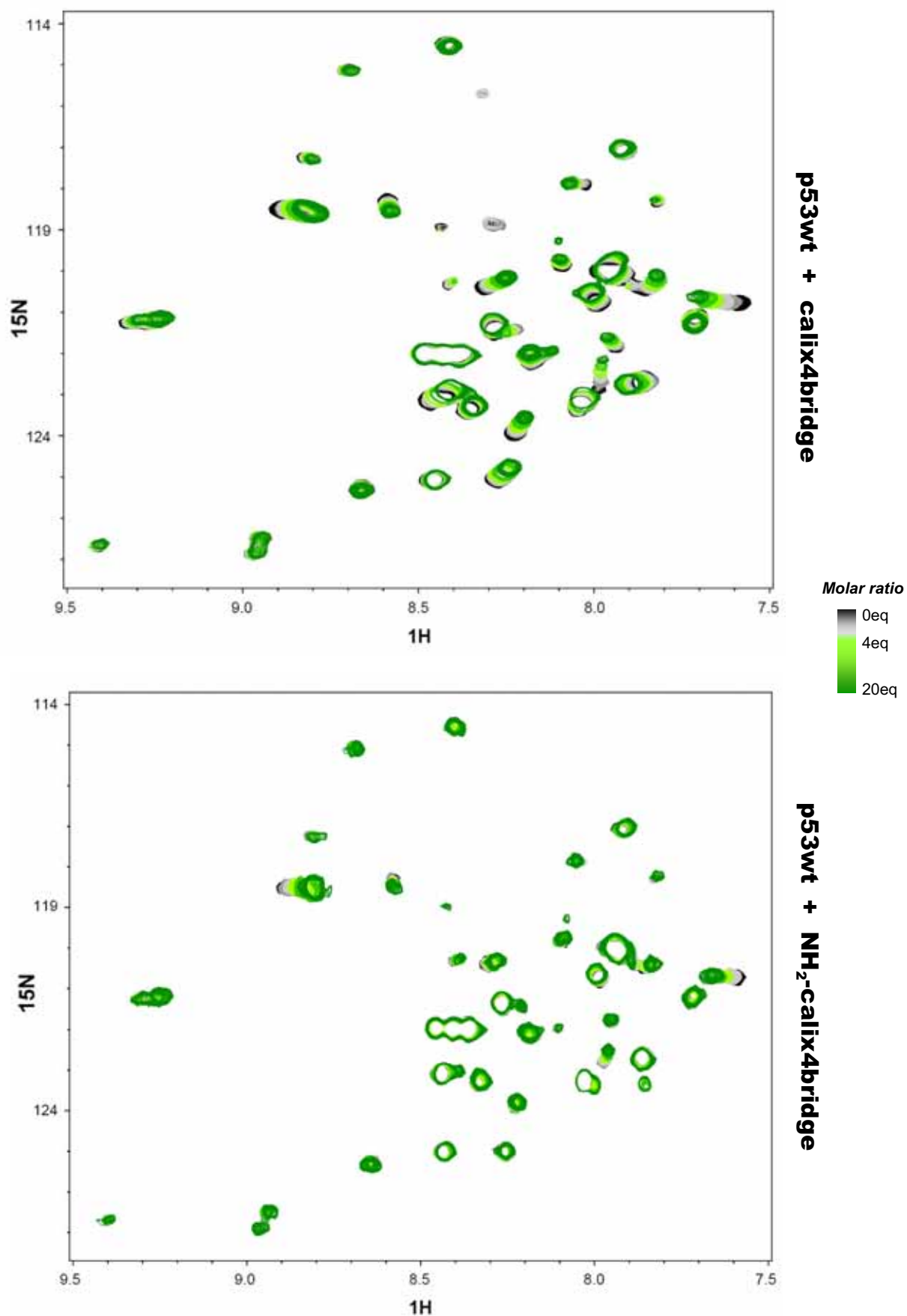
Figure 2.19. ^{15}N-^{1}H-HSQC overlaid spectra of the titration of 125μM ^{15}N-p53wt with calix4bridge (top) and NH$_2$-calix4bridge (bottom), in water at pH 7.04, 298K. Molar ratios consider the tetrameric protein.
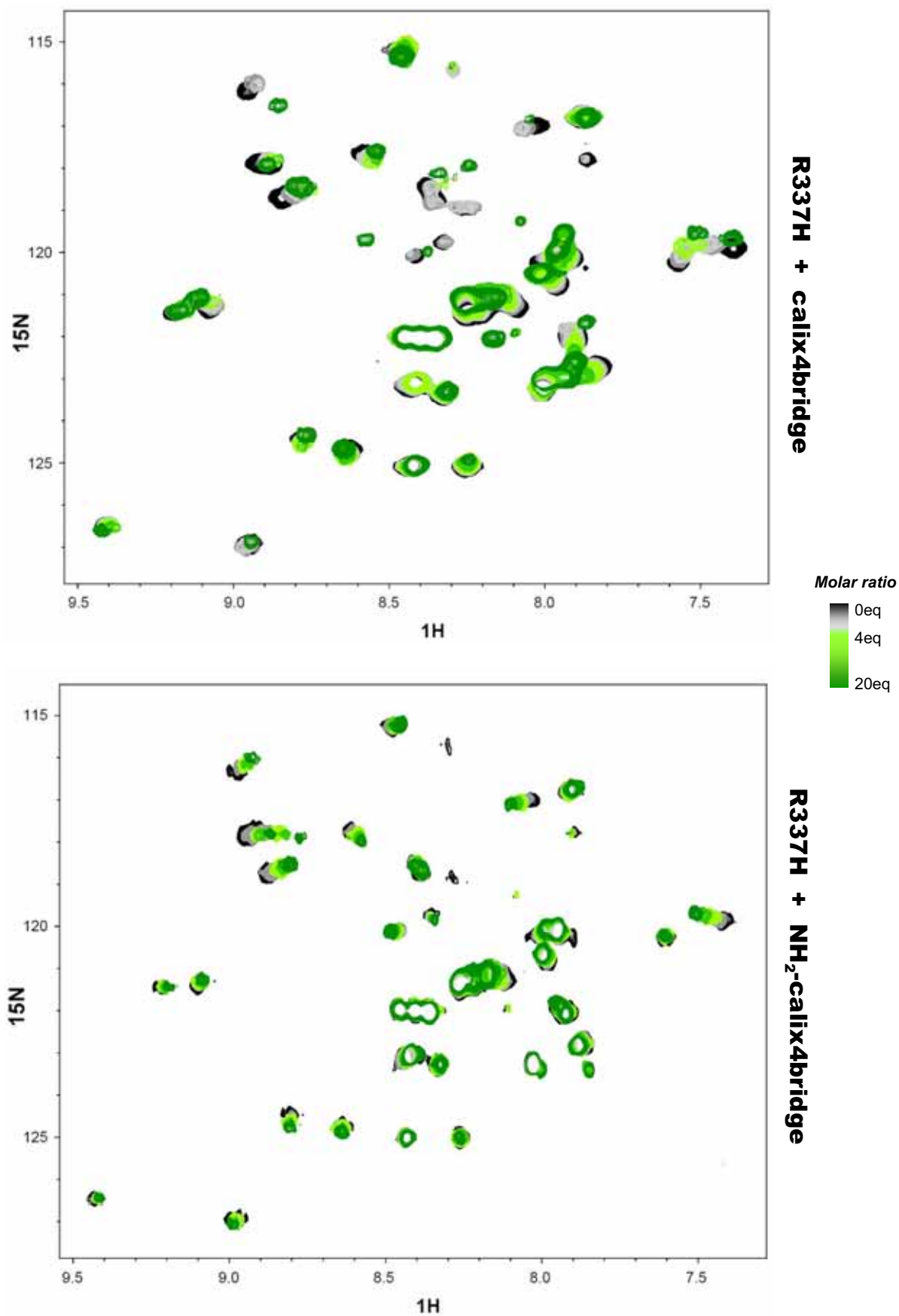
Figure 2.20. ^{15}N-^{1}H-HSQC overlaid spectra of the titration of 125μM ^{15}N-R337H (tetramer) with calix4bridge (top) and NH$_2$-calix4bridge (bottom), in water at pH 7.04, 298K. Molar ratios calculated over tetramer.
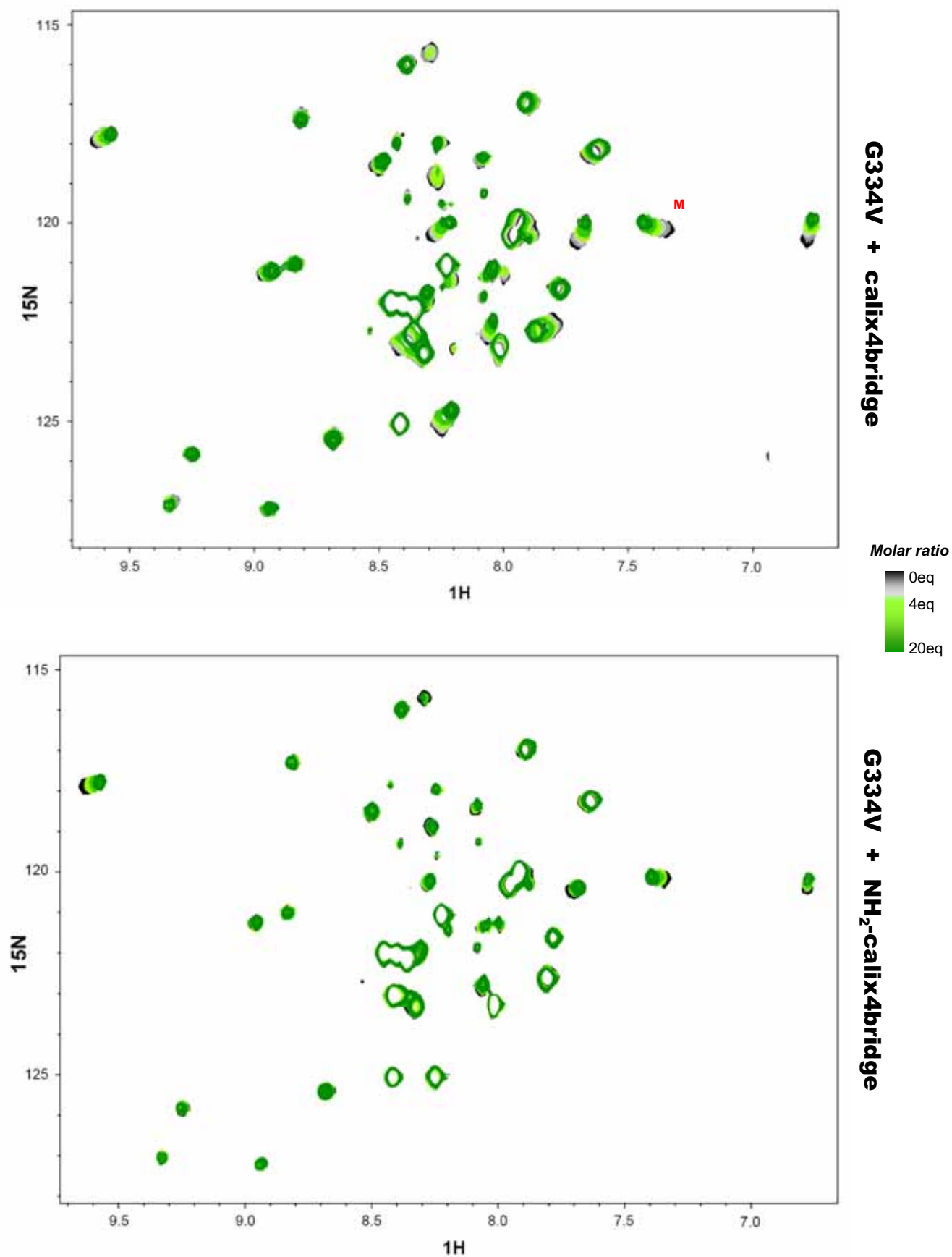
**Figure 2.21.** ^{15}N-^{1}H-HSQC overlaid spectra of the titration of 125μM ^{15}N-G334V with calix4bridge (top) and NH$_2$-calix4bridge (bottom), in water at pH 7.04, 298K. Molar ratios consider the tetrameric protein.

2.3.1.2. NH$_2$-calix4bridge by ^{15}N-^{1}H-HSQC perturbation

The guanidinium group is a key player in molecular recognition processes, and testament of that is how much wise Nature uses arginine at protein interfaces.[23,24]

In order to assess the contribution of the guanidinium groups in the binding of calix4bridge to the protein, the four guanidinium moieties were replaced by amino ones, thus resulting in the 5,11,17,23-tetraaminomethyl-25,26-27,28-biscrown-3-calix[4]arene, named **NH$_2$-calix4bridge** for shorter.
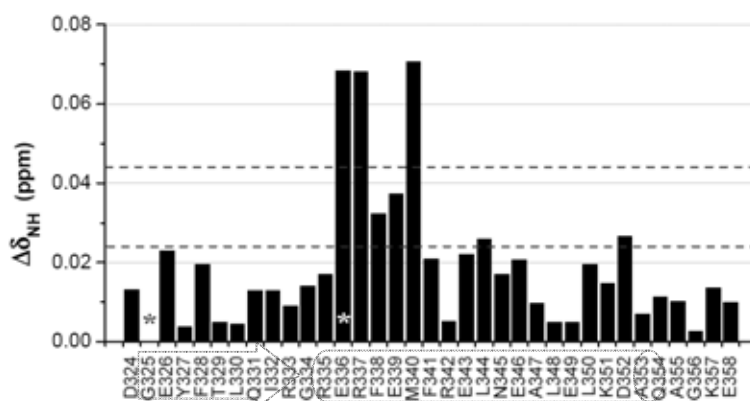

NH$_2$-calix4bridge
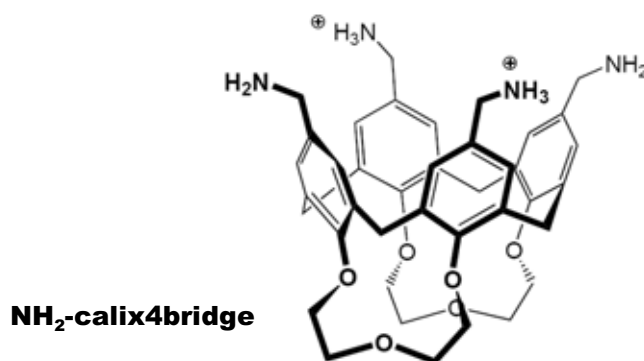
If the amino groups of this calix[4]arene were protonated, they would also establish hydrogen bonds with the carboxylates. However, since amino groups are less basic than guanidinium ones, probably not all the amines will be charged at the working pHs,[4,25] thereby reducing a source of ligand anchoring. Moreover, the amino group also decreases the length of the hanging "branches" in the upper-rim, and they might become too short as to interact efficiently with the carboxylate moieties. In addition, the interaction between an amino group and a carboxylate also misses the ability to chelate and adopt the aromatic-like disposition of the guanidinium-carboxylate couple.

The effects of the amino-version **NH$_2$-calix4bridge** were structurally evaluated by NMR, under the same conditions described for calix4bridge (water at pH 7.0, 298K).

(a) Protein p53wt

The changes in the HSQC spectra of the wild-type p53TD during the titration with NH$_2$-calix4bridge were basically the same than those described for the guanidinium ligand, but the shifts achieved with the same amount of ligand were smaller and still far from saturation (**Figure 2.19**).

Resonances M340 and R337 were again the most sensitive ones (**Figure 2.23**, compare with **Figure 2.12**). Their perturbation was adjusted to the approximate model for one-ligand-to-one-dimer (equation **[7]**), and resulted in a dissociation constant *ca.* 1mM. This value was in total agreement with the shorter changes. The large decrease of the affinity –nearly four times lower– further underscored the important role played by the guanidinium groups in the interaction with p53wt.

Figure 2.22. p53wt chemical shift mapping upon addition of 16 equivalents of NH$_2$-calix4bridge (mean shift: 0.024ppm, and mean shift plus one standard deviation: 0.044ppm)
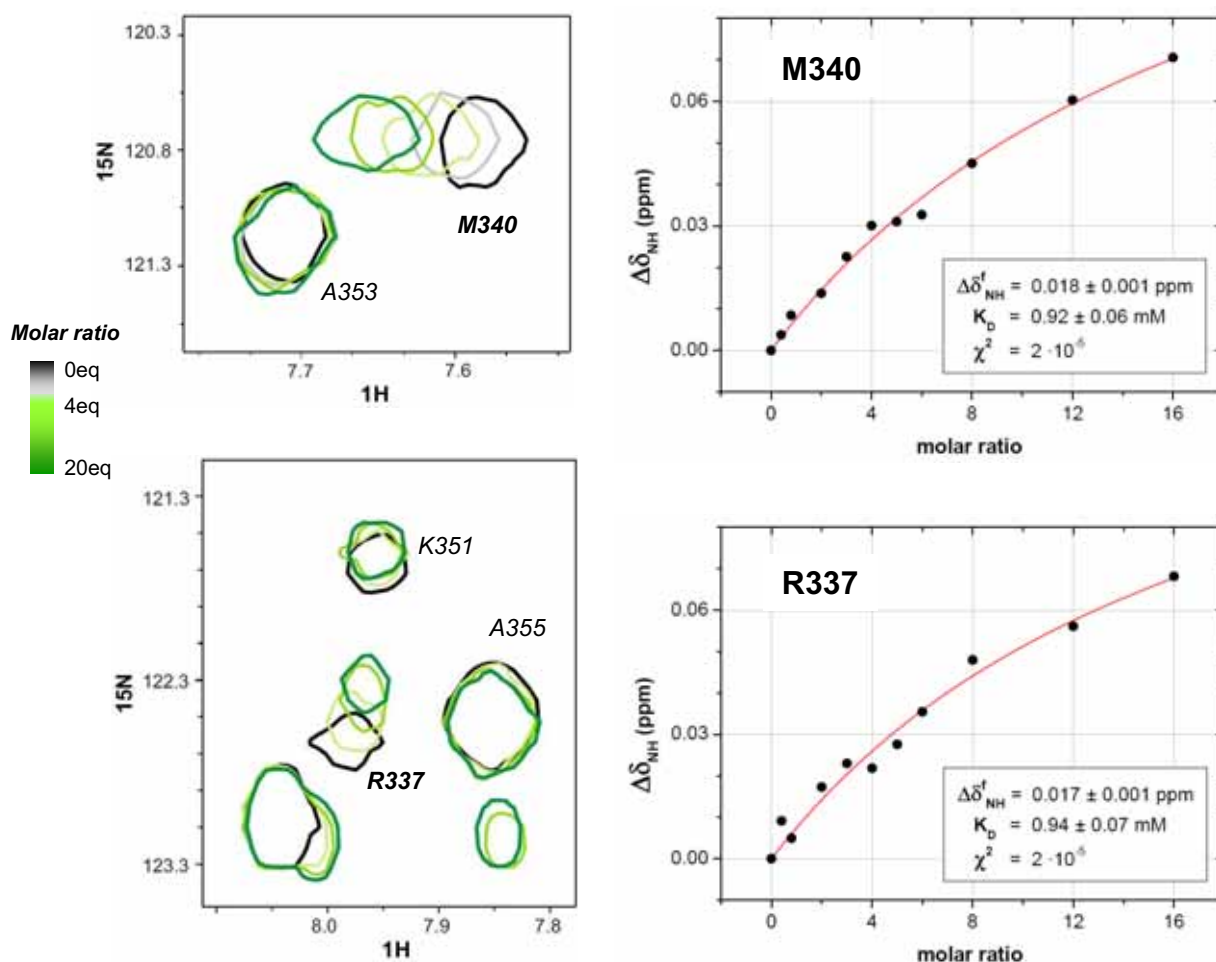

Figure 2.23. CSP of residues R337 and M340 upon addition of NH$_2$-calix4bridge, and their fit to the lock-and-key model considering 1-ligand-to-1-dimer.

The mapping of the protein at the end of the titration with NH_2-calix4bridge (*i.e.* 16eq of ligand, still sub-saturating conditions) was the same than for calix4bridge, but the mean shift was the half (~0.024ppm, **Figure 2.22**). The minor differences in the mapping profile between both ligands could be due to the large experimental error of the small shifts for NH_2-calix4bridge.

(b) Mutant R337H

The HSQC spectra of mutant R337H in the presence of NH_2-calix4bridge evolved in a completely different way to that the described for the tetraguanidinium calix4bridge (**Figure 2.20**). The resonances were only shifted unidirectionally during the titration, and their intensity was hardly affected. The mapping profile for R337H (**Figure 2.24**) was strikingly similar to the mapping of R337H during the first stage of the titration with calix4bridge (**Figure 2.14**). In fact, most of the resonances showed the same shifting direction (**Figure 2.25**, compare with **Figure 2.13**), although for some residues the length of the preturbation was now larger. Interestingly, resonances which shifted and disappeared in the first stage of calix4bridge titration (*e.g.* M340), now covered shorter distances and their intensity was unaltered.
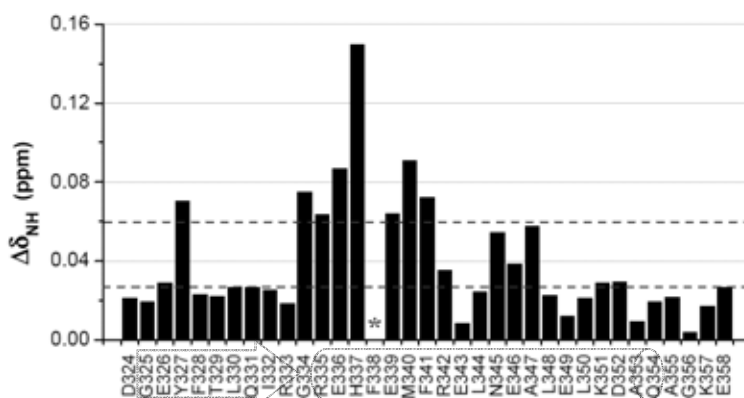
Figure 2.24. CSP mapping of mutant R337H in the presence of 20eq of NH_2-calix4bridge (relative to 125µM tetramer). The dashed lines mark the mean shift: 0.03ppm, and the mean shift plus one standard deviation: 0.06ppm. * marks that no reliable data was available.

From the HSQC spectra it appeared that NH_2-calix4bridge was not able to promote on R337H the structural rearrangements described for calix4bridge. The reason might be the lower affinity displayed by the amino-ligand, although two possible models could justify the experimental data.

On the one hand, the affinity of the amino-ligand was so low that it might be only possible to detect one single binding event; hence, without guanidinium groups, the ligand would not stabilize or promote the new conformation on the protein for the second binding (**Figure 2.15**), and the changes would only correspond to the binding of the first molecule of NH_2-calix4bridge. The final species detected would be the singly-bound "intermediate" P_4L, which would markedly differ from
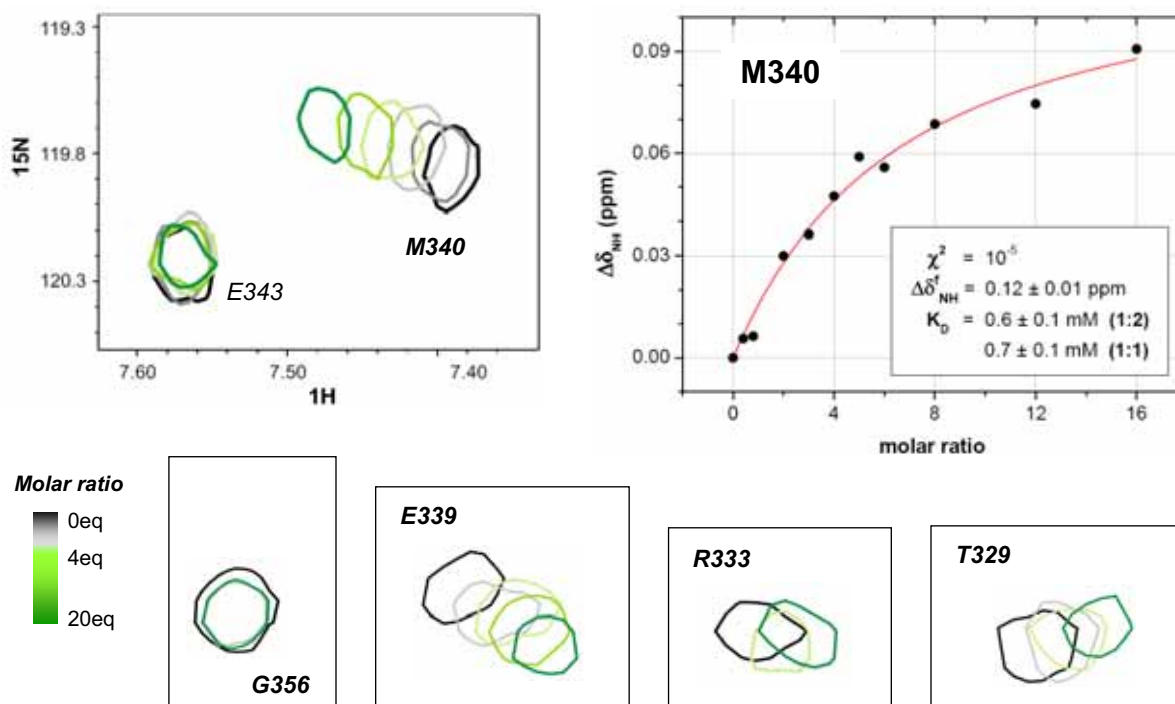
Figure 2.25. Detailed evolutions of some resonances of R337H upon addition of NH$_2$-calix4bridge (see **Figure 2.13** to compare with calix4bridge). Shifts in M340 have been plotted and fit to 1-dimer-to-1-ligand (1:2) and to 1-tetramer-to-1-ligand (1:1) models.

that of calix4bridge (**Figure 2.26**). This could explain why the shift for several residues –namely, those in the binding site– was not as large as in the first stage of calix4bridge titration (*e.g.* M340). Given that the intensity of the spectra (*i.e.* the resonance broadness) was maintained, no significant conformational rearrangements should be taking place either; however, the structure of the protein should be slightly perturbed by the first binding in order to modify the second binding site affinity.
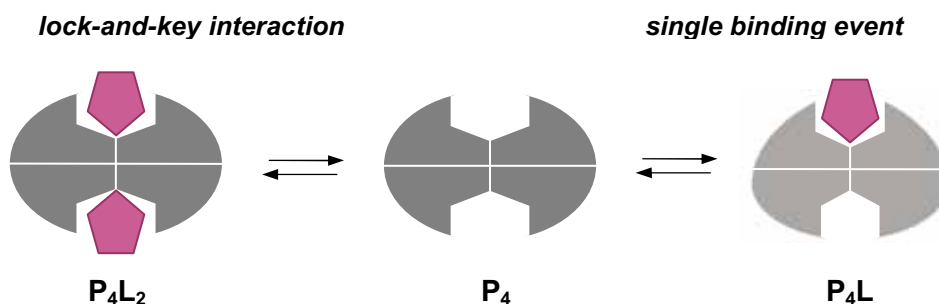
Figure 2.26. Two hypothetical mechanisms for the low affinity interaction of NH$_2$-calix4bridge with R337H.

On the other hand, a second possible mechanism might be that NH$_2$-calix4bridge bound to R337H as a lock to a key, and therefore, both binding sites for R337H would be equivalent and independent. Hence, the binding would not promote any structural change in the protein, and the reason might be again the low affinity displayed by the amino groups, which could not tightly anchor the ligand into the binding site and stabilize a new conformation (**Figure 2.26**).

The CSP of resonance M340 was taken as probe to estimate the affinity of NH$_2$-calix4bridge (**Figure 2.25**). For both hypothetical models (binding of only one or two ligands), the resulting dissociation constants were about ~0.7mM, which would correspond to a really low affinity interaction.

In conclusion, regardless of the mechanism, the crucial role of the guanidinium group in the interaction of calix4bridge with R337H was determinant, and it appeared to be the driving force that stabilized or promoted rearrangements on the protein conformation.

(c) Mutant G334V

Similar to the behavior of p53wt, the changes promoted by the interaction of NH$_2$-calix4bridge with G334V were like those described for the guanidinium-ligand, but to a lesser extent (**Figure 2.21**). In fact, the shifts were so minute that only for a small number of resonances it was possible to detect a slight unidirectional movement. The two hypotheses suggested for R337H: binding of only the first ligand molecule or a lock-and-key binding of two molecules (**Figure 2.26**), could also justify the experimental data for G334V.

Adjusting the shift of resonance "M" to the lock-and-key model (**Figure 2.27**) resulted in a dissociation constant larger than 1.5mM, which would correspond to an extremely low affinity interaction. Hence, once again, the results evidenced the vital importance of the guanidinium groups for calix4bridge interaction.
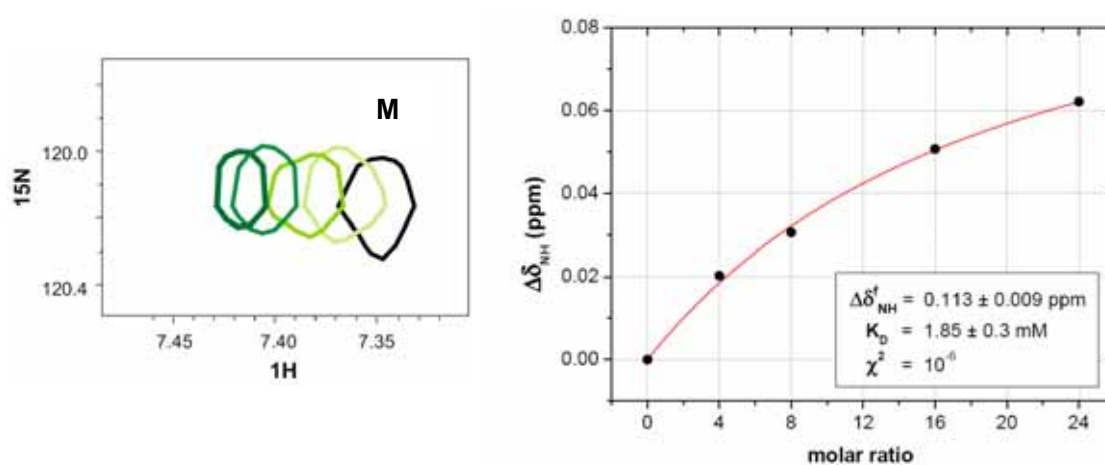
Figure 2.27. Progress of resonance "M" of G334V upon addition of NH$_2$-calix4bridge (4, 8, 16 and 24eq relative to 100µM tetramer). Shifts adjusted to the 2 equivalent and independent binding sites model proposed for p53wt.
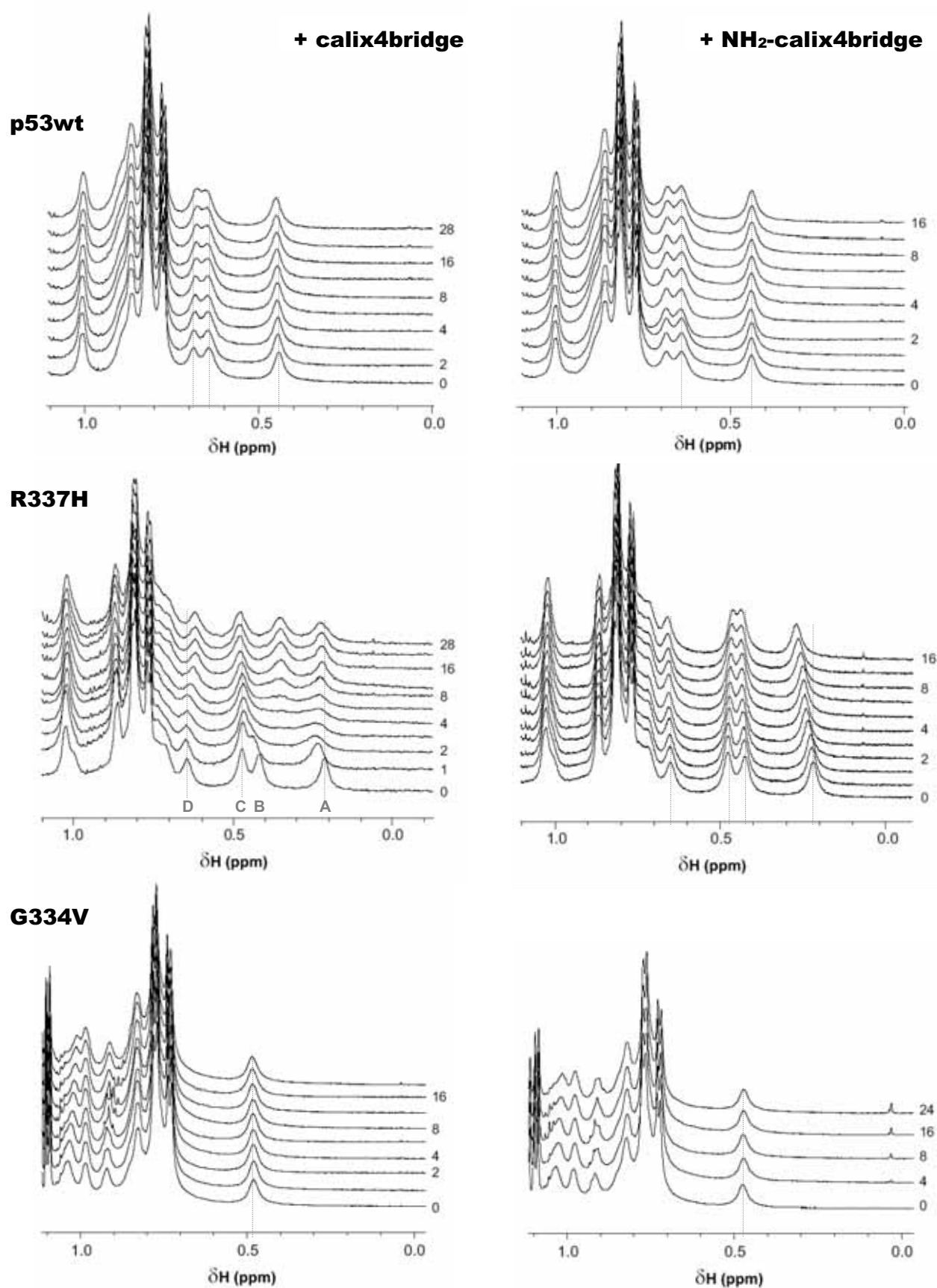
Figure 2.28. Up-field ^{1}H-resonances evolution during the titration with calix4bridge (left panels) and NH$_2$-calix4bridge (right panels) of p53wt (top panels), R337H (middle panels) and G334V (bottom panels). Ligand molar ratios (relative to tetramer) are indicated at the right of the spectra.

2.3.1.3. Up-field ¹H perturbation

The multidimensional experiments presented in the previous sections provided valuable information about the structure, the mechanism and the thermodynamics of the molecular recognition event. Further assessment of the changes experienced by the protein upon interaction with the ligand was achieved through the qualitative analysis of the ^{1}H up-field region (comprised between 0.4 and -1.0ppm). The protons close to the center of aromatic rings within the protein, could also act as sensitive conformational probes.[26-28]

Changes in the up-field ^{1}H region of the proteins upon addition of calix4bridge are shown in **Figure 2.28**. R337H was the most affected protein and, interestingly, the resonances in the up-field region displayed a parallel behavior to that described for the HSQC.

Mutant R337H has four resonances in this region (A: 0.22ppm; B: 0.43ppm; C: 0.49ppm; and D: 0.65ppm). Two stages were clearly distinguished during the titration. Through the first stage (<4 equivalents), two of the resonances (A and B) were shifted and broadened, up to nearly disappear; whereas the other two remained unaltered. The shifts were towards the down-field, which could suggest that their corresponding protons were separating from the aromatic rings. In the second stage, disappeared signals emerged again. One (presumably B) appeared in an upper-field position than formerly, and the addition of more ligand increased its intensity. The other one (A) reappeared close to where it previously was, and it was shifted backwards to nearly the free protein position; after 8 equivalents, the resonance stopped and intensified. That the resonances went back to the up-field might suggest that they returned close to their aromatic ring current. The other two resonances (C and D) only experienced a small shift between 4 and 8 equivalents. Each of the resonances was considerably broader at the end of the titration, as would correspond to the several dynamic processes occurring at the same time: interaction with the ligand and structural rearrangements.

These results strongly supported the model previously proposed for the interaction of calix4bridge with R337H: two sequential binding sites with (moderate) structural rearrangements. The conformational changes were not transforming the protein structure; rather they looked as minor rearrangements –likely from the accommodation of the ligand or from protonation events.

Contrariwise, the up-field ^{1}H resonances of p53wt and G334V were hardly perturbed. For p53wt this also supported the proposed lock-and-key model. For G334V, it would indicate that changes in the structure might not be significant, or at least they could not be detected here.

Even more interesting was to observe the effects of the amino ligand NH_2-calix4bridge in the up-field resonances. As expected from the previous results, p53wt and G334V were unaffected. For R337H changes were moderate, but evident. In agreement with the HSQC spectra, the perturbation could be justified by both mechanisms: the lock-and-key or the single binding. The comparison of the initial points of the titration of R337H with calix4bridge, with the last point of the titration with NH_2-calix4bridge (**Figure 2.29A**), nicely showed how changes in the first stage of calix4bridge binding followed the same trace than changes promoted by NH_2-calix4bridge (or *vice*

versa). Moreover, it was required four times more amino-ligand to achieve the same perturbation than with the guanidinium-calix4bridge.

The shifting of the resonance A of R337H in the NH_2-calix4bridge titration was adjusted to a one-to-one model (only one ligand interacting per tetramer, **Figure 2.29B**). The resulting dissociation constant was *ca.* 1mM; this was larger than the estimated from the HSQC shifts –probably the small shifts made the data fairly inaccurate– but still provided a good idea of the low affinity of the amino-ligand.

Regrettably, the protein up-field ^1H resonances herein analyzed were not identified, which limited the information of these data.
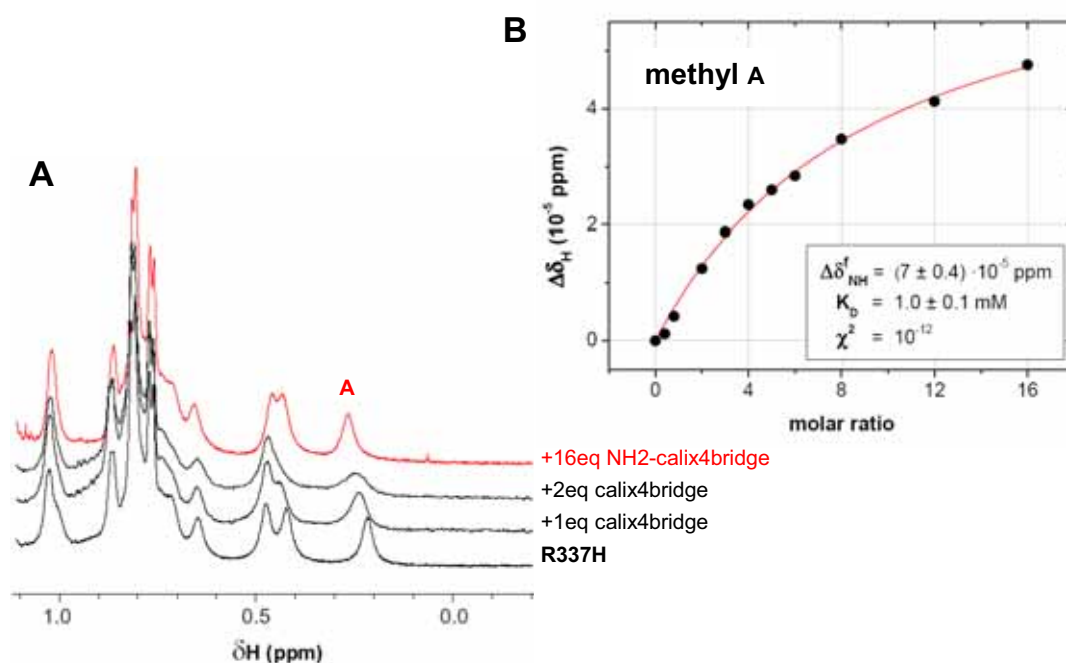
Figure 2.29. (A) Comparison of the ^1H up-field region of R337H during the first stage of calix4bridge titration and at the end of NH_2-calix4bridge titration (top red spectrum). **(B)** Chemical shift perturbation of resonance A in the up-field ^1H spectrum of R337H when titrated with NH_2-calix4bridge (see Figure 2.28).

2.3.2. NMR on the ligand

So far, NMR experiments for mapping the protein binding site confirmed that calix4bridge was binding on p53wt where it had been designed to. However, the other part of the puzzle remained to be solved: how did the ligand interact?

2.3.2.1. ^{1}H spectrum of calix4bridge

In order to analyze the changes of calix4bridge upon interaction with the protein, the assignation of the proton resonances for the free ligand was first required. Due to the conformational rigidity of the molecule, most of the protons are diasterotopic[e] and thereby distinguishable by NMR. In fact, almost every single proton could be unequivocally assigned. In **Figure 2.31** there is the detail of the identification; protons were named with a capital letter and a number; for shorter.

Since most of the calix4bridge signals were nearby the water band (~4.76ppm), the spectrum for the molecule was seriously affected if sequences with water suppression were used (*i.e.* Watergate, presat…). In **Figure 2.30**, the comparison of two spectra with and without water suppression shows to what extent the spectrum was perturbed.

This critical observation limited the experimental conditions in the NMR experiments based on the ligand resonances. Only sequences without water suppression pulses should be used; consequently, water had to be kept to a minimum and samples had to be prepared in "pure" deuterated water ("100", *i.e.* 99.99% D); otherwise, the large water band would overlap the surrounding calixarene signals.

2.3.2.2. ^{1}H chemical shift perturbation & line broadening

(a) Titrating the protein

The detailed analysis of the ^{1}H spectra acquired during the protein titration (sections 2.3.1.1 and 2.3.1.2) also provided valuable information about what happened to the ligand in the presence of the protein. Unfortunately, those experiments were recorded with the Watergate sequence, which ruined the majority of the ligand resonances. Nevertheless, by only considering the aromatic resonances –which were unaffected by the water suppression–, a great deal of information could be also obtained (**Figure 2.30**).

According to the binding model, the perfect symmetry of calix4bridge should be partially lost upon binding to p53TD, given that the binding pocket of the protein is of lower symmetry than the free ligand. Hence, equivalent protons in the free calixarene would become different upon binding, and

---

[e] **diasterotopic:** chemically equivalent but magnetically different
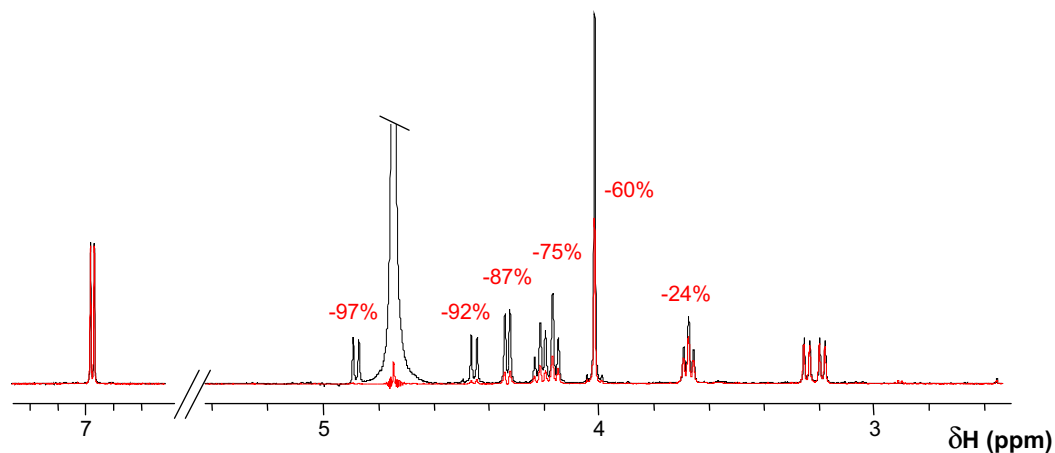
Figure 2.30. Effects of water suppression on calix4bridge ^{1}H spectrum. In black, the [1]H-spectrum (600MHz, D_2O "100"); in red, the [1]H-spectrum with Watergate suppression (600MHz, H_2O + 90% D_2O, irradiating at 4.76ppm with 54dB). Percentages indicate the degree of reduction caused by the pre-saturation sequence (spectra normalized on the aromatic resonances).
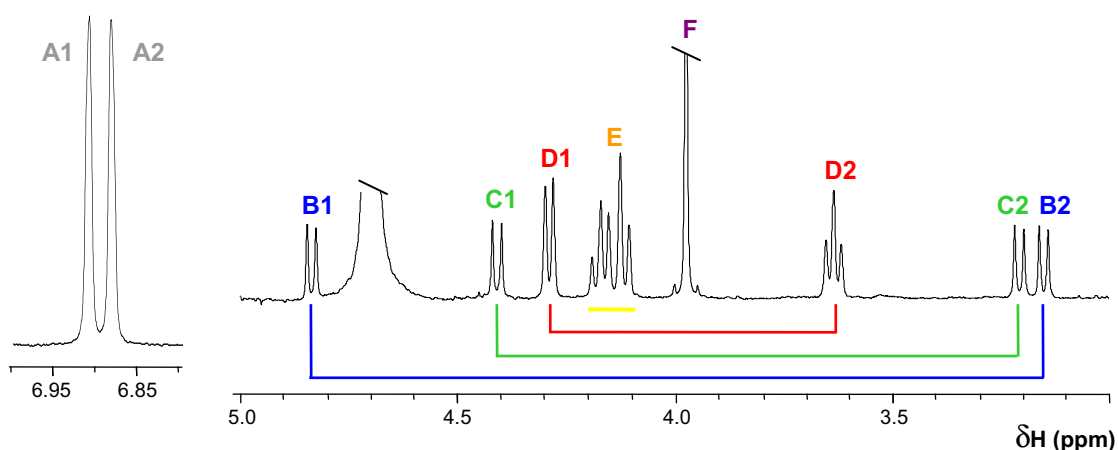
	δ_H (ppm)	J (Hz)	H
A1	6.906		4
A2	6.881		4
B1	4.834	12.2	2
C1	4.408	12.5	2
D1	4.288	10.9	4
E_{1-3}	4.169	11.8	4
E_{4-5}	4.115	10.9	4
F	3.973		8
D2	3.634	10.5	4
C2	3.208	12.6	2
B2	3.152	12.2	2
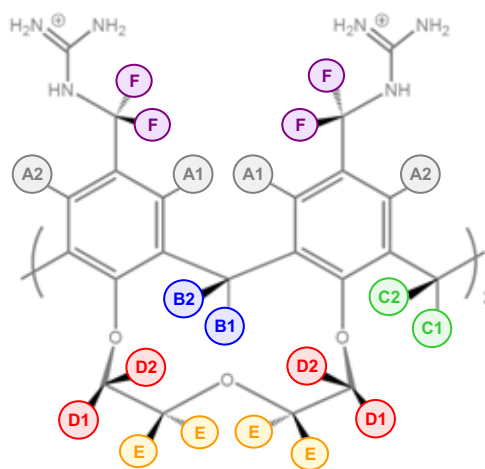
Figure 2.31. Calix4bridge ^{1}H assignation (600mHz, D_2O "100"). Each resonance was arbitrarily named under a capital letter and a number.

the former resonances of the free ligand would not only shift towards the bound form, but also split in two (**Figure 2.32**).
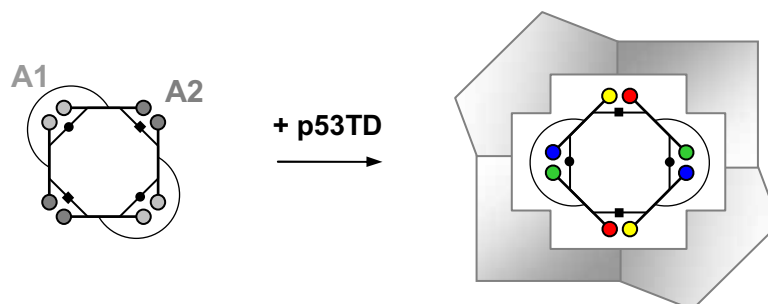
Figure 2.32. Schematic illustration of calix4bridge free (symmetry *C2v*) and bound to the protein (symmetry *C2*). Equivalent aromatic protons are represented as balls of the same color. The positions of methylene protons B1/B2 are indicated in black dots (●) and C1/C2 in black squares (■).

All these phenomena could be clearly detected in the ^{1}H spectra. The upper panels of **Figure 2.33** show the progress of the aromatic protons of calix4bridge during the titration of protein with increasing amounts of ligand. Initially –at the low ligand-to-protein ratios– the resonances of the ligand better represented those of the complex with the protein; whereas at the end of the titration –when the ligand concentration was large and close to saturation– the resonances better resembled those of the free ligand.

The shift-and-split phenomena were marked for p53wt and G334V titrations (and changes were similar for both proteins). In fact, the aromatic resonances at the end of the titration did not completely reach their free-ligand sharp shape, which reflected the low affinity constants for the interaction with these proteins (section 2.3.1.1). On the contrary, the tighter binding and slower chemical exchange for R337H caused that the ligand resonances in the bound form were not clearly appreciated, since under sub-saturating conditions the broad ligand resonances overlapped with the protein ones.

The lower panels of **Figure 2.33** show the results of the titrations with the amino-calixarene NH$_2$-calix4bridge, which displayed lower affinity for the proteins (section 2.3.1.2). The highest ratio recorded for p53wt and R337H (*i.e.* 16 equivalents of ligand) was far from saturation, and the split of ligand resonances was evident. The pattern for G334V was completely different, and resonances showed as singlets even at the lowest ratios, which might be attributed to the loose fitting of the ligand and to the extremely low affinity of the interaction.

The shift-and-split evolution was also observed for other ligand resonances. For instance, singlet F, despite being affected by the water suppression pulse, was intense enough as to be distinguished among the protein resonances (**Figure 2.34B**).
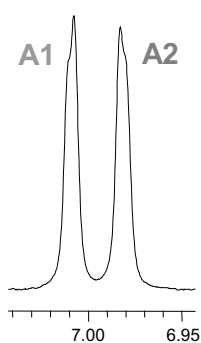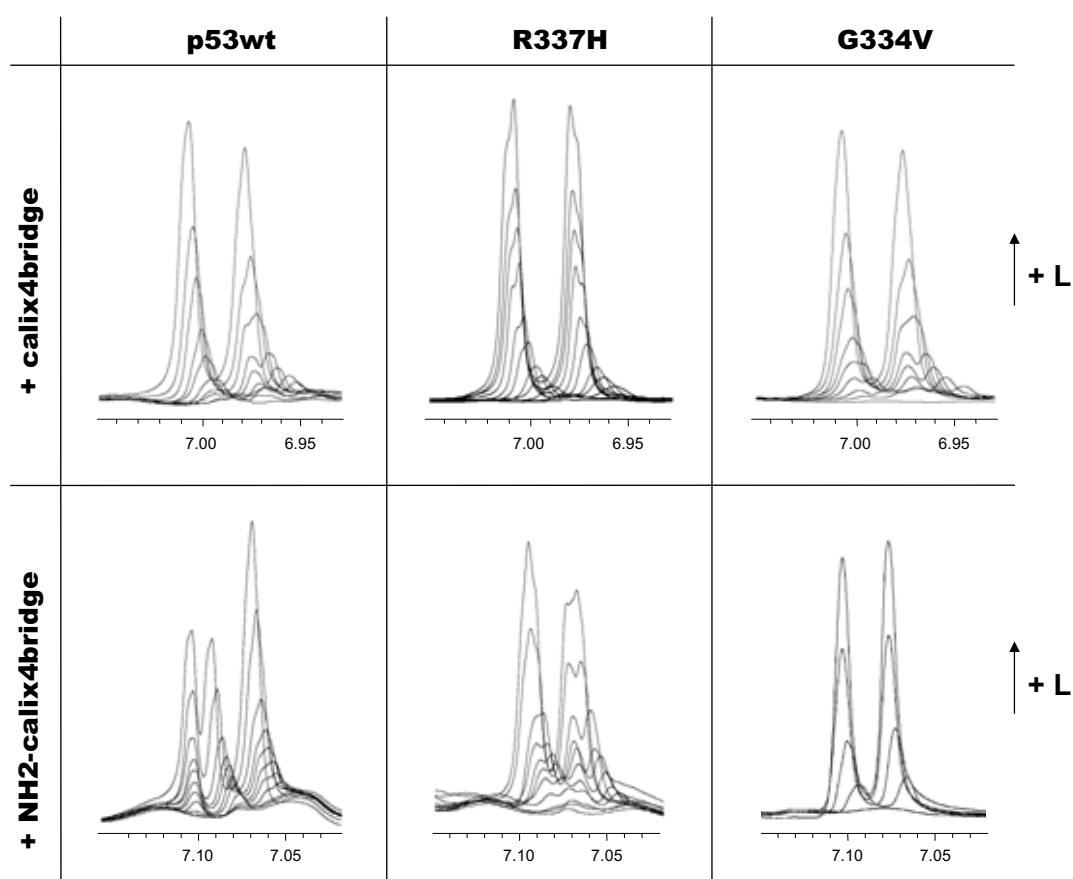
Figure 2.33. Next to these lines, aromatic resonances of calix4bridge (600MHz, D_2O). For NH_2-calix4bridge, they only differ slightly in the chemical shift. Above these lines, there are represented the stacked ^{1}H-spectra expanded in the aromatic region of calix4bridge (upper panels) and NH_2-calix4bridge (lower panels), recorded during the titration of protein with ligand (600MHz, 298K, 90%H_2O + 10%D_2O, pH 7, 125μM of tetramer; ratios in **Figure 2.28**).

Nevertheless, not all calix4bridge resonances had to split. The methylene protons B1/B2 and C1/C2 preserved their symmetry upon binding to the protein (**Figure 2.32**) and, accordingly, only one peak was observed during the titration (**Figure 2.34A**).

All these observations led to the important conclusion that calix4bridge had a preferred orientation to interact with the protein.
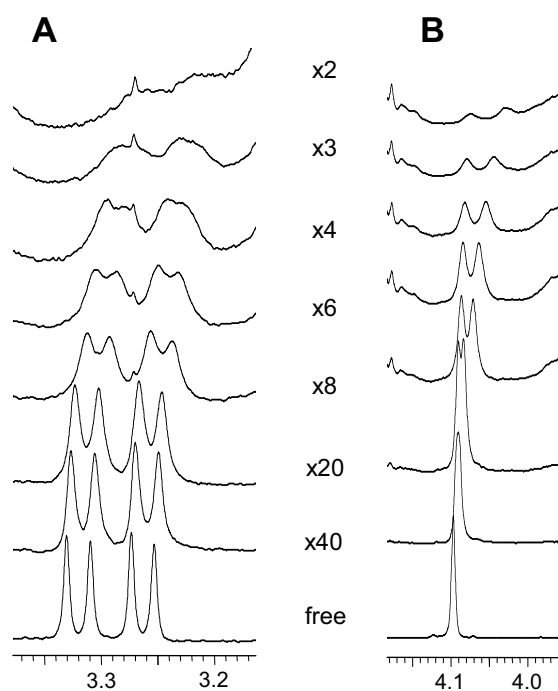
Figure 2.34. (A) Shift of resonances B2 and C2 and **(B)** shift-and-split of the singlet F in the titration of 500µM calix4bridge with p53wt (600MHz, 298K, D_2O at pD 7.4). Molar ratios correspond to ligand-to-tetramer.

(b) Titrating the ligand

To gain insights into the affinity from the ligand point of view, the ligand must be in large excess over the protein. Hence, the ligand resonances are ruled by the free species but they display changes –subtle or obvious– resulting from the interaction with the protein. However, this is only applicable in fast chemical exchanges. Perturbation in the chemical shift and the linewidth of the ligand resonances are the two factors more sensitive to protein binding.

The shifting and broadening effects of p53wt on the [1]H-resonances of calix4bridge were evaluated by titration of a small amount of protein (~4µM tetramer) with large excesses of the ligand (from 75µM to 1.4mM). The results are shown in **Figure 2.35**; only the intense and clear singlet F (Ar-CH_2-guanidinium) has been illustrated.

Changes in the chemical shift and the linewidth of the ligand resonances depend on the affinity for the protein; therefore, the binding constants for the interaction can be obtained through the mathematical analysis of these data.[29-31] Since calix4bridge and p53wt underwent a fast chemical exchange, and a large excess of ligand was used in this experiment ($[L] \approx [L]_T \gg [P_4]_T$), any observable parameter A for the ligand could be expressed as:

$$A = A_F + 2 \frac{[L]_T \, [P_4]_T}{K_D + [L]_T^2} A_B \qquad [11]$$

whereby A_F is the value for the free ligand and A_B for the bound one. In the approximation used to work out the solution for $[P_4L_2]$, the actual 1:2 protein-ligand stoichiometry was preserved.
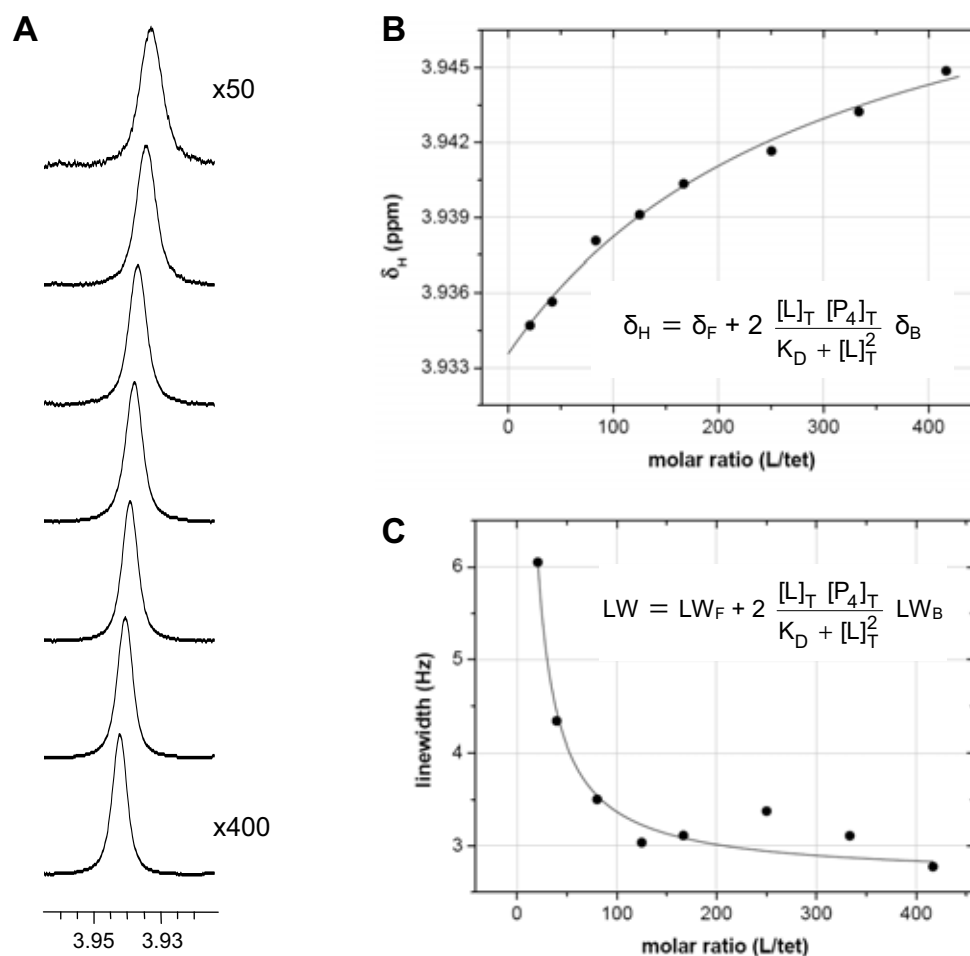
Figure 2.35. CSP and line broadening effects of p53wt on resonance F of calix4bridge (ligand ratios relative to 4.5μM tetramer). **(A)** Evolution during the titration; to better appreciate the changes, the spectra of the lower excesses of ligand have been intensified. Changes in **(B)** the chemical shift and **(C)** the linewidth broadening are plotted against the ligand molar ratio (relative to tetramer). Calculated curves could fit the data although the resulting parameters (not shown) were not accurate, probably because of the large experimental error.

The chemical shift changes and the linewidth broadening were fit to their corresponding equation [11] (**Figure 2.35B** and **C**). The calculated curves could visibly "fit" the data, although the resulting parameters were unreliable due to their large uncertainties. In addition, several "solutions" could result depending on the initial conditions given to the solver tool. Fielding and co-workers[32] recently reported that affinity constants obtained from line broadening measurements must be treated with caution because of their potentially large errors; those authors even suggest to perform multiple experimental determinations to ensure reproducibility and assess the reliability of the quantitative results.

It was not the aim of this chapter the perfect study of line broadening and chemical shift perturbation of ligand signals, and hence, this matter was not further explored. However, it was interesting to observe how the ligand resonances can also be used as probes for protein

interaction. In addition, it is possible to work out exact analytical solutions for the experimental data, even for systems with larger stoichiometries.

2.3.2.3. [1]H Saturation Transfer Difference

The evolution of the ligand resonances in the presence of protein (section 2.3.2.2a) suggested that calix4bridge might adopt a favored orientation to interact with the protein. However, those experiments were insufficient to know what it was like. Saturation transfer experiments helped in determining the ligand binding mode. In particular, [1]H-STD led to the most revealing results.

Several factors are key determinants for the success of an STD experiment. One is the system itself: the kinetics of the binding process should be slow enough as to transfer saturation to the bound ligand, but fast enough as to have free saturated ligand in solution (*i.e.* $10^{-3} > K_D > 10^{-8}$ M). Experimental conditions can be adjusted in order to set the kinetics in the right range. The other essence for success is the selective and efficient saturation of the protein.

For the case of calix4bridge, several experimental parameters had to be modified to detect an optimal STD signal.

The first point was to use a [1]H-STD sequence without water suppression; otherwise, the saturated calix4bridge resonances would have been useless. Finding the appropriate pulse sequence was easy; working in "pure" D_2O was not. The thorough precautions taken to avoid "H_2O-hydration" seriously complicated and limited the *modus operandi*. Since the pH could not be carefully controlled, STD experiments were only performed with p53wt, which was more robust to pH variations than R337H; its affinity was lower but still within the range of STD experiments.

Finding a selective frequency to saturate the protein was certainly not a problem, since the first ligand resonance in the upper field appeared at 3ppm. Some methyls from the protein at ~0.7ppm were selected to irradiate the macromolecule (>2ppm far from the ligand), and the length of the pulse was increased up to 3s.[33] An STD blank experiment (recorded without protein) proved that the calixarene was indeed unaffected by the saturation pulse (**Figure 2.36**).

Finally, the temperature and the ligand excess were adjusted in order to increase the saturation transfer, and thus obtaining measurable differences in convenient times. Decreasing the temperature did help. Initially, this was attributed to kinetic effects: lowering the temperature slowed the dissociation, and thereby saturation could be better transferred.[34] However, in a recent work by Jiménez-Barbero and co-workers,[35] the increase in the STD effect at lower temperatures is attributed to the more efficient saturation of the protein, specially if it is small (5-30kDa) and not effectively irradiated –*i.e.* the case for p53wt. Although this would be the predominant factor for the STD enhancement, temperature also affects other factors relevant to STD intensity, such as the dissociation rate and the longitudinal relaxation.

In addition to cool the system, increasing the amount of protein also resulted in an improvement of the STD signals.[34] The low affinity might be now the reason.

The final, optimized STD spectrum is shown in **Figure 2.36**.
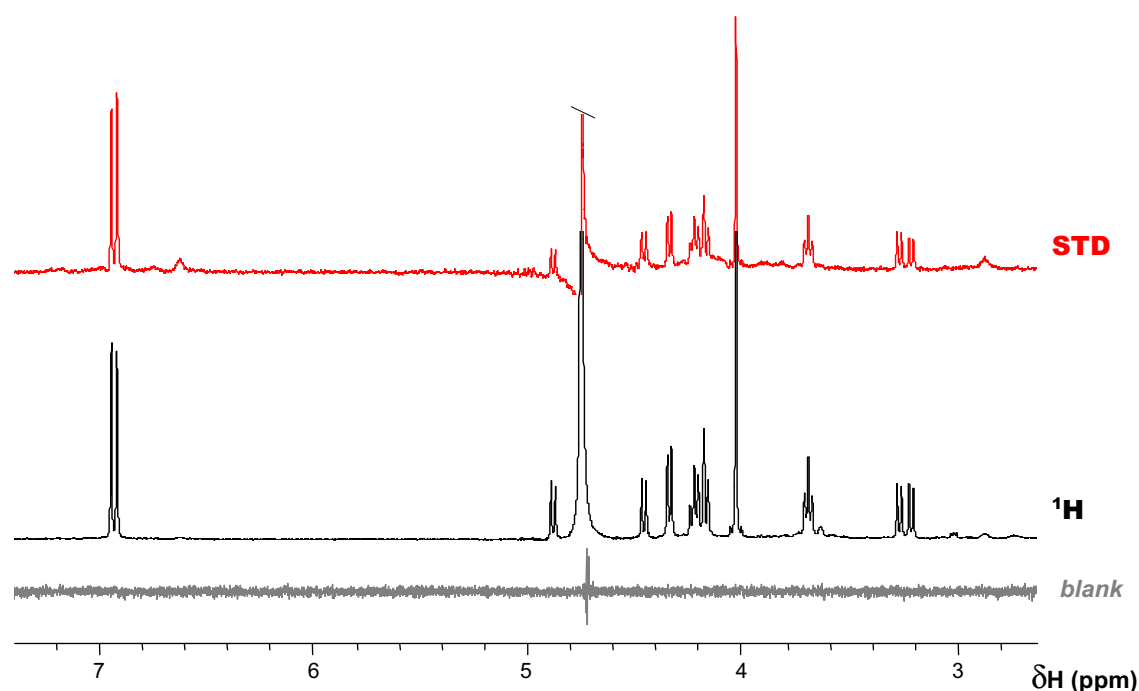
Figure 2.36. ^{1}H (black) and ^{1}H-STD (red) experiments on a 12.5μM (tetramer) p53wt sample in the presence of 1mM calix4bridge (600MHz, D_2O, 288K). STD experiment was recorded with 1024 scans, using 50ms Guassian shaped pulses during 3s for saturation at 0.72ppm, and a 20ms spinlock to remove residual protein resonances (experiment time: 2.5h). Calix4bridge signals were not affected by the selective saturation pulse as shows the blank STD experiment (grey).

Although STD experiments are typically employed for mapping the ligand epitope, the saturation transfer phenomenon can also prove the specificity of the protein-ligand interaction. The latter was achieved by the analysis the STD evolution during the titration of a minute amount of protein (~4.5μM tetramer) with large ligand excesses (from 75μM to 1.4mM). The perfect control of the concentrations of protein and ligand in each point of the titration was accomplished by the convergent strategy (see Experimental Section).

STD signal intensity depends on both ligand excess and ligand concentration, and they both were simultaneously varied during the titration. In order to compare the STD of the several samples, it was required to use the so-called STD amplification factor (equation [12]).

$$\text{STD amplification factor} = \frac{I_o - I_{sat}}{I_o} \text{ x ligand excess} \qquad [12]$$

The evolution of the STD amplification factor for some of the protons of calix4bridge (*i.e.* F, A2, C1 and D2) during the titration (**Figure 2.37**) shows that even if the fraction of saturated ligand

decreased at higher ligand excesses, the absolute STD signal intensity increased in the form of a saturation curve. Said *saturation* was the sticking evidence that the interaction of calix4bridge with p53wt was *specific*. Otherwise, the STD amplification factor would have increased indefinitely. The STD data from that titration were adjusted to the equation [13] (**Figure 2.37** and **Table 2.2**).

$$STD_{ampl} = \frac{STD_{MAX} \times [L]_T}{K_D + [L]_T}$$
[13]
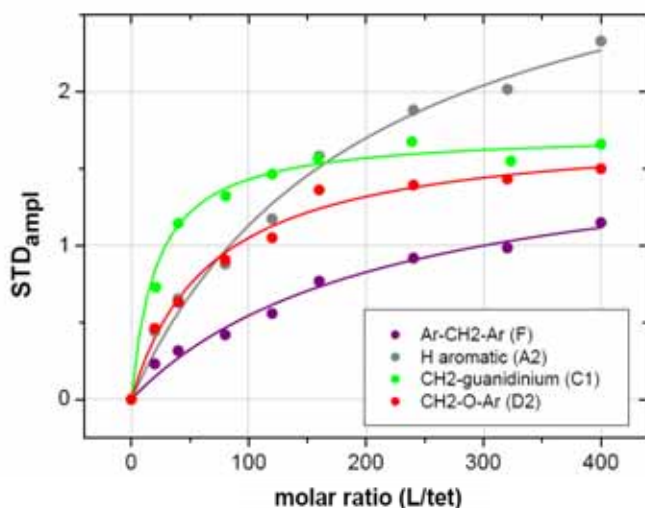
Figure 2.37. STD amplification factor as a function of calix4bridge excess (ligand-to-tetramer molar ratio). Convergent titration performed over ~4.5µM tetramer p53wt (600MHz, D_2O, 283K).

The saturation transferred to the ligand depends on the proximity to the receptor, although the size of the observed STD signal not only depends on that. Saturation of the protons of the ligand in the bound state is counteracted by their longitudinal relaxation times, T1, in the free state;[36] hence, a large STD effect can be misinterpreted for a strong contact when long saturation times are used. This effect is especially worrisome for molecules with protons differing markedly in their T1 values, as was the case of calix4bridge (**Table 2.3**). T1 for the aromatics protons was nearly twice longer than for the rest, and consequently, their STD would be overestimated when using presaturation times as long as 3 seconds. In fact, such was the effect of T1 on the STD intensity, that the hypothetical degrees of saturation calculated normalizing the STD_{MAX} from the STD titration experiment (**Table 2.2**, *"% saturation"*) were nonsense: no logical ligand orientation could justify them.

The STD misinterpretation was bypassed tracing the STD build-up curves, *i.e.* the STD effect as a function of protein presaturation times (equation [14]).[29,36] To eliminate the T1 bias, the parameter taken as an indicator of the proximity to the receptor was the slope of the STD build-up curve at zero saturation time (equation [15]).

Table 2.2. Parameters from the adjustment of the STD amplification factor as a function of calix4bridge concentration.

	STD_{MAX}	K_D (mM)	χ^2	"% saturation" [a]
F	1.72 ± 0.17	0.79 ± 0.16	0.003	50
A1	3.43 ± 0.31	0.94 ± 0.17	0.006	100
A2	3.42 ± 0.27	0.74 ± 0.12	0.008	100
B1	1.31 ± 0.19	0.20 ± 0.11	0.029	38
B2	1.85 ± 0.15	0.017 ± 0.005	0.015	54
C1	1.54 ± 0.08	0.06 ± 0.02	0.017	45
C2	1.75 ± 0.14	0.13 ± 0.04	0.029	51
D1	1.51 ± 0.09	0.19 ± 0.04	0.008	44
D2	1.77 ± 0.17	0.25 ± 0.16	0.004	52
E_{1-3}	1.64 ± 0.10	0.18 ± 0.04	0.011	48
E_{4-5}	1.51 ± 0.09	0.23 ± 0.05	0.006	44

[a] "% saturation" corresponds to the STD_{MAX} values normalized, thus representing the hypothetical proximity to the protein.

	T1 (s)	
	calix	**calix + p53**
F	0.68	0.68
A1	1.36	1.22
A2	1.30	1.18
B1	0.49	0.77
B2	0.53	0.54
C1	0.52	0.45
C2	0.54	0.55
D1	0.51	0.49
D2	0.54	0.54
E_{1-3}	0.44	0.44
E_{4-5}	0.51	0.50

Table 2.3. Longitudinal relaxation of calix4bridge protons, free and in the presence of protein p53wt (ligand-to-tetramer ratio: 80). As expected, some of the T1s slightly decreased. B1 results were largely inaccurate due to its proximity to the water band (600MHz, D_2O, 288K, inversion recovery pulse sequence)

$$STD = STD_{max} \times [1 - \exp(-k_{sat} \times t_{sat})]$$ [14]

$$v_o = STD_{max} \times k_{sat}$$ [15]

Several ^{1}H-STD spectra were recorded at saturation times ranging from 0.2 to 3 seconds on the same sample (1mM calix4bridge, 12.5μM tetramer p53wt, D_2O, 288K), and the STD amplification factors were subsequently determined for each of the protons and fit to equation [14] (**Figure 2.38** and **Table 2.4**). Normalization of the slopes, v_o, ultimately resulted in saturation percentages that were directly proportional to the proximity to the protein, assigning the 100% to the closest proton. The representation of the degrees of saturation on the structure of calix4bridge (**Figure 2.38**) evidences how the ligand oriented to interact with the protein.
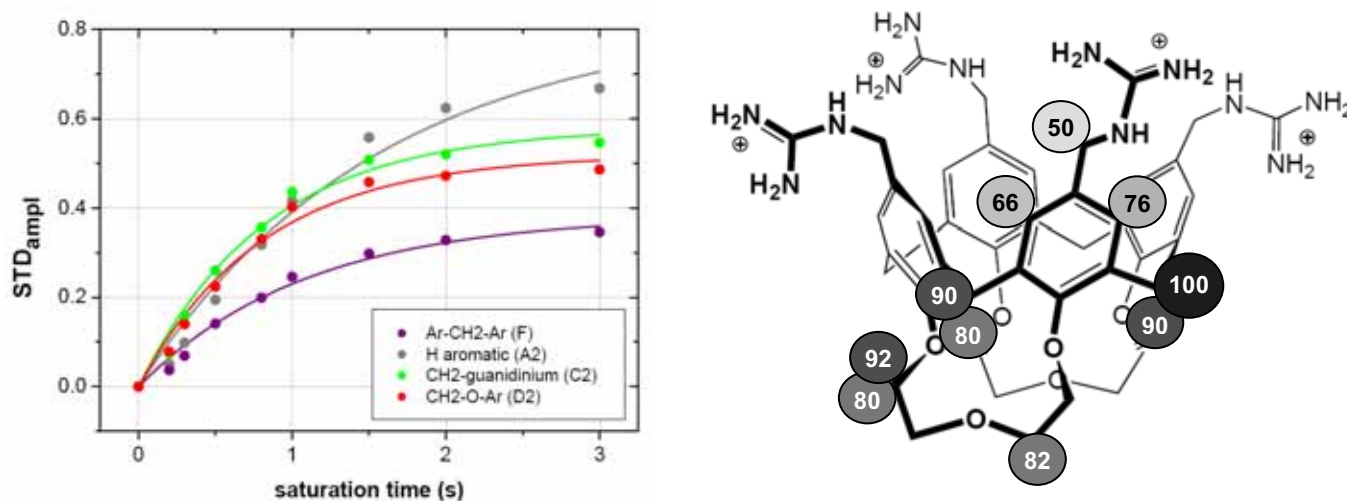
Figure 2.38. STD build-up curves of calix4bridge protons with different T1 (see **Table 2.3**) and different STD (1mM ligand + 12.5μM p53w tetramer, 600MHz, D_2O, 288K). The relative degrees of saturation for the each individual proton (normalized to that of C2) are represented on the structure of the molecule.

In the light of these results, it is certainly concluded that calix4bridge interacted with p53wt as it had been designed to do. Moreover, since protons at the same "level" within the molecule (*i.e.* the two aromatic protons, or methylenes B1/C1 or B2/C2) received different degrees of saturation, the molecule did adopt a preferred orientation into the protein binding pocket.

To further confirm that STD results were not artifactual, the same STD experiment was performed for NH$_2$-calix4bridge, and the ligand mapping was successfully reproduced (these results are provided in the Supplementary Material).

Table 2.4. Parameters from the mathematical adjustment of the STD built-up curves and saturation percentages of calix4bridge.

	STD_{max}	k_{sat} (s^{-1})	χ^2	v_o (s^{-1})	% saturation
F	0.38 ± 0.02	0.91 ± 0.11	0.0003	0.35	**50**
A1	0.71 ± 0.07	0.64 ± 0.12	0.0007	0.46	**65**
A2	0.83 ± 0.09	0.64 ± 0.12	0.0009	0.53	**76**
B1	0.40 ± 0.02	1.39 ± 0.18	0.0004	0.55	**79**
B2	0.51 ± 0.02	1.23 ± 0.11	0.0004	0.63	**90**
C1	0.47 ± 0.02	1.31 ± 0.17	0.0006	0.62	**89**
C2	0.58 ± 0.03	1.20 ± 0.13	0.0007	0.70	**100**
D1	0.46 ± 0.02	1.21 ± 0.13	0.0004	0.56	**80**
D2	0.52 ± 0.02	1.23 ± 0.14	0.0006	0.64	**92**
E$_{1-3}$	0.44 ± 0.02	1.31 ± 0.15	0.0008	0.57	**82**
E$_{4-5}$	0.42 ± 0.02	1.35 ± 0.16	0.0004	0.57	**82**

[a] STD_{max} from the STD build-up curves and STD_{MAX} from the ligand titration experiment do not correspond to the same parameter. In the STD build-up curves, it represents the maximum observable STD if long saturation times are used, for a given ligand excess. In the ligand titration, STD_{MAX} corresponds to the maximum observable STD amplification factor that can be reached increasing the ligand excess, for a given saturation time. Since both experiments were not done under the same experimental conditions, it was not possible to compare STD at 3s from the STD build-up curves with the STD value obtained for the same ligand excess in the titration.

2.3.2.4. Transferred nOe

Some preliminary transferred nOe experiments were done in order to further characterize calix4bridge binding mode. As occurred with the ^{1}H-STD experiments, several experimental parameters had to be adjusted before getting tr-nOes; hence, it was required to move to a lower magnetic field (500MHz), cool the system (288K), decrease the ligand excess (500μM ligand and 12.5μM tetramer p53wt) and short the mixing time to avoid spin-diffusion but still have enough intensity (100ms for the samples with protein).

Calix4bridge was one of those medium-size molecules with nearly null nOes. Decreasing the temperature helped in detecting small negative nOes in its NOESY spectrum (**Figure 2.40A**). Some of the expected nOes were not even detected, probably due to their low intensity. The NOESY spectrum strikingly changed in the presence of protein (**Figure 2.40B**). On the one hand, the intensity of the cross-peaks increased (*i.e.* more negative), hence, confirming the interaction with the protein. On the other hand, new cross-peaks appeared. Whether the new cross-peaks belonged to the ligand itself (those that before were not observed for the low intensity) or to spin-diffusion effects promoted by the interaction with the protein, could not be solved from the NOESY

spectrum. In addition, the quantitative analysis of these data was precluded because most of the protons experiencing nOes were also strongly *J*-coupled (*e.g.* geminal protons).

In order to distinguish the real nOes from the spin-diffusion, and to avoid zero-quantum up-down peaks, the ROESY spectra were also recorded (**Figure 2.41**). Molecules always display positive ROESY cross-peaks, and spin-diffusion effects can be discriminated because they appear as negative cross-peaks.

Two remarkable changes were detected in the ROESY spectrum of calix4bridge in the presence of protein, and they both involved protons from the lower loops. The most visible difference was the appearance of a new spin-diffusion cross-peak between protons E and D2; interestingly, the already existent spin-diffusion cross-peak between E and D1 increased its intensity. The other change concerned the system of protons C1-D1, whose nOe signal was also more intense in the presence of protein. These changes were in agreement with the design model were the lower rim of the calixarene was envisioned into the protein pocket; hence, protein nuclei would act as transductors of the nOe, **Figure 2.39**. Said fitting was likely favoring a given conformation of the biscrown loops.

Since the affinity of calix4bridge for p53wt was rather low, no intermolecular tr-nOe was detected (nor even increasing the protein concentration).

These findings were interesting and agreed with the design model, although no reliable quantification was possible because ROESY cross-peaks were contaminated with TOCSY signals[f]. Given that the ligand binding mode was already determined by STD, no further tr-nOe experiments were done.
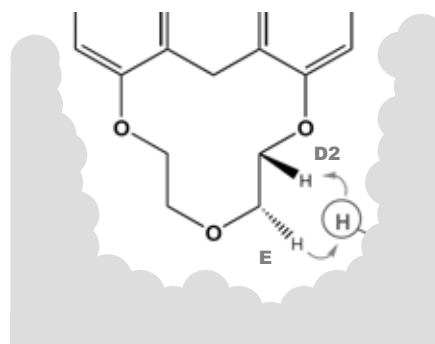
Figure 2.39. Illustration for new tr-nOes between protons in the lower-rim.

---

[f] There are pulse sequences which remove the TOCSY contamination from ROESY cross-peaks; however, they were not used in these preliminary experiments.
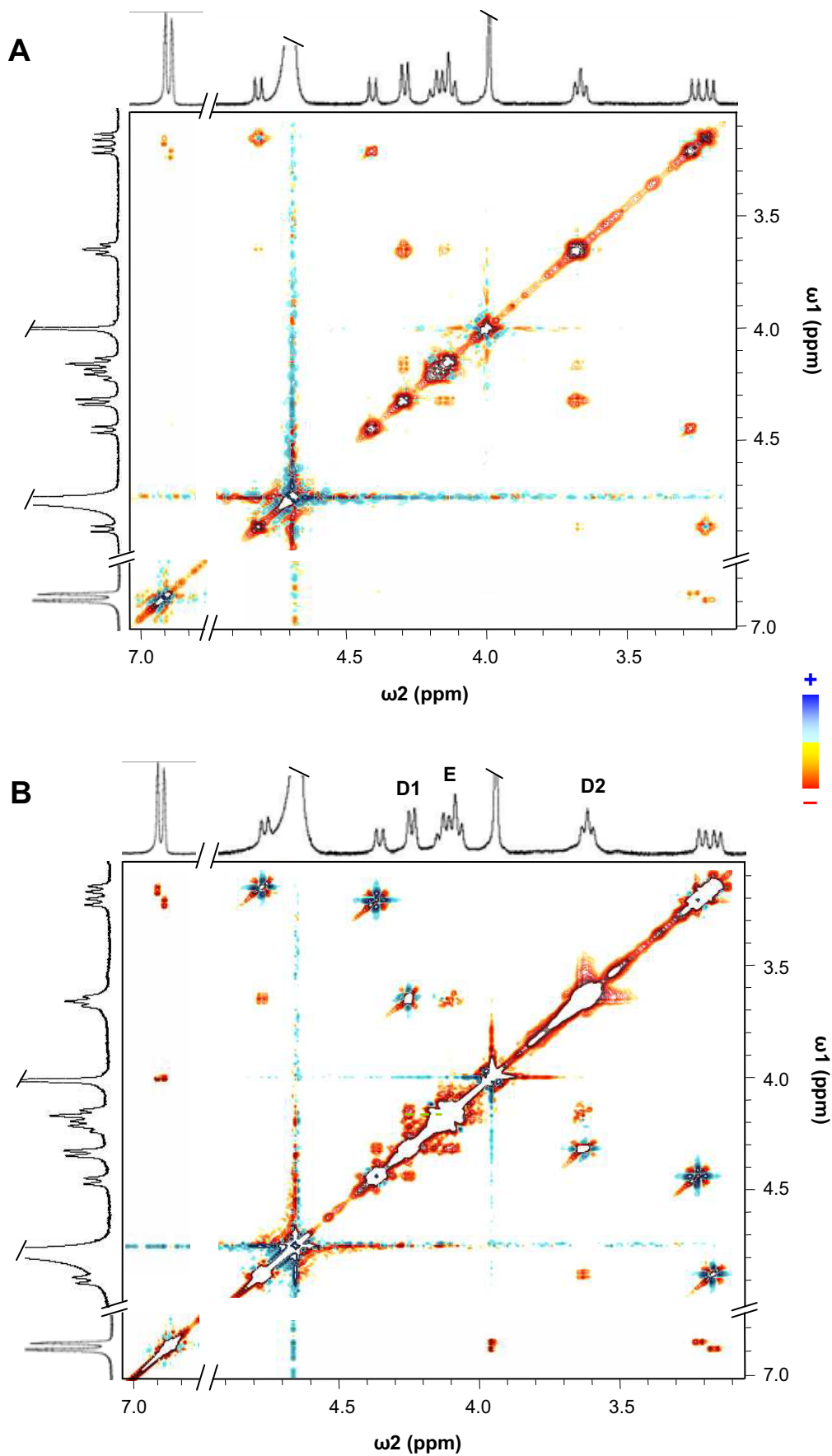
Figure 2.40. NOESY spectra of 500µM calix4bridge **(A)** free and **(B)** in the presence of 12.5µM (tetrameric) p53wt (500MHz, 288K, D$_2$O).
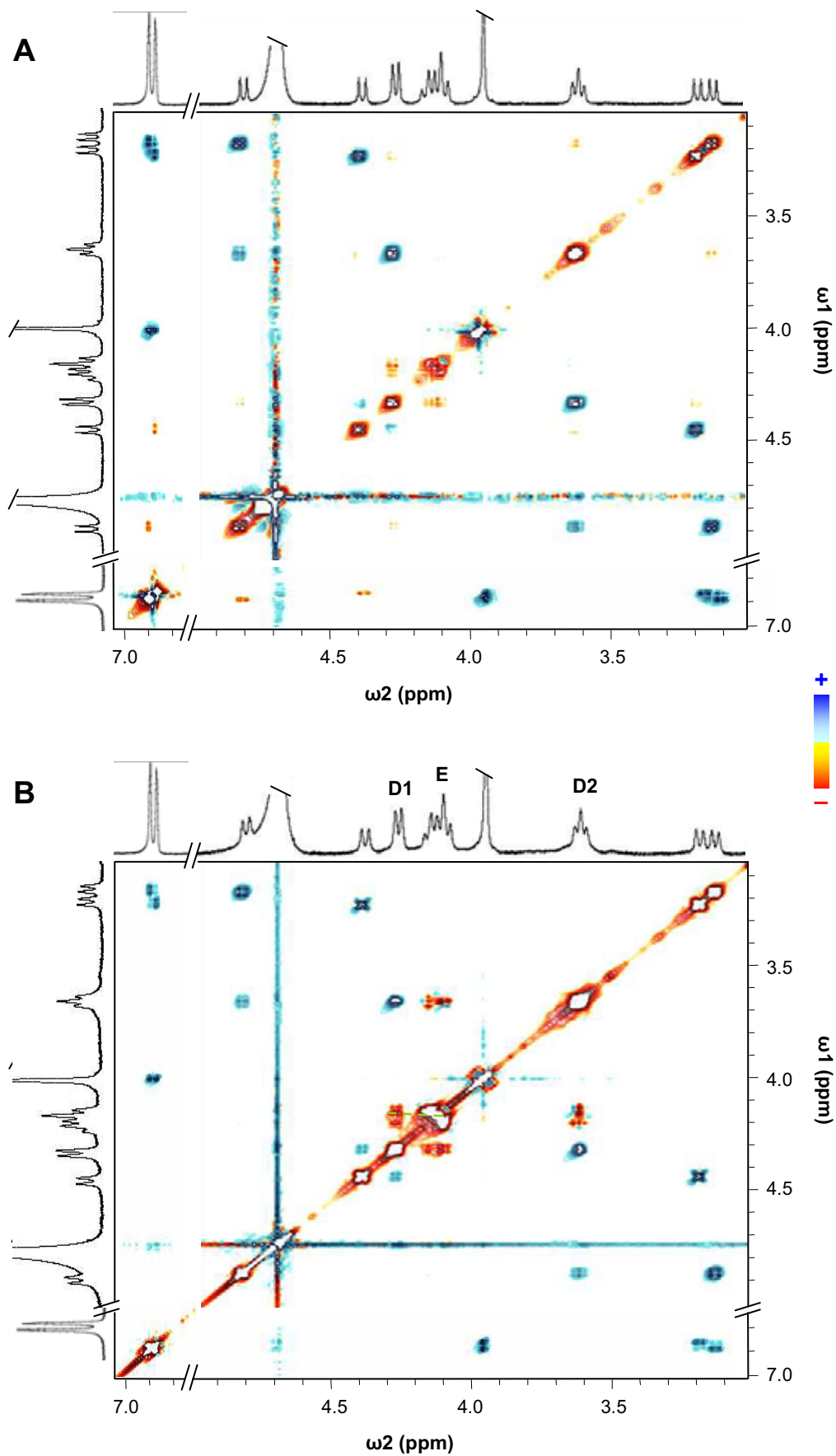
Figure 2.41. ROESY spectra of 500µM calix4bridge **(A)** free and **(B)** in the presence of 12.5µM (tetrameric) p53wt (500MHz, 288K, D$_2$O).

2.5 Isothermal Titration Calorimetry

Thus far, experimental results for the complex p53TD-calix4bridge asserted the structural model and the induced thermal stabilization of the mutant proteins. Despite the fact that a feasible mechanistic model for the binding could be also hypothesized, the complexity of the system did not enable the determination of basic thermodynamic parameters required to better describe and understand the molecular recognition event.

Isothermal Titration Calorimetry (ITC) was chosen to overcome the lack of thermodynamic characterization. Unfortunately, a considerable number of inconveniences resulting from inherent experimental limitations of the system, made the ITC results inappropriate for an accurate analysis.

Firstly, the limited availability of ligand did not permit the repetition of the titrations to ensure their reproducibility. In addition, it also restrained the concentration working range, and the amount of protein employed might have not been sufficient for good quality results.[37]

The rest of pitfalls were the result of working in plain water. The inability to control the ionic strength made that the "buffers" of the protein sample and of the ligand stock did not match, thereby maximizing the dilution heat and breaking one of the more basic rules for ITC success.[12] Said heat could not be offset by a blank dilution experiment over water, since water could not reproduce the crowded, self-buffered solution of protein.

In this respect, a titration over the negative control L344P informed about the real effects of diluting the ligand into the protein solution (**Figure 2.42**). The dilution heats were larger, as corresponds to dilute an organic molecule (charged and hydrophobic) into an ionic solution.[38]

In addition, the calixarene was a synthetic organic molecule; although it was purified, residual amounts of other organic species (*e.g.* sub-products, solvents or salts) were still present, and they also contributed to the dilution heat. This is well illustrated in **Figure 2.42**, where the dilution heats from two different batches of calix4bridge are compared; their dilution heats are clearly different.

In conclusion, working in water introduced an unavoidable source of experimental error in the large dilution heat of the ligand, which could not be controlled either corrected. The situation was further hampered for the system p53TD-calix4bridge, whose (specific) interaction heat was minuscule compared to that of the dilution; by all means this adversely affected the accuracy of the experimental data. As a consequence, the results from the ITC experiments were not reliable.

Figure 2.43 shows overlapped the resulting ITC data for the titration of the four proteins with calix4bridge. One of the more relevant features was the different energetic behavior between p53wt and R337H (that apparently exhibited a profile entropy driven – enthalpy opposed, *i.e.* positive heats), and G334V (that displayed a favorable enthalpy conduct, *i.e.* negative heats). The difference could be real, but it could be artifactual as well. The doubt arose because the titrations for p53wt and R337H, on one hand, and those for G334V and L344P, on the other, were performed with different batches of calixarene.
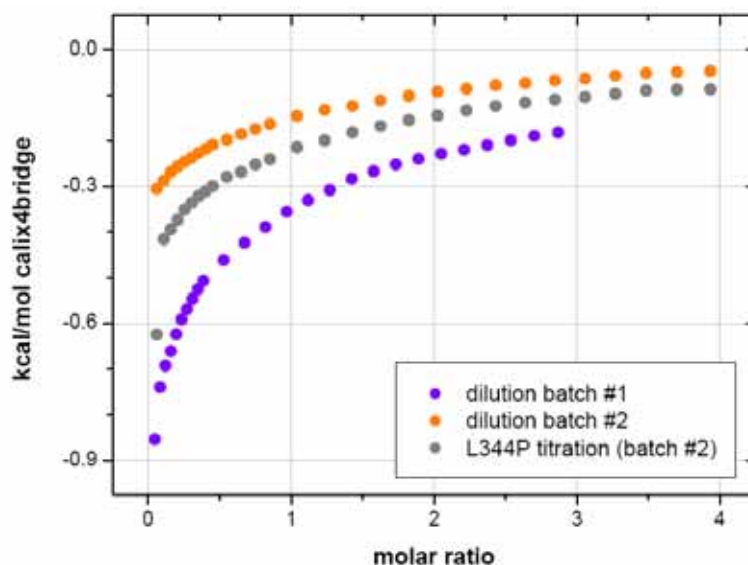
Figure 2.42. Inconveniences of working in water. Heats measured in the dilution of calix4bridge from different synthetic batches (● and ●) over water and over 400µM monomeric L344P (●). The protein sample was titrated with batch #2. The concentration of both batches was ensured to be equal by UV. Molar ratios calculated considering 400µM of protein.
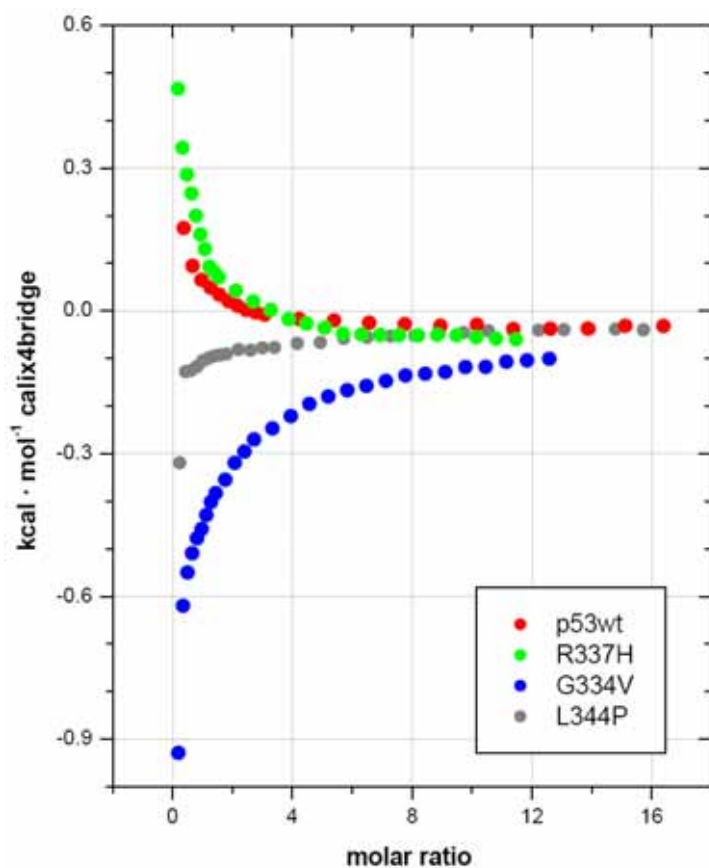
Figure 2.43. ITC results of calix4bridge and p53wt (red), R337H (green), G334V (blue) and L344P (grey), once subtracted the corresponding water dilution blank. Molar ratios correspond to ligand-to-tetramer; although for L344P no tetramer can be formed, this scale allows better comparison with the other proteins.

Whether endothermic or exothermic, all proteins showed a hyperbolic evolution of the heat during the titration. That profile had little to do with the "standard" ITC sigmoidal curves (obtained under appropriate concentrations).[37] However, they neither looked like the featureless straight lines which should be expected for a weak interaction. Probably the different shape reflected of a much more complex binding process than the standard one-to-one from book examples,[39,40] or it was simply a false trend due to the water inconveniences.

Curves seemed to get to saturation, although saturation did not get to zero-heat. Interestingly, the final asymptotes for the several proteins got to similar negative heats, which might be the result of the difference in ionic strength between the protein solution and the water dilution blank.

ITC could not provide reliable information due to the inaccuracy and uncertainty in the experimental calorimetric results; hence, the fine thermodynamic characterization for calix4bridge binding remains undetermined.

2.5 Towards the detection of the tetrameric complex

The thermal stabilization promoted by calix4bridge on the mutant proteins could be indeed associated to the stabilization of the tetrameric ensemble. Moreover, several experimental evidences suggested that one tetramer might interact with two ligands; however, no direct observation of such ligand-bound tetramer was yet achieved.

2.5.1 Protein chemical cross-linking

In a first raw approach, the protein was covalently cross-linked in the presence of calix4bridge.[41] Two different chemical cross-linkers were used: glutaraldehyde, which reacts with the protein amines, and EDC+NHS (ethanolamine + *N*-hydroxysuccinimide),[42] which link the carboxylates (from glutamate, aspartate and the C-termini) and the amino groups (from lysines and the N-termini) through an amide bond.

The results from the cross-linking of the proteins p53wt and R337H in the presence of calix4bridge are shown in **Figure 2.44**. No changes in the band pattern were detected when glutaraldehyde was used, which could suggest that calix4bridge did not affect the tetramerization equilibrium under the cross-linking conditions. In the cross-linking with EDC+NHS, the computational analysis revealed a slight real fade of the tetrameric band for R337H (the low quality of the figure may not allow detecting the subtle change). This was the opposite of the expected; however, it could be that the bound ligand acted as a "shield" for the carboxylates and did not enable them to react with the EDC+NHS.

This hypothesis was assessed cross-linking the proteins in the presence of NH_2-calix4bridge. The amino groups of this ligand could not interact as tightly as the guanidinium groups of calix4bridge did, but if they were close enough to a carboxylate moiety, they might even get linked to it. Moreover, since the four amino groups of one molecule of ligand were supposed to interact with different monomers, the ligand might act itself as a cross-linker of the tetramer. **Figure 2.45** shows the results. Although subtly, the band of the tetramer in the EDC+NHS cross-linking became brighter in the presence of NH_2-calix4bridge, while the monomer and the dimer ones faded. This would agree with the proposed "shielding" hypothesis for calix4bridge and could even be considered as an evidence of the interaction with the tetrameric assembly.

In the glutaraldehyde cross-linking for NH_2-calix4bridge some changes were also detected, although they were in the opposite direction: the tetramer band faded. This could be because the large ligand concentration (*i.e.* the large concentration of amino groups) decreased the effective concentration of reactive glutaraldehyde.

p53wt   **R337H**
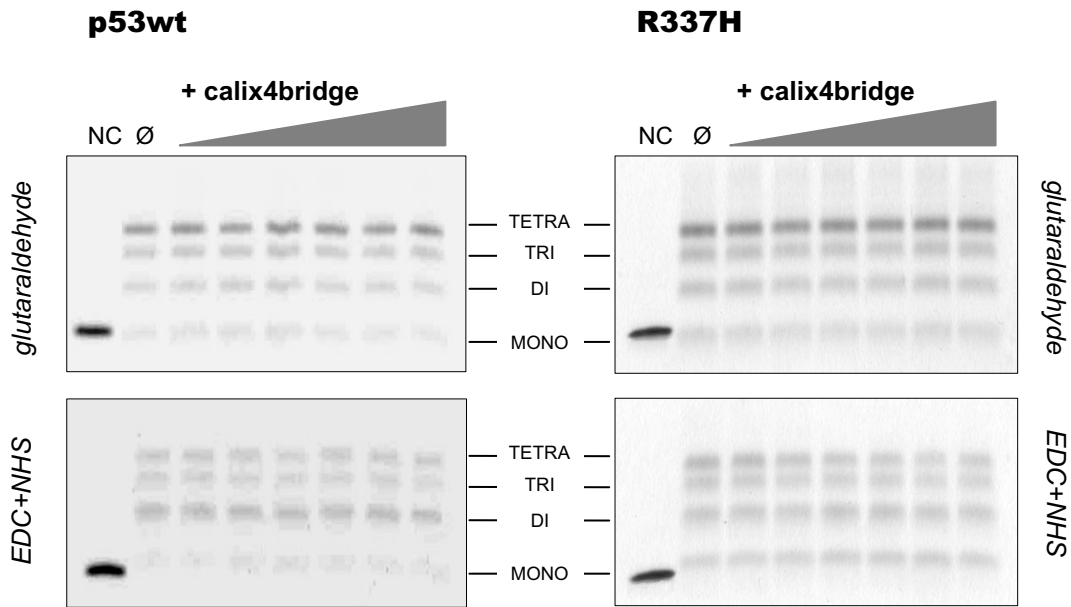
Figure 2.44. SDS-PAGE analysis of cross-linked samples of 25µM (tetramer) p53wt (left) and R337H (right) in the presence of calix4bridge (ligand-to-tetramer ratios: 0.8, 2, 4, 6, 8, 16eq), using 0.1% glutaraldehyde (upper panels), or 20mM EDC + 5mM NHS (lower panels), for 25min at 37ºC. Ø: cross-linked protein without ligand. NC: non-cross-liked protein.

p53wt   **R337H**
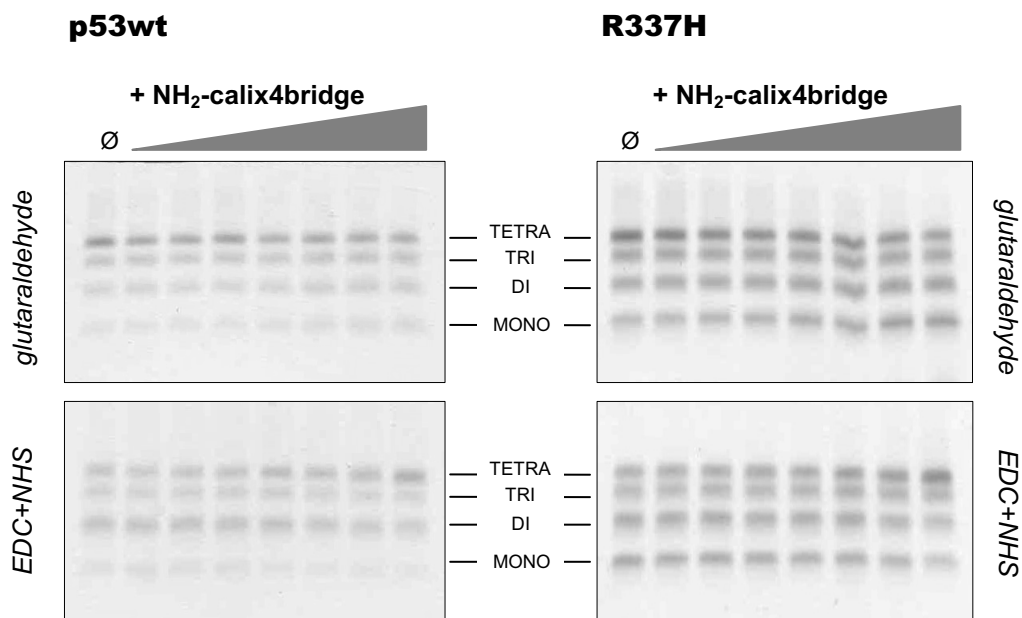
Figure 2.45. SDS-PAGE analysis of cross-linked samples of 25µM (tetramer) p53wt (left) and R337H (right) in the presence of NH$_2$-calix4bridge (ligand-to-tetramer ratios: 0.8, 2, 4, 6, 8, 16, 24eq), using 0.1% glutaraldehyde (upper panels) or 20mM EDC + 5mM NHS (lower panels), for 25min at 37ºC. Ø: cross-linked protein without ligand.

Regardless of the agreement between the cross-linking results and the calix4bridge model, these results should be taken with caution. The working conditions greatly differed from other biophysical experiments (*e.g.* the presence of cross-linker, the change of viscosity by the glycerol, the uncontrolled pH, the temperature of cross-linking) and the interaction between the protein and the ligand was be certainly perturbed by these factors.

2.5.2 Mass spectrometry

The presence of the tetramer was rather clear from the results of several biophysical experiments (CD, DSC, NMR or chemical cross-linking). However, no explicit evidence about the number of molecules of calix4bridge bound to the protein was achieved yet. Fortunately –at the end of this thesis–, it was possible to perform some preliminary experiments by ESI-MS that eventually provided the striking experimental evidence that two molecules of calix4bridge interacted with one tetramer of protein. Results are displayed in **Figure 2.46** and **Figure 2.47**.

The non-covalent complex of the tetrameric protein with one and with two molecules of ligand was successfully detected, although the experimental conditions were not thoroughly optimized in these trials. Free tetramer was also observed, which could be due to several factors; besides the non-optimal ionization conditions or the short ligand excess used, the most important of said factors was the weakness of hydrophobic interactions in the gas-phase.[43] Although for calix4bridge the guanidinium groups were found to be essential for protein interaction (section 2.3.1.2), an important contribution to the affinity relied on the interaction between the hydrophobic pocket of the protein and the non-polar lower rim and the aromatic platform of the calixarene; hence, this side of the interaction would be weakened in the gas-phase.

Interestingly, for p53wt and mutant G334V the ratio of tetramer with one ligand molecule and with two ligand molecules was approximately 2:1 (**Figure 2.46**), as would correspond to a probabilistic occupation of two binding sites of the same affinity.
On the contrary, the binding of calix4bridge to R337H (under the same conditions than for the other proteins) was hardly detected in the gas-phase; indeed, to get some complex the ligand excess had to be greatly increased (**Figure 2.47**). Given that in the solution-phase the affinity for R337H was higher than for the other proteins, MS-ESI results underscored the importance of the hydrophobic component for the interaction of R337H and calix4bridge (specially for the second binding site).

Another interesting feature in these preliminary MS spectra was that the detected amount of monomeric species seemed to decrease in the presence of the ligand. However, this observation should be taken really cautiously, since the presence of non-bound ligand (a charged molecule) might affect the ionization process.
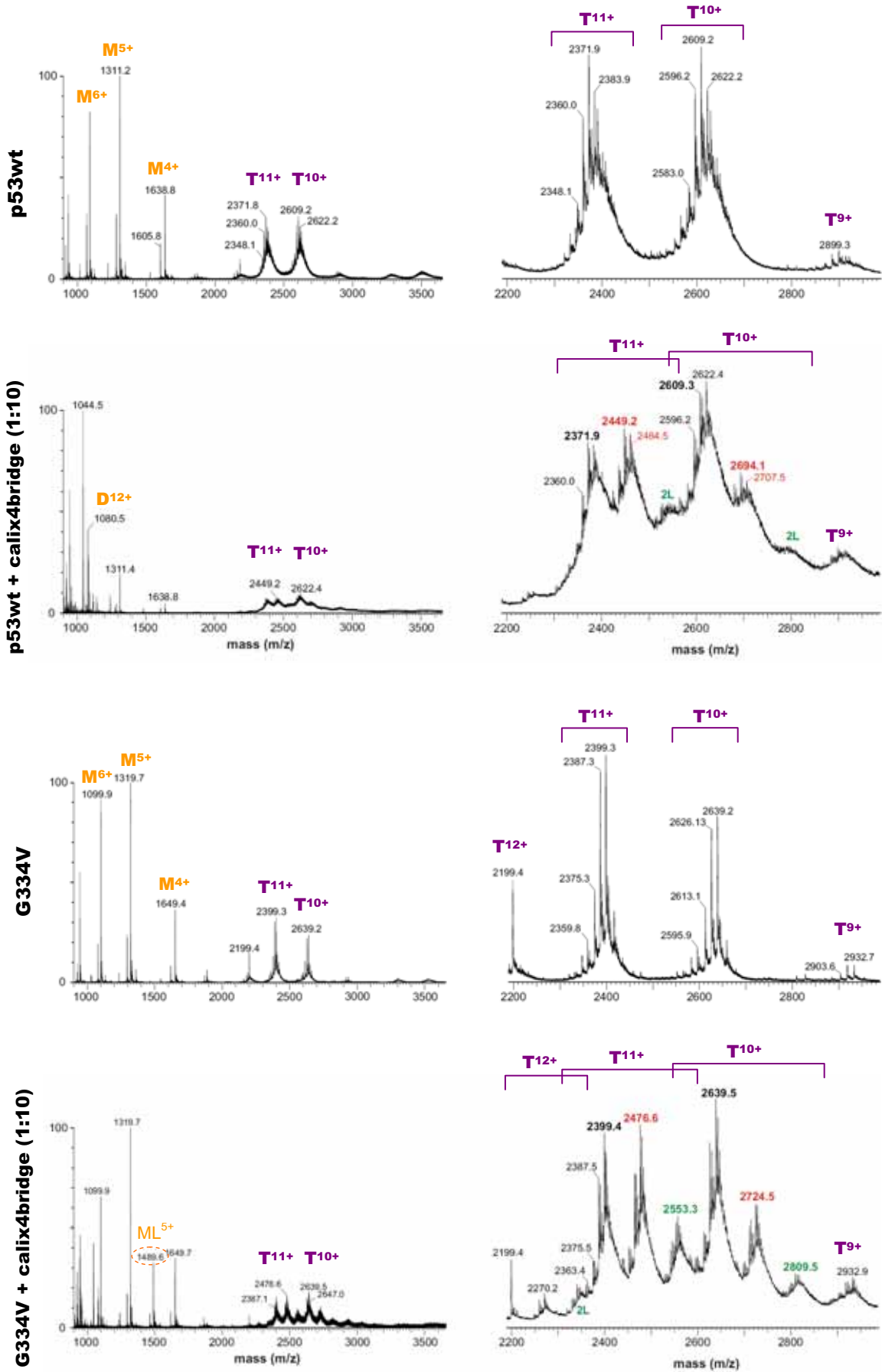
Figure 2.46. ESI-MS spectra for p53wt and G334V (12.5µM tetramer) with calix4bridge (130µM).
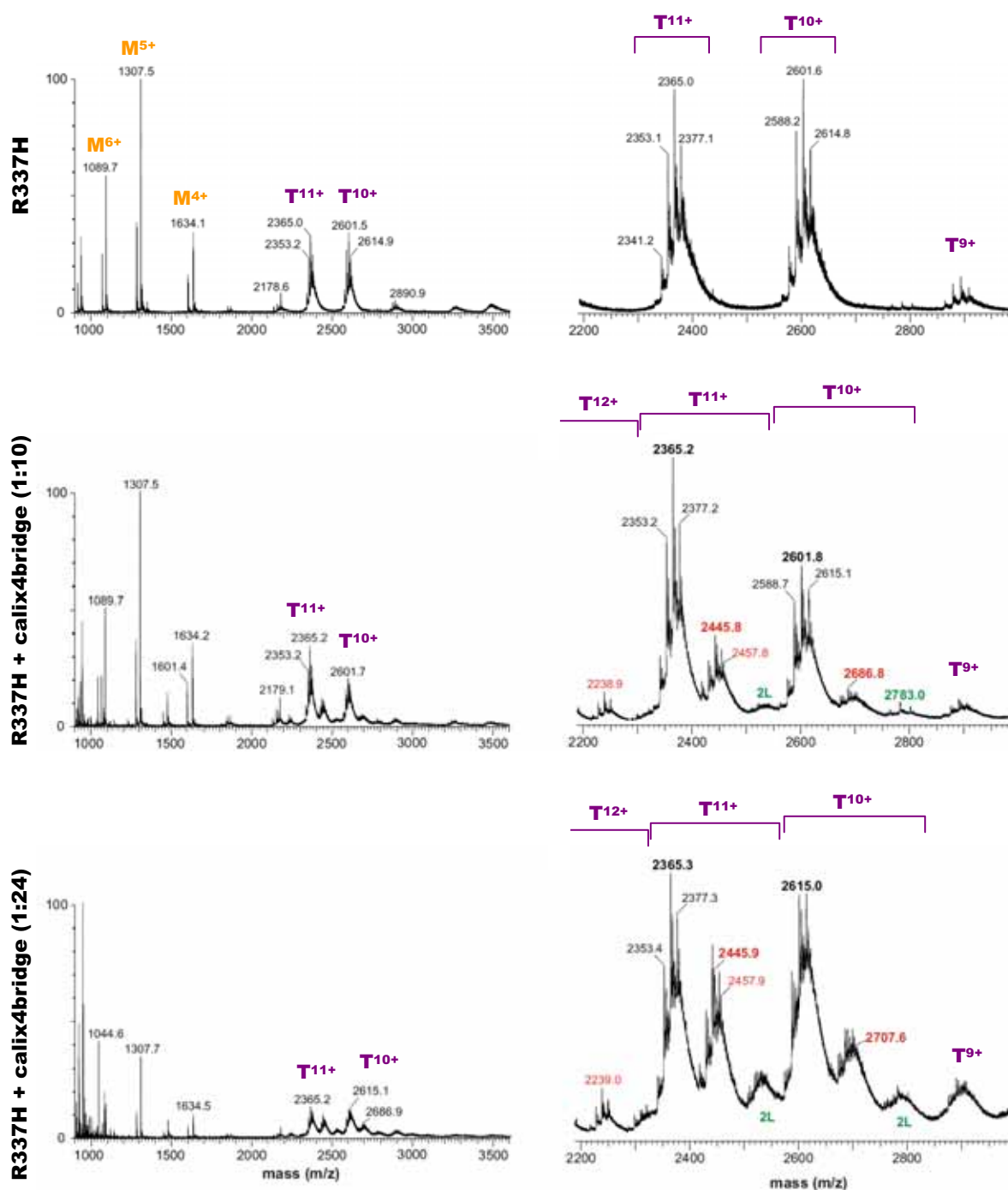
Figure 2.47. ESI-MS spectra for 12.5µM R337H (tetramer) in the presence of 10eq and 24eq of ligand (relative to tetramer), in 10mM sodium acetate buffer, at pH 7. **T** corresponds to tetramer, and **M** to monomer. Red masses indicate the complex with one molecule of ligand and in green with two.

Mutant L344P was used as negative control to evaluate to what extent nonspecific ionic interactions could affect in the MS detection, since it is well-known that MS has a bias towards electrostatic interactions. The spectra of L344P are provided in the Supplementary Material; some dimeric L334P bound to one ligand was detected, which agreed with other techniques that had already detected the existence of nonspecific interactions between L344P and calix4bridge.

In conclusion, although MS experiments do not provide reliable information about binding affinities –specially if they are composed of both hydrophobic and electrostatic components[43]– the results shown here also provided information beyond the right stoichiometry of the complexes. The hydrophobic-electrostatic balance for each of the three protein-ligand complexes could be compared in the basis of the relative detection of the complexes; hence, the hydrophobic component seemed to weight more for R337H than for p53wt and G334V, although it would not mean that the electrostatic component for R337H was not important or lesser than for the others. Despite the fact that it could not be said whether hydrophobic or electrostatic interactions ruled the binding of calix4bridge in the solution-phase, the differences detected in the gas-phase may reflect the different affinity described for each of the three proteins.

2.5.3 Crystallography: first trials

On going work.

In hot pursuit of complete characterization, the complex of the calix4bridge and the tetramerization domain of p53 was tried to crystallize. As was mentioned in section 1.3.6, protein crystals were obtained with the synthetic p53TD under the two different conditions described in the literature.[44,45] Given that calix4bridge interaction was not supposed to be affected by the absence of the terminal unstructured tails from the recombinant protein, using the nicked synthetic domain should not represent an inconvenient.

For the crystallization of the protein-ligand complex two strategies were followed in parallel: soaking and co-crystallization, both by the hanging-drop method.

On the one hand, some pre-formed protein crystals were soaked into a solution containing the ligand and incubated for variable times. According to the lock-and-key binding model, calix4bridge should not alter the protein structure. The analysis of the reported p53TD crystal structure,[44] revealed that the ligand binding site (*i.e.* the hydrophobic pocket) was perfectly accessible. Furthermore, the crystal channels, which were mainly defined by this region, were big enough as to enable the calix4brige molecule to diffuse through them, although the big size of the ligand would slow the diffusion process. Therefore crystallization of the complex by soaking might be feasible.

The evolution of pre-formed protein crystals of different morphologies soaked in ligand-containing solutions over the time is shown in **Figure 2.48**. As expected, calix4bridge always precipitated when it was added to the high saline crystallization buffer; hence, the effective ligand concentration in the drop was extremely minimized, and the diffusion into the protein crystal would not be efficient. The big crystals obtained in Tris buffer[44] (**Figure 2.48A**) remained apparently unperturbed by the presence of the calixarene; this could be either because no ligand was diffused into the crystal, or because if it diffused, it preserved the protein net. Unfortunately, it was then found that those protein crystals were a macle (see section 1.3.6) and the evaluation of the incorporated ligand into the protein crystal in this king of packing would not be reliable.

Contrariwise, protein crystals obtained in HEPES[45] were progressively damaged when soaked into the calix4bridge solution (**Figure 2.48B**). Destruction of the protein crystal could suggest that ligand and protein interacted.
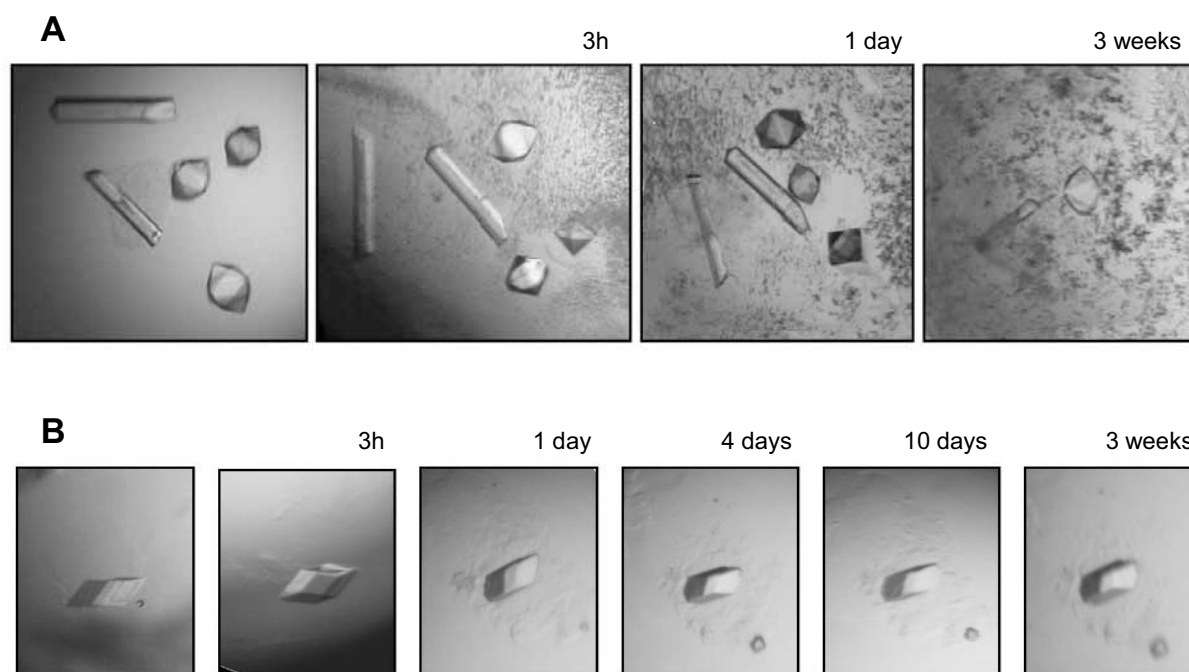
Figure 2.48. p53TD crystals soaked into a solution containing 2mM calix4bridge (at pH 7.5). (**A**) Crystals of different morphologies obtained in Tris/formate/sulfate buffer[44] and (**B**) crystal obtained in HEPES/citrate buffer.[45] The initial pictures correspond to the protein crystals at time 0. The cloudy mass in **A** corresponds to precipitated calix4bridge. In **B** ligand precipitation was not so appalling.

On the other hand, the challenge was also undertaken by direct co-crystallization of the protein-ligand complex. Initial trials were carried out in the buffers already used to crystallize the protein, tuning parameters such as the pH or the precipitant (*i.e.* sodium formate) concentration. Whatever the conditions were, free calix4bridge (**Figure 2.49A**, control drop) always precipitated. In fact, it did crystallize into rectangular crystals whose size and morphology depended on the pH and the salt concentration. Interestingly, a totally different pattern was observed in the presence of protein. For most of the conditions, the drop remained transparent, but crystals were formed in some instances (namely, Tris buffer at pH 7.5-8). They were also rectangular, and the thickness critically depended on the precipitant concentration, becoming mere threadlike needles at the highest ones. These crystals developed from a same nucleation core, always at the edges of the drop, whereas the free calixarene crystals were independent and stuck in the middle of the drop.

If those crystals belonged to free ligand or to the protein-ligand complex is still undetermined, since it has not been possible to analyze or diffract them yet.
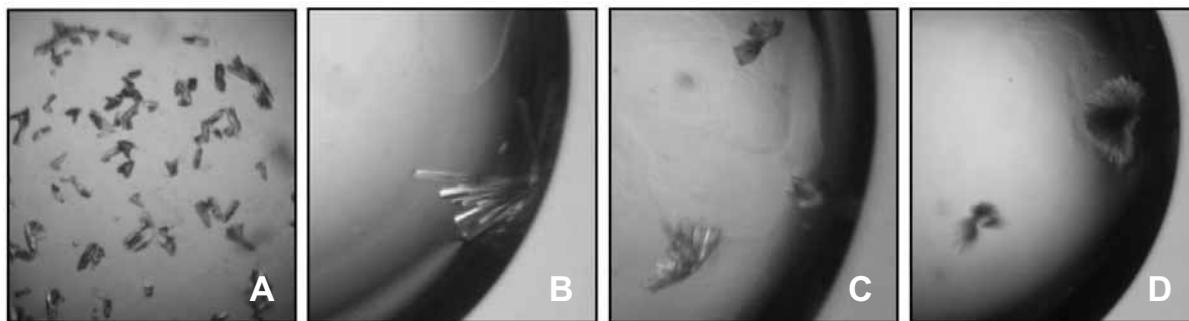
Figure 2.49. Co-crystallization trials in 50mM Tris-HCl pH 7.5 with sodium formate and 0.5M ammonium sulfate. The free calixarene control (middle section of the drop, sodium formate at 3M) is shown in (**A**), and the rest of pictures correspond to drops for pre-incubated samples of p53TD and calix4bridge (10mg/mL of protein and 2mM of ligand) crystallized with sodium formate at (**B**) 3M, (**C**) 3.5M and (**D**) 4M.

2.5. Calix4bridge summarized

Calix4bridge is a tetraguanidinium biscrown calix[4]arene molecule rationally designed to interact with the tetramerization domain of p53. The hydrophobic lower rim of the calixarene can – theoretically– fit into a small hydrophobic pocket present on the protein surface which is outlined by the four monomeric units. The upper rim of the ligand, featuring four guanidinomethyl moieties, may additionally chelate carboxylate residues exposed on the protein surface belonging to different monomers. Due to the high symmetry of the protein there are two of these binding sites; hence, two molecules of calix4bridge would interact with p53TD and hold together its four monomers. Such ability would be really precious for mutated domains with compromised tetramerization abilities (*e.g.* R337H or G334V) since the interaction with the calixarene would stabilize the tetrameric structure.

To validate the rational model, a battery of biophysical experiments has been performed between the synthetic calixarene and the tetramerization domains of proteins p53wt, R337H, G334V and L344P. The experimental results are consistent enough as to confidently affirm that calix4bridge specifically interact with the tetramerization domain of p53 as it has been designed to do. Moreover, the interaction stabilizes the tetrameric assembly of structured mutant proteins.

The thermal stability induced by calix4bridge on the proteins (determined by DSC and CD) proves the existence of interaction. Furthermore, calix4bridge also promotes kinetic stabilization, delaying the spontaneous denaturation process of proteins over the time; this would be a very promising ability to avoid, for instance, misfolding disorders in proteins.

Regarding the structure of the complex, both ^{15}N-^{1}H-HSQC experiments on the protein and ^{1}H-STD experiments on the ligand perfectly agree with the rational model. On the one hand, the hydrophobic pocket of the protein is the most sensitive region to the presence of ligand. On the other hand, the lower rim of calix4bridge is the region that becomes closest to the protein. In fact, the calixarene interacts with the protein in a favored orientation, which may be conditioned by a preferred conformation of the lower loops (as the STD, the tr-nOe and the ^{1}H spectra suggest).

The detection by ESI-MS of the tetrameric protein bound to two molecules of the calixarene provides the most strinking evidence of the existence of the complex and its 1:2 stoichiometry.

The NMR results also provide information about the mechanisms and the affinity of the binding. Interestingly, each protein behaves in a different way.

The two binding sites for p53wt are equivalent and independent (*i.e.* lock-and-key model), and the thermodynamic dissociation constant is estimated to be ~280μM (this value is an overestimation due to the approximate model used to calculate it).

Contrariwise, the binding of the two molecules of calix4bridge on R337H proceeds sequentially (likely in a cooperative manner), and the interaction of the ligand promotes some structural rearrangements, which are not felt equally for those residues within the binding site and for those on the outer surface. The affinity for R337H is nearly one order of magnitude higher than for p53wt.

The mutation H337 itself may affect the structure of the binding site, thus conditioning the said affinity. However, the differences in affinity and mechanism can also rise from the more flexible structure of R337H; differing from the well-packed and stable p53wt, R337H can probably rearrange to adopt a "more optimal" binding site, thereby establishing tighter interactions with the bound ligand.

The flexibility hypothesis can not be extended to mutant G334V; the interaction of two molecules of calix4bridge with G334V is likely to be also sequential, but the affinity is much lower (in the same range or larger than for p53wt). The mutation in this protein does not enable a convenient packing of the tetramer, and this probably results in an "unsuitable" binding site –perhaps too large– in which the calixarene binds rather loosely –although it binds and stabilizes the tetramer.

Regarding the driving force in calix4bridge interaction, the marked decrease in the affinity of a calixarene analog in which the four guanidinium moieties have been substituted by amino groups underscores the crucial role of the guanidinium-carboxylate chelation. Nonetheless, the hydrophobic component of the interaction is also essential, and may explain the relative low detection of the complex in the gas phase.[43] In fact, the ESI-MS results suggest that the hydrophobicity is more important in the interaction with mutant R337H than with the other proteins, which could be also the reason for its higher affinity.

In addition to the structured proteins, the effect of biscrown calixarene on the unstructured mutant L344P has been also evaluated. L344P has been used as negative control, and the results clearly indicate that the calixarene does not specifically interact with this protein and, of course, can not recover the tetrameric state.

All these results lead to certainly conclude that calix4bridge behaves as it has been designed to do. This ligand may be somehow considered as a "pharmacological chaperone", in the sense that its interaction with the mutated proteins can *stabilize* the native tetrameric assembly. However, this is only valid for mutated proteins which assemble the tetramer by themselves. Perhaps, calix4bridge should be better described as a "thermodynamic stabilizer" since it can simply shift the thermodynamic equilibrium towards a preexistent tetrameric form.

Although only three structured mutants have been tested, the "stabilizer-effect" may also be expected for other mutants of p53TD, as far as they can adopt a native-like tetrameric structure without negatively perturbing the binding site.

In addition to this thermodynamic-stabilizing property, calix4bridge can also *kinetically* stabilize the proteins towards spontaneous denaturation (at low temperature). This effect would resemble the "kinetic native-state stabilizers" described by Kelly and co-workers,[46-48] with the difference that calix4bridge also presents the ability to stabilize the native state of mutated proteins.

Bibliography

1. Arduini, A. *et al.* Calix[4]arenes Blocked in a Rigid Cone Conformation by Selective Functionalization at the Lower Rim. *The Journal of Organic Chemistry* **60**, 1454-1457 (1995).
2. Galán, H., de Mendoza, J. & Prados, P. Conformational Control of Calix[6]arenes Through Multiple Bridges. *European Journal of Organic Chemistry* **19**, 4093-4097 (2005).
3. Mammen, M., Choi, S. K. & Whitesides, G. M. Polyvalent Interactions in Biological Systems: Implications for Design and Use of Multivalent Ligands and Inhibitors. *Angew. Chem. Int. Ed Engl.* **37**, 2754-2794 (1998).
4. Sakai, N. & Matile, S. Anion-mediated transfer of polyarginine across liquid and bilayer membranes. *J. Am. Chem. Soc.* **125**, 14348-14356 (2003).
5. Fukada, H., Sturtevant, J. M. & Quiocho, F. A. Thermodynamics of the binding of L-arabinose and of D-galactose to the L-arabinose-binding protein of Escherichia coli. *Journal of Biological Chemistry* **258**, 13193-13198 (1983).
6. Brandts, J. F. & Lin, L. N. Study of strong to ultratight protein interactions using differential scanning calorimetry. *Biochemistry* **29**, 6927-6940 (1990).
7. Manly, S. P., Matthews, K. S. & Sturtevant, J. M. Thermal denaturation of the core protein of lac repressor. *Biochemistry* **24**, 3842-3846 (1985).
8. Sanchez-Ruiz, J. M. Ligand effects on protein thermodynamic stability. *Biophys. Chem.* **126**, 43-49 (2007).
9. Johnson, C. R., Morin, P. E., Arrowsmith, C. H. & Freire, E. Thermodynamic analysis of the structural stability of the tetrameric oligomerization domain of p53 tumor suppressor. *Biochemistry* **34**, 5309-5316 (1995).
10. Waldron, T. T. & Murphy, K. P. Stabilization of proteins by ligand binding: application to drug screening and determination of unfolding energetics. *Biochemistry* **42**, 5058-5064 (2003).
11. Privalov, G. P. & Privalov, P. L. Problems and prospects in microcalorimetry of biological macromolecules. *Methods Enzymol.* **323**, 31-62 (2000).
12. Ladbury, J. E. & Doyle, M. L. *Biocalorimetry 2. Applications of calorimetry in the biological science*. Wiley, West Sussex (2004).
13. Prabhu, N. V. & Sharp, K. A. Heat capacity in proteins. *Annu. Rev. Phys. Chem.* **56**, 521-548 (2005).
14. Shrake, A. & Ross, P. D. Ligand-induced biphasic protein denaturation. *J. Biol. Chem.* **265**, 5055-5059 (1990).
15. Greenfield, N. J. Analysis of circular dichroism data. *Methods Enzymol.* **383**, 282-317 (2004).
16. Pace, C. N. & McGrath, T. Substrate stabilization of lysozyme to thermal and guanidine hydrochloride denaturation. *J. Biol. Chem.* **255**, 3862-3865 (1980).
17. van Nuland, N. A. *et al.* The NMR determination of the IIA(mtl) binding site on HPr of the Escherichia coli phosphoenol pyruvate-dependent phosphotransferase system. *FEBS Lett.* **315**, 11-15 (1993).
18. Li, X., Zhang, J., Cao, Z., Wu, J. & Shi, Y. Solution structure of GOPC PDZ domain and its interaction with the C-terminal motif of neuroligin. *Protein Sci.* **15**, 2149-2158 (2006).
19. Gunther, U., Mittag, T. & Schaffhausen, B. Probing Src homology 2 domain ligand interactions by differential line broadening. *Biochemistry* **41**, 11658-11669 (2002).
20. Gunther, U. L. & Schaffhausen, B. NMRKIN: simulating line shapes from two-dimensional spectra of proteins upon ligand binding. *J. Biomol. NMR* **22**, 201-209 (2002).
21. Craven, C. J. *et al.* Complexes formed between calmodulin and the antagonists J-8 and TFP in solution. *Biochemistry* **35**, 10287-10299 (1996).
22. Johnson, P. E. *et al.* Calcium binding by the N-terminal cellulose-binding domain from Cellulomonas fimi beta-1,4-glucanase CenC. *Biochemistry* **37**, 12772-12781 (1998).
23. Jones, S. & Thornton, J. M. Principles of protein-protein interactions. *Proc. Natl. Acad. Sci. U. S. A* **93**, 13-20 (1996).
24. Bogan, A. A. & Thorn, K. S. Anatomy of hot spots in protein interfaces. *J. Mol. Biol.* **280**, 1-9 (1998).
25. Nishihara, M. *et al.* Arginine magic with new counterions up the sleeve. *Org. Biomol. Chem.* **3**, 1659-1669 (2005).
26. Perkins, S. J. & Wuthrich, K. Conformational transition from trypsinogen to trypsin: 1H nuclear magnetic resonance at 360 MHz and ring current calculations. *Journal of Molecular Biology* **138**, 43-64 (1980).
27. Hinshelwood, J. & Perkins, S. J. Conformational changes during the assembly of factor B from its domains by (1)H NMR spectroscopy and molecular modelling: their relevance to the regulation of factor B activity. *J. Mol. Biol.* **301**, 1267-1285 (2000).
28. Hoyt, D. W., Harkins, R. N., Debanne, M. T., O'Connor-McCourt, M. & Sykes, B. D. Interaction of transforming growth factor alpha with the epidermal growth factor receptor: binding kinetics and differential mobility within the bound TGF-alpha. *Biochemistry* **33**, 15283-15292 (1994).
29. Mayer, M. & James, T. L. NMR-based characterization of phenothiazines as a RNA binding scaffold. *J. Am. Chem. Soc.* **126**, 4453-4460 (2004).
30. Koekoek, H. & Robillard, G. T. Substrate specificity via ternary complex formation with glutamate dehydrogenase. *Eur. J. Biochem.* **79**, 85-92 (1977).
31. Miller, J., Witzemann, V., Quast, U. & Raftery, M. A. Proton magnetic resonance studies of cholinergic ligand binding to the acetylcholine receptor in its membrane environment. *Proc. Natl. Acad. Sci. U. S. A* **76**, 3580-3584 (1979).
32. Fielding, L., Rutherford, S. & Fletcher, D. Determination of protein-ligand binding affinity by NMR: observations from serum albumin model systems. *Magn Reson. Chem.* **43**, 463-470 (2005).
33. Meyer, B. & Peters, T. NMR spectroscopy techniques for screening and identifying ligand binding to protein receptors. *Angew. Chem. Int. Ed Engl.* **42**, 864-890 (2003).

34. Mayer, M. & Meyer, B. Group epitope mapping by saturation transfer difference NMR to identify segments of a ligand in direct contact with a protein receptor. *J. Am. Chem. Soc.* **123**, 6108-6117 (2001).
35. Groves, P. *et al.* Temperature dependence of ligand-protein complex formation as reflected by saturation transfer difference NMR experiments. *Magn Reson. Chem.* **45**, 745-748 (2007).
36. Yan, J., Kline, A. D., Mo, H., Shapiro, M. J. & Zartler, E. R. The effect of relaxation on the epitope mapping by saturation transfer difference NMR. *J. Magn Reson.* **163**, 270-276 (2003).
37. Velazquez, C. A. & Freire, E. ITC in the post-genomic era...? Priceless. *Biophys. Chem.* **115**, 115-124 (2005).
38. Matulis, D., Rouzina, I. & Bloomfield, V. A. Thermodynamics of DNA binding and condensation: isothermal titration calorimetry and electrostatic mechanism. *J. Mol. Biol.* **296**, 1053-1063 (2000).
39. Sikora, C. W. & Turner, R. J. Investigation of ligand binding to the multidrug resistance protein EmrE by isothermal titration calorimetry. *Biophys. J.* **88**, 475-482 (2005).
40. Karsten, W. E. & Cook, P. F. An isothermal titration calorimetry study of the binding of substrates and ligands to the tartrate dehydrogenase from Pseudomonas putida reveals half-of-the-sites reactivity. *Biochemistry* **45**, 9000-9006 (2006).
41. Kluger, R. & Alagic, A. Chemical cross-linking and protein-protein interactions--a review with illustrative protocols. *Bioorganic Chemistry* **32**, 451-472 (2004).
42. Lambert, B. & Buckle, M. Characterisation of the interface between nucleophosmin (NPM) and p53: potential role in p53 stabilisation. *FEBS Lett.* **580**, 345-350 (2006).
43. Robinson, C. V. *et al.* Probing the Nature of Noncovalent Interactions by Mass Spectrometry. A Study of Protein-CoA Ligand Binding and Assembly. *Journal of the American Chemical Society* **118**, 8646-8653 (1996).
44. Jeffrey, P. D., Gorina, S. & Pavletich, N. P. Crystal structure of the tetramerization domain of the p53 tumor suppressor at 1.7 angstroms. *Science* **267**, 1498-1502 (1995).
45. Mittl, P. R., Chene, P. & Grutter, M. G. Crystallization and structure solution of p53 (residues 326-356) by molecular replacement using an NMR model as template. *Acta Crystallogr. D. Biol. Crystallogr.* **54**, 86-89 (1998).
46. Johnson, S. M. *et al.* Native state kinetic stabilization as a strategy to ameliorate protein misfolding diseases: a focus on the transthyretin amyloidoses. *Acc. Chem. Res.* **38**, 911-921 (2005).
47. Miroy, G. J. *et al.* Inhibiting transthyretin amyloid fibril formation via protein stabilization. *Proc. Natl. Acad. Sci. U. S. A* **93**, 15051-15056 (1996).
48. Foss, T. R., Kelker, M. S., Wiseman, R. L., Wilson, I. A. & Kelly, J. W. Kinetic stabilization of the native state by protein engineering: implications for inhibition of transthyretin amyloidogenesis. *J. Mol. Biol.* **347**, 841-854 (2005).